

Utah State University

DigitalCommons@USU

All Graduate Theses and Dissertations

Graduate Studies

5-2014

Linking Montane Soil Moisture Measurements to Evapotranspiration Using Inverse Numerical Modeling

Ling Lv

Utah State University

Follow this and additional works at: <https://digitalcommons.usu.edu/etd>



Part of the [Soil Science Commons](#)

Recommended Citation

Lv, Ling, "Linking Montane Soil Moisture Measurements to Evapotranspiration Using Inverse Numerical Modeling" (2014). *All Graduate Theses and Dissertations*. 3323.

<https://digitalcommons.usu.edu/etd/3323>

This Dissertation is brought to you for free and open access by the Graduate Studies at DigitalCommons@USU. It has been accepted for inclusion in All Graduate Theses and Dissertations by an authorized administrator of DigitalCommons@USU. For more information, please contact digitalcommons@usu.edu.



LINKING MONTANE SOIL MOISTURE MEASUREMENTS TO
EVAPOTRANSPIRATION USING INVERSE
NUMERICAL MODELING

by

Ling Lv

A dissertation submitted in partial fulfillment
of the requirements for the degree

of

DOCTOR OF PHILOSOPHY

in

Soil Science

Approved:

Scott B. Jones, Ph.D.
Major Professor

Roger K. KJelgren, Ph.D.
Committee Member

Lawrence E. Hipps, Ph.D.
Committee Member

Shih-Yu Wang, Ph.D.
Committee Member

R. Douglas Ramsey, Ph.D.
Committee Member

Mark McLellan, Ph.D.
Vice President for Research and
Dean of the School of Graduate Studies

UTAH STATE UNIVERSITY
Logan, Utah

2014

Copyright © Ling Lv 2014

All Rights Reserved

ABSTRACT

Linking Montane Soil Moisture Measurements to Evapotranspiration
Using Inverse Numerical Modeling

by

Ling Lv, Doctor of Philosophy

Utah State University, 2014

Major Professor: Scott B. Jones
Department: Plants, Soils and Climate

The mountainous areas in the Intermountain West (IMW) of the North America are considered as the major water reservoir for the Western US. Summer evapotranspiration (ET) and soil moisture are key factors affecting the annual water yield in the montane region of the IMW. This research estimated ET of four common vegetation types (aspen, conifer, grass, and sage) and areal soil moisture in an advanced instrumentation site located at the T.W. Daniel Experimental Forest (TWDEF). Among instrumented forest research sites worldwide, TWDEF is one of a few with triplicate measures of meteorological parameters, radiation, and soil moisture within four common vegetation types in the IMW. This unique dataset enables study and understanding of the ecological and hydrological responses to climate change in Utah and the IMW region. In a second phase of this study, summer water uses from the four common vegetation types were simulated using a numerical simulation model, Hydrus-1D. The simulation was

informed by soil moisture measurements at three depths (0.1 m, 0.25 m, and 0.5 m) and by ET measured from an eddy covariance tower. The results confirmed the value of numerical simulations as a viable alternate method to estimated ET where no direct ET measurements are available. It also provided comparison of water use by these vegetation species including both high and low water years. In the third phase of this study, a comparison was made between the intermediate-scale areal soil moisture measured by a Cosmic-ray neutron probe (CRNP) and the in situ TDT soil moisture network at the TWDEF site. Improved correlations were obtained, especially after shallow rainfall events, by including numerically simulated soil moisture above 0.1 m where no measurements were available. The original CRNP calibration exhibited a dry bias during spring/early summer, leading to the need for a site-specific enhanced calibration, which improved the accuracy of the CRNP soil moisture estimate at the TWDEF site.

(151 pages)

PUBLIC ABSTRACT

Linking Montane Soil Moisture Measurements to Evapotranspiration
Using Inverse Numerical Modeling

Ling Lv

Evapotranspiration (ET) and soil moisture play important roles in annual water delivered from snowpack to reservoirs, lakes and streams. Indeed, ET and soil moisture are key factors dictating the performance of the regional climate models in the intermountain west (IMW) of the USA. Water resources management and climate modeling require accurate prediction of ET and areal soil moisture for reliable estimates of ongoing and future water needs. This research has examined ways to estimate ET from four common vegetation types in the IMW (aspen, conifer, grass, and sage) using local soil moisture measurements from an advanced instrumentation network located in the T.W. Daniel Experimental Forest (TWDEF). The TWDEF is located within the Bear River Range of the Wasatch Cache National Forest in Northern Utah. Among instrumented forest research sites worldwide, TWDEF is unique, providing triplicate measures within a mixed forest system common to the IMW. Observations included continuous meteorological measurements such as air temperature, humidity, solar radiation, wind speed, soil moisture and others. In situ soil moisture values were measured at 0.10-, 0.25- and 0.50-m depths within each of the four vegetation types. In addition, areal soil moisture was measured using a Cosmic-ray neutron probe (CRNP) located in the middle of the site. This unique dataset enables study of the hydrological

processes in Utah and the IMW region. Estimates of ET from aspen, conifer, grass and sage were simulated using a numerical model. Simulated ET values were compared with measured ET from an eddy covariance tower. Results suggest the numerical model is a viable method to estimate ET where no direct ET measurements are available. The simulations also enabled comparison of summer ET among vegetation species including both high and low water years. Finally, a comparison was made between the intermediate-scale areal soil moisture measured by the Cosmic-ray neutron probe (CRNP) and the in situ time domain transmissometry (TDT) soil moisture network at the TWDEF site. Improved correlations were obtained by including numerically simulated soil moisture above 0.1 m where no measurements were available. The original CRNP calibration showed a dry bias during spring/early summer, leading to the need for an additional site-specific calibration, which improved the accuracy of the CRNP soil moisture estimate at the TWDEF site.

ACKNOWLEDGMENTS

I would like to express sincere gratitude to the members of my doctoral committee: Dr. Scott B. Jones, Dr. Lawrence E. Hipps, Dr. Shih-Yu Wang, Dr. Roger K. Kjelgren, and Dr. R. Douglas Ramsey. Thank you for your time, support, encouragement, and expertise throughout this process. I especially thank my committee chair and supervisor, Dr. Jones. Thank you for being patient and supportive all the time. I would have never completed this work without your support and guidance. You are an amazing mentor.

My special thanks to my co-authors, Dr. David A. Robinson at the NERC-Center for Ecology & Hydrology, and Dr. Trenton E. Franz at University of Nebraska-Lincoln, Lincoln, Nebraska for his assistance in interpreting the results.

I also want to thank Jobie Carlisle, and my lab-mates for their help during my field work at T.W. Daniels Experimental Forest, Logan, UT, USA. Thanks to Dr. Lawrence E. Hipps and Pawel Szafruga for assisting me to analyze data from eddy covariance measurements. Thanks to Bill Mace for technical support. I would like to thank Dr. Jiri Simunek for the timely reply to my questions on the Hydrus-1D model.

Further thanks go to the Chinese Scholarship Council and to the Graduate School of Utah State University for financial support during my doctoral study.

I also want to extend gratitude to the Department of Plants, Soils and Climate, and its talented and dedicated faculty and staff. I love my Utah State experience and am very proud of being part of such a renowned department.

Last but not least, I want to thank all the wonderful people, such as Jiyuan Wang, Enzhu Hu, Xystus N Amakor, and etc., who have helped me go through my doctoral study.

Finally, I want to dedicate this dissertation to my parents and my family. Their love, care, patience, and big hearts led me to where I am today. They raised me and taught me tolerance, honesty, and wisdom. Family is what keeps me warm all the time.

This research was supported by a National Science Foundation (NSF) EPSCoR grant EPS 1208732 awarded to Utah State University, as part of the State of Utah Research Infrastructure Improvement Award. Earlier support was provided by a project of USDA-CSREES Special Research Grant no. 2008-34552-19042 from the USDA Cooperative State Research, Education, and Extension Service and by the Utah Agricultural Experiment Station, Utah State University, Logan, UT, 84322-4810.

Ling Lv

CONTENTS

| | Page |
|--|------|
| ABSTRACT..... | iii |
| PUBLIC ABSTRACT | v |
| ACKNOWLEDGMENTS | vii |
| LIST OF TABLES | xi |
| LIST OF FIGURES | xiii |
| CHAPTER | |
| 1 INTRODUCTION | 1 |
| 1.1 ET Assessment Techniques..... | 2 |
| 1.2 Soil Moisture Assessment Techniques..... | 4 |
| 1.3 Research Objectives | 5 |
| References | 7 |
| 2 T.W. DANIEL EXPERIMENTAL FOREST INSTRUMENTATION AND MONITORING..... | 13 |
| 2.1 Introduction | 14 |
| 2.2 Site Descriptions | 16 |
| 2.3 Instruments and Environmental Measurements | 19 |
| 2.3.1 Meteorological Measurements..... | 19 |
| 2.3.2 Soil Moisture Measurement..... | 21 |
| 2.3.3 Eddy Covariance..... | 24 |
| 2.3.4 Other Data..... | 26 |
| 2.3.5 Data Availability..... | 26 |
| 2.3.6 Example of Data Application..... | 27 |
| References | 27 |
| 3 EVAPOTRANSPIRATION IN A SEMI-ARID MOUNTAIN ECOSYSTEM FROM INTEGRATED NUMERICAL MODELING AND ENVIRONMENTAL DATA..... | 43 |
| 3.1 Introduction | 44 |
| 3.2 Theoretical Considerations..... | 48 |
| 3.2.1 Root Water Uptake | 49 |
| 3.2.2 Initial and Boundary Conditions..... | 50 |

| | | |
|---|--|-----|
| 3.2.3 | Inverse Modeling Procedure | 51 |
| 3.3 | Materials and Methods | 52 |
| 3.3.1 | Study Area and Experimental Data..... | 52 |
| 3.3.2 | Eddy Covariance Measurement | 55 |
| 3.4 | Statistical Analysis | 57 |
| 3.5 | Results and Discussions | 57 |
| 3.5.1 | Precipitation | 57 |
| 3.5.2 | Soil Moisture and Water Transport Calibration..... | 57 |
| 3.5.3 | Comparison of Simulated and Measured ET | 59 |
| 3.5.4 | Plant Water Use Characteristics..... | 61 |
| 3.5.5 | ET and Soil Moisture | 63 |
| 3.6 | Conclusions | 65 |
| | References | 66 |
| 4 MEASURED AND MODELED SOIL MOISTURE COMPARED WITH COSMIC- RAY NEUTRON PROBE ESTIMATES IN A MIXED FOREST | | 90 |
| 4.1. | Introduction | 90 |
| 4.2. | Theoretical Considerations..... | 92 |
| 4.3. | Materials and Methodologies | 94 |
| 4.3.1. | Study Area | 94 |
| 4.3.2. | TDT Soil Moisture Sensor Network..... | 96 |
| 4.3.3. | Portable TDR Soil Moisture Measurements | 97 |
| 4.3.4. | Soil Texture Mapping | 97 |
| 4.3.5. | CRNP Calibration | 99 |
| 4.3.6. | Numerical Model Simulation of Near Surface Soil Moisture | 100 |
| 4.3.7. | Comparison of CRNP with Distributed Sensor Network | 101 |
| 4.4. | Results and Discussions | 102 |
| 4.4.1. | Soil Moisture Comparison of CRNP with the TDT Network..... | 102 |
| 4.4.2. | Vegetation Related Soil Moisture Distribution Within the TWDEF Site..... | 104 |
| 4.4.3. | Seasonal Change of Soil Moisture Distribution..... | 105 |
| 4.4.4. | Recalibration of CRNP for the TWDEF Site..... | 106 |
| 4.5. | Conclusions | 107 |
| | References | 108 |
| 5 SUMMARY AND CONCLUSIONS | | 124 |
| 5.1 | Summary of Findings | 124 |
| 5.2 | Conclusions | 127 |
| APPENDICES | | 128 |
| CURRICULUM VITAE..... | | 132 |

LIST OF TABLES

| Table | Page |
|--|------|
| 2-1. Instrumented Experimental sites of nature ecosystems in the Western US..... | 31 |
| 2-2. Summary of instrumentation installed at the T.W. Daniel Experimental Forest (TWDEF) site..... | 32 |
| 3-1. Feddes Parameters defining root water uptake reduction coefficient, $\alpha(h)$ for studied vegetation types (Havranek and Benecke, 1978; Kelliher et al., 1993; Kolb and Sperry, 1999; Running, 1976; Ryel et al., 2002; Ryel et al., 2010; Taylor and Ashcroft, 1972) | 74 |
| 3-2. Albedos and extinction coefficients of TWDEF plants types (Betts and Ball, 1997; Black et al., 1991; Brantley and Young, 2007; Chen et al., 1997; Kiniry et al., 2011) | 74 |
| 3-3. Vegetation physiological stages for plant types at the TWDEF. The LAI_0 and LAI_{max} were from previous studies (Barr et al., 2004; Clark and Seyfried, 2001; Gifford et al., 1984; Lecain et al., 2000)..... | 75 |
| 3-4. The snow ablation date for different vegetation sites in water year of 2009, 2010, 2011, and 2012. Drifted and accumulated snow generally builds up on grass A and sage A plots resulting in later snowmelt compared to grass and sage plots .. | 76 |
| 3-5. The total ET (averaged from 4-year simulation) of aspen and conifer as compiled from the literature | 77 |
| 3-6. Significance testing of total evaporation, transpiration, and ET for each vegetation type compared for the same growing seasons (confidence level of $\alpha=0.05$). Units are in cm of water loss | 78 |
| 3-7. Significance testing for each vegetation type during the four simulated growing seasons of 2009, 2010, 2011, and 2012 (confidence level of $\alpha=0.05$). Units are in cm of water loss | 79 |
| 4-1. Tree size distribution and characteristics determined from seven-100 m ² plots at the TWDEF research site, and the estimated aboveground and root biomass (Jenkins et al., 2003)..... | 113 |
| 4-2. Summary of measured and derived parameters used in the universal calibration function (equation 4-4) | 114 |

| | | |
|------|--|-----|
| 4-3. | Examples of numerically fitted (Hydrus-1D) soil hydraulic parameters for each vegetation type | 115 |
| 4-4. | Variogram nugget and sill from soil moisture measurements for each of four different sampling dates. The variogram was fitted using an exponential model. To the soil water moisture measurements obtained by a portable time domain reflectometry (TDR) | 116 |

LIST OF FIGURES

| Figure | Page |
|--|------|
| 1-1. Schematic illustration of Hydrus-1D model to simulate evaporation, transpiration. The Penman-Monteith equation and root water uptake were coupled in it. Here ET is evapotranspiration, θ is volumetric soil moisture, θ_r is residual soil moisture, θ_s is saturated soil moisture, K_s is saturated soil water conductivity, α and n are the shape factors to describe van Genuchten equation, which is a relationship of soil moisture and soil matric potential..... | 12 |
| 2-1. The over view of the TWDEF study site in Northern Utah and the layout of the data collection network contained within the fenced perimeter. A Cosmic-Ray Neutron Probe (CRNP), USU Doc Daniel Snotel site, and GPS station are also shown. The labels indicated the plots in each vegetation type, where the first letter represents vegetation type (a=aspen, c=conifer, g=grass, and s=sage), the second letter stands for the plot A, B, and C. For example, AA stands for the plot A of aspen. | 33 |
| 2-2. (a) Deviation of monthly air temperatures from 5-year average monthly air temperature during water years 2008-2012, and (b) annual accumulative precipitation (AP), annual snow water equivalent (SWE), and annual reference ET (ET_0) during water years 2008-2012 period at the USU Doc Daniel Snotel site, which is approximately 50 m away from the southwest edge of the TWDEF site. Reference ETs were estimated from the FAO-56 Penman-Monteith equation. ... | 34 |
| 2-3. Sample data for comparison of the (a) air temperature, (b) air vapor pressure at dew point, (c) net radiation and (d) wind speed in the open areas (grass and sagebrush) and underneath the tree canopies (aspen and conifer) during the summer time when the vegetation canopy was fully developed..... | 35 |
| 2-4. Sample data for Comparing of the effect of vegetation canopies on snow depth. Four snow pits were excavated near the grass plot. The offset in the snow depth sensor is because of vegetation growth after snow melt..... | 36 |
| 2-5. Sample data comparison of (a) GPS snow depth (SD) and (b) snow water equivalent (SWE) measurements with SNOTEL and hand measurements. Taking the GPS as the center location, the hand measurements transects were taken in four directions (45° , 135° , 180° , 225°) and at distances of 2.5 m, 5m, 7.5m, 10m, 15m, 20m and 25m. | 37 |
| 2-6. Monthly-precipitation (a) and -snow water equivalent (SWE) (b) during the 2008-2012 water years of measurement at the USU Doc Daniel Snotel site..... | 38 |

- 2-7. Thirty-minute averaged sample data of soil moisture (a1, a2, a3, and a4) and soil temperatures (b1, b2, b3, and b4) at depths of 10 cm, 25 cm, and 50 cm in one plot each of aspen, conifer, grass and sagebrush during the 2010 water year. 39
- 2-8. Comparison of areal soil moisture measured by the CRNP with aggregate estimates from the TDT-sensor network at the 10 cm depth. Each TDT soil moisture measurements was distance weighted from the CRNP sensor location as described in Chapter 4. 40
- 2-9. Illustration of footprint radius of Eddy covariance (EC) tower at TWDEF site under stable neutral and unstable weather conditions which are 500-, 370-, and 85 m, respectively. The EC footprint is calculation using the Method of Hsieh et al.(2000). Because of the heterogeneous landscape, only area enclosed within the EC footprint with a wind direction between 257° and 330° is considered acceptable data. The summer dominant wind direction is 294°(black arrow line in the graph). The footprint of Cosmic-Ray Neutron Probe (CRNP) is estimated at 385 m at the TWDEF elevation. 41
- 2-10. Sample eddy covariance measurements exhibiting the hourly energy flux including solar radiation (Rs), net radiation (Rn), soil heat flux (G), latent heat flux (LE), and sensible heat flux (H). The lack of LE and H on day 206 is because the wind direction was out of the acceptable range, i.e., 257°-330°. The LE and H are estimated after energy balance closure check. 42
- 3-1. Root distribution density in the vegetation, aspen = A, conifer = C, sage = S, and grass = G for plots A, B, and C. Root density as a function of depth was interpreted from the 2004 soil pedon surveys. Because the root depth of the conifer plot C did not extend below 62 cm while the other two went beyond 1.2 m., we separated the analyses to shallow and deep rooted plots. 80
- 3-2. The T.W. Daniel Experimental Forest (TWDEF) site located in Northern Utah, illustrating the data collection network distributed within the study site. The site is surrounded by a perimeter fence with 12 primary/secondary weather stations and associated subplots. The Doc Daniel Snotel site is located at the Eastern edge of the TEDEF enclosure. The source of the DEM was from the U.S. Geological Survey (USGS) in spatial resolutions of 1 arc-second (30 m)..... 81
- 3-3. The mean and standard deviation of minimum soil moisture measured by TDT sensor in water years 2009, 2010, 2011, and 2012 for each subplot at 10-, 25-, and 50 cm depths. The x-axis designates each subplot, where the first letter represents vegetation type (a=aspen, c=conifer, g=grass, and s=sage), the second letter stands for the plot A, B, and C, and the last number represents the subplots number, i.e. 1 through 3. 82

- 3-4. Total precipitation for grass (left), and temporal variation in snow water equivalent (SWE) at the USU Doc Daniel Snotel site (right) for water years 2009, 2010, 2011, and 2012..... 83
- 3-5. Example simulated soil moisture calibrations from measured values at 10-, 25-, and 50- cm depths in Aspen, Conifer, Grass/Forbs and sagebrush sites during the study periods of 2009, 2010, 2011, and 2012. 84
- 3-6. Example of simulated hydraulic properties and corresponding 95% confidence intervals for (a) soil moisture and (b) hydraulic conductivity (K) for the top layer of AA1, which is subplot one of plot A in aspen..... 85
- 3-7. Comparison of soil core sampled with Hydrus-1D simulated soil moisture distribution profiles among the four vegetation types plots (aspen, conifer, grass/forbs, and sagebrush) on Sep. 14th, 2011. The first letter of legend represents vegetation type (a=aspen, c=conifer, g=grass, and s=sage), the second letter stands for the plot A, B, and C, and the last number represents the subplots number, i.e. 1 through 3. Sage B simulation was unavailable due to failure of the TDT soil moisture sensors. 86
- 3-8. Comparison between the calculated ET from eddy covariance tower and the numerically simulated ET (mean±1 standard deviation). The mean numerically simulated ET was computed from 18 subplots, 9 in grass and 9 in sagebrush, with error bars representing one standard deviation from the means. 87
- 3-9. Numerically simulated (Hydrus-1D) average daily evaporation rates, transpiration rates, and evapotranspiration (ET) rates for aspen, conifer, grass and sage during the growing seasons of 2009, 2010, 2011, and 2012. 88
- 3-10. Normalized daily ET rate (ratio of daily ET rate to reference ET rate) as a function of soil moisture in the near surface layer (10 cm depth) for aspen, conifer (deep-rooted conifer = drC, shallow-rooted conifer = srC), grass and sage during the growing seasons of 2009, 2010, 2011, and 2012. 89
- 4-1. The overview of the TWDEF study site in the Northern Utah and the layout of the data collection network contained within the fenced perimeter. A Cosmic-ray Neutron Probe (CRNP) and its associated footprint are also shown. The time domain transmissometry (TDT) soil moisture sensors are shown as triangles around each plot weather station. The clay content (%) distribution inside the TWDEF site is displayed on the right upper corner. 117
- 4-2. (a) Comparison between TDT weighted average soil moisture of 0.1 m, 0.25 m, and 0.5 m depth ($\bar{\theta}_{TDT}$) and the average areal soil moisture measured by CRNP (θ_v) during the growing seasons of 2011 and 2012. (b) Comparison between Hydrus-1D weighted soil moisture ($\bar{\theta}_{H1D}$) of 0.03 m, 0.05 m, 0.1 m, 0.25 m, and

- 0.5 m depth and the average areal soil moisture measured by CRNP (θ_v) during the growing seasons of 2011 and 2012. The soil moistures at 0.03 m and 0.05 m were extracted from the Hydrus-1D estimation. The soil moistures at 0.1 m, 0.25 m, and 0.5 m were measured by TDT sensors. 118
- 4-3. The seasonal evolution of soil moisture under the four vegetation types as measured by the portable time domain Reflectometry (TDR) probe on June 07, 2012, July 06, 2012, August 01, 2012, and September 02, 2012 at the TWDEF site. 119
- 4-4. Clay content distribution within each vegetation type based on electromagnetic induction mapping and correlation between clay content and electrical conductivity (ECa). From top to bottom, the box chart shows the max value (top whisker), 75th percentile, mean (dash line), median (solid line), 25th percentile, and min value (bottom whisker) for each vegetation group, respectively. Dots indicate the 95th and 5th confidence interval. 120
- 4-5. Temporal evolution of soil moisture during the summer of 2012 within each of 3 soil clay content regimes illustrated in Figure 1. The mean soil moisture flanked by one standard deviation for each soil clay fraction are plotted from portable TDR measurements made on June 07, 2012, July 06, 2012, August 01, 2012, and September 02, 2012 at the TWDEF. 121
- 4-6. Comparison of CRNP-based soil moisture estimates as a function of fast neutron intensity using the parameters published by Desilets et al. (2010) against recalibrated parameters for the TWDEF. The discrete data points are derived from the Hydrus-1D weighted average areal soil moisture ($\bar{\theta}_{H1D}$) and the relative fast neutron intensity (N/N_0) obtained during the growing season of 2012. 122
- 4-7. Comparison of soil moisture estimated from the weighted TDT sensors ($\bar{\theta}_{TDT}$), the universal calibration function (θ_v), and from the recalibrated parameters (θ_v') during the snow-free season of 2013. 123

CHAPTER 1

INTRODUCTION

Mountain areas in the Intermountain West (IMW) are considered to be a major water reservoir in the Western US. Climate studies (Cayan et al., 2001, 2010) estimate future warming and drying trends in a region already plagued by drought. Future water resources of the IMW are being strained and threatened from a rapid increase in water demand and the projected decrease in precipitation. Episodic events of extreme drought will compound the problem of increased demand and this may interact with projected climate change in unforeseen and potentially worrisome ways (Wang and Gillies, 2012). Therefore, it is important to quantify each component involved in hydrological processes for water resources management. Water inputs in this region are extensively monitored by the Snowpack Telemetry (SNOTEL) networks. Water loss through evapotranspiration (ET) and water storage as soil moisture have received far less attention. Limited quantification of ET and soil moisture restricts not only water resources management but is also a significant limitation for high-resolution climate modeling in the IMW (Henderson-Sellers et al., 1995; Shao and Henderson-Sellers, 1996; Wang et al., 2009). The availability of replicated, plant-species-dependent, determination of ET and soil moisture within a montane setting of the T.W. Daniel Experimental Forest provides a significant resource and opportunity to better inform models and water management decisions.

To understand the important roles of ET and soil moisture in land-atmosphere interactions, early research mainly focused on the fundamental principles of silviculture,

disturbance ecology and ecosystem properties in relation to succession (Anhold et al., 1996; Ballard and Long, 1988; Clayton, 2003; Dean and Long, 1992) in western mountains. Only recently have appropriate instruments and sensors been available to monitor these environmental properties and make state-of-the-art estimates of evapotranspiration and energy balance in montane regions.

1.1 ET Assessment Techniques

Evapotranspiration is the sum of evaporation from soil and transpiration from vegetation. Evaporation is the process of water vaporization and removal from an evaporating surface. Transpiration is the process of water vaporization in plant tissues and the vapor removal to the atmosphere (Allen et al., 1998). Direct ET observation techniques are based on (1) water mass balance, such as soil and plant weighing lysimeter (Andales et al., 2009) or catchment water budget analysis (Wilson et al., 2001). (2) Energy balance and turbulent transfer theory, such as Bowen ratio (Angus and Watts, 1984; Fritschen, 1965; Tomlinson, 1996) and eddy covariance (Ivans et al., 2006; Shi et al., 2008). In addition, there are techniques to estimate either evaporation (E), such as soil heat pulse analysis and surface chamber systems (Denmead, 1984) or transpiration (T), including sap flow methods (Wilson et al., 2001; Wullschlegel et al., 1998), plant chamber systems, and isotopic tracers (Denmead, 1984), etc. Several studies have reviewed the pros and cons of the existing observation techniques (Drexler et al., 2004; Rana and Katerji, 2000; Shuttleworth, 2007; Verstraeten et al., 2008; Wang and Dickinson, 2012).

At the same time, ET can be estimated indirectly by a large number of more- or less- empirical models. Based on the working principle or driving meteorological variables, the current ET models are categorized into Monin-Obukhov similarity theory (Wang and Dickinson, 2012), temperature based approaches, radiation based approaches, and combination equations including resistance type approaches (Bormann, 2011). The simplest model is the temperature based approach, such as Hargreaves Equation (Hargreaves and Allen, 2003), which is recommended for periods of one month or more. The most widely applied combination equations based ET model is the Penman-Monteith (PM) equation, which is driven by meteorological data, and defined as aerodynamic resistance and canopy resistance. Obtaining reliable values of canopy resistance is complicated and therefore for certain situations limits application of the PM equation (Jarvis and McNaughton, 1986). Furthermore, reference ET is based on the PM equation for a reference surface, which is a hypothetical grass reference crop with an assumed crop height of 0.12 m, a fixed surface resistance of 70 s/m and an albedo of 0.23 (Allen et al., 1998). The reference ET can be converted to actual ET by multiplying a crop coefficient. The crop coefficient varies with vegetation species, soil moisture conditions, and vegetation growth stage, etc (Allen et al., 2005). Currently, crop coefficients are only available for limited plant species, mainly for economic crops and grasses. Few studies of the crop coefficients are available for vegetation in natural ecosystems, especially for plants in high elevations. Radiation-based models, such as the Priestley-Taylor model (Priestley and Taylor, 1972) were developed to estimate ET in energy limited ecosystems. The empirical or semi-empirical ET models mentioned above require local

calibration. Testing the accuracy and performance of these model is laborious, time-consuming and costly (Allen et al., 1998).

Numerous models have been developed to estimate the sub-components of ET. For example, the root water uptake model of Feddes (Feddes et al., 2001) is a physiological model to simulate plant transpiration. Instead of measuring meteorological data, soil matric potential or soil moisture was measured within root zone. The root water extraction was solved numerically as a sink term that was added to the vertical water-flow equation. Root water extraction has also been coupled within climate models, such as general circulation models and numerical weather prediction models (Feddes et al., 2001) or hydrologic models, such as the soil-water-atmosphere-plant model (Kroes et al., 2000) and hydrus-1D (Simunek et al., 2008) (Figure 1-1). The soil evaporation component could also be estimated from separate models, such as the model expressed by Camillo and Gurney (1986) and the advection-diffusion equation (Or et al., 2013).

1.2 Soil Moisture Assessment Techniques

Soil moisture is the source of available water to plants and microbes (Jung et al., 2010). In dry lands particularly, soil moisture is one of the major controls on the structure and diversities of ecosystems. The standard reference method for determining soil moisture is to oven dry mineral soils at 105 °C, or organic soils and gypsiferous soils at 70 °C (Robinson et al., 2008). In the past decade, new soil moisture measurement technologies have been developed such as neutron thermalization sensors, electromagnetic sensors, and heat pulse sensors. These new soil moisture measurement methods can be combined with wireless data transfer for automated, seamless, and real-

time data collection. Such measurement methods enhance our ability to capture the spatial and temporal soil moisture dynamics (Abdu et al., 2008; Blonquist et al., 2005a, 2005b; Jones et al., 2005; Robinson et al., 2003). While, these measurements are made at a point-scale or involving a relatively small soil volume, atmospheric and land-surface applications generally require large area- or volume-averaged soil moisture estimation. Therefore, point measurements must be scaled up to larger areas. However, the inherent small-scale heterogeneity of soils makes such up-scaling difficult. Soil physicists have made some progress with this issue, but it still is a longstanding unresolved research problem (Jury et al., 2011). Although satellite remote sensing methods are becoming available at large scales, there are other limitations, including shallow measurement depth, limited capability to penetrate vegetation or snow, inability to measure soil ice, sensitivity to surface roughness, discontinuous temporal coverage and a short life span of satellite missions (Zreda et al., 2008). The Cosmic-ray Neutron Probe (CRNP) is a novel non-invasive technique (Shuttleworth et al., 2010) to measure the areal averaged soil moisture of an effective depth on the order of decimeters within a radial footprint of several hundred meters (Zreda et al., 2008, 2012). Franz et al. (2012) suggested the CRNP to be highly sensitive to the shallow subsurface soil moisture, but a lack of shallow (< 10 cm) soil moisture measurements limited their conclusions in this regard.

1.3 Research Objectives

The dynamics and magnitude of ET and soil moisture in the mountain ecosystems in the IMW remain poorly documented, despite their great importance to water resources. The primary objective of this research was to describe an experiment at the T.W. Daniel

Experimental Forest (TWDEF) located in Northern Utah and, to employ those data to quantify the water use (ET) of the vegetation types common in this region. In addition, numerical modeling is employed as a tool to simulate the soil moisture content in the top 10 cm, where measurements were unavailable. Lastly, we compared a point-scale soil moisture measurement array against the Cosmic-Ray Neutron Probe (CRNP) areal soil moisture determination.

The specific objectives were to:

1. Analyze environmental data from the T.W. Daniel Experimental Forest Research site.
2. Estimate evaporation and transpiration from four vegetation types common to montane areas of the IMW, using inverse numerical modeling of soil moisture measurements.
3. Compare these ET estimates with Eddy Covariance measurements at the TWDEF.
4. Determine the ability of near-surface soil moisture estimates made by a large footprint neutron count-based soil moisture sensor (i.e., via Cosmic-ray neutron probe) to TDR/TDT-based near-surface soil moisture estimates combined with numerical simulation of near-surface soil moisture.

The remainder of this dissertation is organized as follows: Chapter 2 frames the setup of instruments and measurements in the dataset, and compares our dataset with existing similar datasets. Chapter 3 introduces the numerical simulation of the ET from four common vegetation types across multiple growing seasons. The statistical comparison of ET among vegetation types and growing season were also discussed in this chapter. In Chapter 4, the comparison of point soil moisture measurements

(TDT/TDR) and the CRNP soil moisture measurements were evaluated in more detail. Repetition of some formulae and facts are thus inevitable in some parts of this dissertation. I ask the disposed reader to excuse this redundancy.

References

- Abdu, H., Robinson, D.A., Seyfried, M., Jones, S.B., 2008. Geophysical imaging of watershed subsurface patterns and prediction of soil texture and water holding capacity. *Water Resour. Res.* 44: W00D18.
- Allen, R.G., Pereira, L.S., Raes, D., Smith, M., 1998. Crop evapotranspiration - Guidelines for computing crop water requirements-FAO Irrigation and drainage paper 56. FAO - Food and Agriculture Organization of the United Nations, Rome.
- Allen, R.G., Pereira, L.S., Smith, M., Raes, D., Wright, J.L., 2005. FAO-56 dual crop coefficient method for estimating evaporation from soil and application extensions. *J. Irrig. Drain. Eng.* 131(1): 2-13.
- Andales, A., Straw, D., Ley, T., Berrada, A., 2009. Alfalfa reference ET from a weighing lysimeter and estimates from the ASCE standardized reference ET equation in the Arkansas Valley of Colorado, World Environmental and Water Resources Congress, pp. 1-9.
- Angus, D.E., Watts, P.J., 1984. Evapotranspiration — How good is the Bowen ratio method? *Agric. Water Manage.* 8(1-3): 133-150.
- Anhold, J.A., Jenkins, M.J., Long, J.N., 1996. Management of lodgepole pine stand density to reduce susceptibility to mountain pine beetle attack. *West. J. Appl. For.* 11(2): 50-53.
- Ballard, L.A., Long, J.N., 1988. Influence of stand density on log quality of lodgepole pine. *Can. J. For. Res.* 18: 911-916.
- Blonquist, J.M.J., Jones, S.B., Robinson, D.A., 2005a. Standardizing characterization of electromagnetic water content sensors. *Vadose Zone J.* 4(4): 1059-1069.
- Blonquist, J.M.J., Jones, S.B., Robinson, D.A., 2005b. A time domain transmission sensor with TDR performance characteristics. *J. Hydrol.* 314(1-4): 235-245.
- Bormann, H., 2011. Sensitivity analysis of 18 different potential evapotranspiration models to observed climatic change at German climate stations. *Clim. Change* 104(3-4): 729-753.

- Camillo, P.J., Gurney, R.J., 1986. A resistance parameter for bare-soil evaporation models. *Soil Sci.* 141(2): 742-744.
- Cayan, D.R., Das, T., Pierce, D.W., Barnett, T.P., Tyree, M., Gershunov, A., 2010. Future dryness in the southwest US and the hydrology of the early 21st century drought. *PNAS*: 21271-21276.
- Cayan, D.R., Dettinger, M.D., Kammerdiener, S.A., Caprio, J.M., Peterson, D.H., 2001. Changes in the onset of spring in the Western United States. *Bull. Am. Meteorol. Soc.* 82(3): 399-415.
- Clayton, J.C., 2003. Effects of clearcutting and wildfire on shrews (Soricidae: Sorex) in a Utah coniferous forest. *West. N. Am. Naturalist* 63(22): 264-267.
- Dean, T.J., Long, J.N., 1992. Influence of leaf area and canopy structure on size-density relations in even-aged lodgepole pine stands. *For. Ecol. Manage.* 49: 109-117.
- Denmead, O.T., 1984. Plant physiological methods for studying evapotranspiration: Problems of telling the forest from the trees. *Agric. Water Manage.* 8(1-3): 167-189.
- Drexler, J.Z., Snyder, R.L., Spano, D., Paw U, K.T., 2004. A review of models and micrometeorological methods used to estimate wetland evapotranspiration. *Hydrol. Processes* 18(11): 2071-2101.
- Feddes, R.A., Hoff, H., Bruen, M., Dawson, T., Rosnay, P. de, Dirmeyer, P. Jockson, R.B., Kabat, P. Kleidon, A., Lilly, A., Pitman, A., 2001. Modeling root water uptake in hydrological and climate models. *Bull. Am. Meteorol. Soc.* 82(12): 2797-2809.
- Franz, T., Mreda, M., Rosolem, R., Ferre, T.P.A., 2012. Field validation of a cosmic-ray neutron sensor using a distributed sensor network, *Vadose zone J.* 11, 4, doi:10.2136/vzj2012.0046.
- Fritschen, L.J., 1965. Accuracy of evapotranspiration determinations by the Bowen ratio method. *Bull. Int. Assoc. Scientific Hydrol.* 10(2): 38-48.
- Hargreaves, G., Allen, R., 2003. History and evaluation of Hargreaves evapotranspiration equation. *J. Irrig. and Drain. Eng.* 129(1): 53-63.
- Henderson-Sellers, A., Pitman, A.J., Love, P.K., Irannejad, P., Chen, T.H., 1995. The Project for Intercomparison of Land Surface Parameterization Schemes (PILPS): Phases 2 and 3. *Bull. Am. Meteorol. Soc.* 76(4): 489-503.

- Ivans, S., Hipps, L., Leffler, A.J., Ivans, C.Y., 2006. Response of water vapor and CO₂ fluxes in semiarid lands to seasonal and intermittent precipitation pulses. *J. Hydrometeorol.* 7(5): 995-1010.
- Jarvis, P.G., McNaughton, K.G., 1986. Stomatal control of transpiration: scaling up from leaf to region. Academic Press, pp. 1-49.
- Jones, S.B., Blonquist, J.M., Robinson, D.A., Rasmussen, V.P., Or, D., 2005. Standardizing characterization of electromagnetic water content sensors. *Vadose Zone J.* 4(4): 1048-1058.
- Jung, M., Reichstein, M., Ciais, P., Seneviratne, S.I., Sheffield, J., Goulden, M.L., Bonan, G., Cescatti, A., Chen, J., de Jeu, R., Dolman, A.J., Eugster, W., Gerten, D., Gianelle, D., Gobron, N., Heinke, J., Kimball, J., Law, B.E., Montagnani, L., Mu, Q., Mueller, B., Oleson, K., Papale, D., Richardson, A.D., Rouspard, O., Running, S., Tomelleri, E., Viovy, N., Weber, U., Williamms, C., Wood, E., Zaehle, S., Zhang, K., 2010. Recent decline in the global land evapotranspiration trend due to limited moisture supply. *Nature* 467(7318): 951-954.
- Jury, W.A., Or, D., Pachepsky, Y., Vereecken, H., Hopmans, J.W., Ahuja, L.R., Clothier, B.E., Bristow, K.L., Kluitenberg, G.J., Moldrup, P., Simunek, J., van Genuchten, M. Th., Horton, R., 2011. Kirkham's legacy and contemporary challenges in soil physics research. *Soil Sci. Soc. Am. J.* 75(5): 1589-1601.
- Kroes, J.G., Wesseling, J.G., Van Dam, J.C., 2000. Integrated modelling of the soil–water–atmosphere–plant system using the model SWAP 2.0 an overview of theory and an application. *Hydrol. Processes* 14(11-12): 1993-2002.
- Or, D., Lehmann, P., Shahraeeni, E., Shokri, N., 2013. Advances in Soil Evaporation Physics—A Review. *Vadose Zone J.* 12(4), doi: 10.2136/vzj2012.0163.
- Priestley, C.H.B., Taylor, R.J., 1972. On the assessment of surface heat flux and evaporation using large-scale parameters. *Mon. Weather Rev.* 100(2): 81-92.
- Rana, G., Katerji, N., 2000. Measurement and estimation of actual evapotranspiration in the field under Mediterranean climate: a review. *Eur. J. of Agron.* 13(2–3): 125-153.
- Robinson, D.A. Campbell, C.S., Hopmans, J.W., Hornbuckle, B.K., Jones, S.B., Knight, R., Ogden, F., Selker, J., Wendroth, O., 2008. Soil moisture measurement for ecological and hydrological watershed-scale observatories: a review. *Vadose Zone J.* 7(1): 358-389.
- Robinson, D.A., Jones, S.B., Wraith, J.M., Or, D., Friedman, S.P., 2003. A review of advances in dielectric and electrical conductivity measurement in soils using time domain reflectometry. *Vadose Zone J.* 2(4): 444-475.

- Shao, Y., Henderson-Sellers, A., 1996. Modeling soil moisture: A Project for Intercomparison of Land Surface Parameterization Schemes Phase 2(b). *J. Geophys. Res.* 101(D3): 7227-7250.
- Shi, T. Guan, D., Wang, A., Wu, J., Jin, C., Han, S., 2008. Comparison of three models to estimate evapotranspiration for a temperate mixed forest. *Hydrol. Processes* 22(17): 3431-3443.
- Shuttleworth, W.J., 2007. Putting the "vap" into evaporation. *Hydrol. Earth Syst. Sci.* 11(1): 210-244.
- Shuttleworth, W.J., Zreda, M., Zeng, X., Zweck, C., Ferre, P.A., 2010. The cosmic-ray Soil Moisture Observing System (COSMOS): a non-invasive, intermediate scale soil moisture measurement network, Proceedings of the British Hydrological Society's Third International Symposium: 'Role of hydrology in managing consequences of a changing global environment, Newcastle University.
- Simunek, J., Sejna, M., Saito, H., Sakai, M., van Genuchten, M.T., 2008. The HYDRUS-1D software package for simulating the one-dimensional movement of water, heat, and multiple solutes in Variably-saturated Media. Department of environmental sciences university of California riverside, California.
- Tomlinson, S.A., 1996. Comparison of Bowen-ratation, eddy correlation, and weighing lysimeter evapotranspiration for two sparse canopy sites in eastern Washington. In: U.S. Geological Survey. Water-Resources Investigations Report 96-4081, Tacoma, WA.
- Verstraeten, W., Veroustraete, F., Feyen, J., 2008. Assessment of evapotranspiration and soil moisture content across different scales of observation. *Sensors* 8(1): 70-117.
- Wang, K., Dickinson, R.E., 2012. A review of global terrestrial evapotranspiration: Observation, modeling, climatology, and climatic variability. *Rev. of Geophys.* 50(2): RG2005.
- Wang, S.-Y., Gillies, R., 2012. Climatology of the U.S. Inter-Mountain West, Modern Climatology, Dr Shih-Yu Wang (Ed.), ISBN: 978-953-51-0095-9, In Tech, Available from: <http://www.intechopen.com/books/modern-climatology/climatology-of-the-u-s-intermountain-west>.
- Wang, S.-Y., Gillies, R.R., Takle, E.S., Gutowski, W.J., Jr., 2009. Evaluation of precipitation in the Intermountain Region as simulated by the NARCCAP regional climate models. *Geophys. Res. Lett.* 36(11): L11704.
- Wilson, K.B., Hanson, P.J., Mulholland, P.J., Baldocchi, D.D., Wullschleger, S.D., 2001. A comparison of methods for determining forest evapotranspiration and its

components: sap-flow, soil water budget, eddy covariance and catchment water balance. *Agric. and For. Meteorol.* 106(2): 153-168.

Wullschleger, S.D., Meinzer, F.C., Vertessy, R.A., 1998. A review of whole-plant water use studies in tree. *Tree Physiol.* 18(8-9): 499-512.

Zreda, M., Desilets, D., Ferré, T.P.A., Scott, R.L., 2008. Measuring soil moisture content non-invasively at intermediate spatial scale using cosmic-ray neutrons. *Geophys. Res. Lett.* 35(21): L21402.

Zreda, M., Shuttleworth, W.J., Zeng, X., Zweck, C., Desilets, D., Franz, T., Rosolem, R., 2012. COSMOS: The COsmic-ray Soil Moisture Observing System. *Hydrol. Earth Syst. Sci. Discuss.* 9(4): 4505-4551.

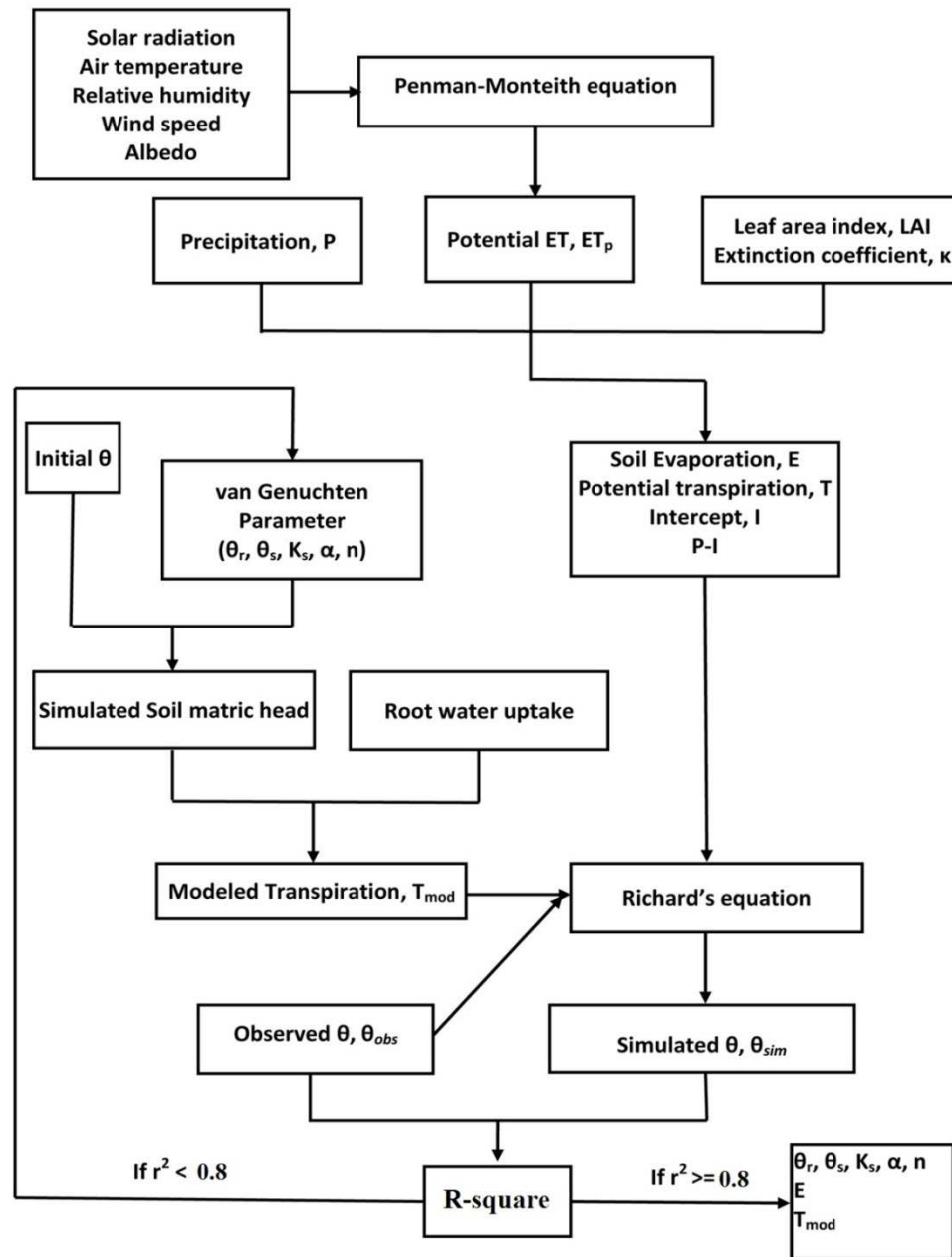


Figure 1-1. Schematic illustration of Hydrus-1D model to simulate evaporation, transpiration. The Penman-Monteith equation and root water uptake were coupled in it. Here ET is evapotranspiration, θ is volumetric soil moisture, θ_r is residual soil moisture, θ_s is saturated soil moisture, K_s is saturated soil water conductivity, α and n are the shape factors to describe van Genuchten equation, which is a relationship of soil moisture and soil matric potential.

CHAPTER 2

T.W. DANIEL EXPERIMENTAL FOREST INSTRUMENTATION
AND MONITORING¹

Abstract. The T.W. Daniel Experimental Forest (TWDEF) is located in the Bear River Range of the Wasatch Cache National Forest in Northern Utah in the United States. The site represents high-elevation (2600 m) environmental conditions of the Intermountain Region within a patchwork of four predominant montane vegetation types (aspen, conifer, grass, and sagebrush). Monitoring began at the study site in 2008 where vegetation type has one primary and two secondary weather stations, each station adjacent to three-3 x 3 meter instrumented vegetation sub-plots. Each of the four primary automated micrometeorological towers (AMT) records air temperature and air vapor pressure, net radiation, precipitation, snow depth, and wind speed and direction as well as snow depth every 30 minutes. Secondary towers provide air temperature and snow depth measurements. Each subplot includes soil measurements at 10-, 25- and 50-cm depths of temperature, electrical conductivity, dielectric permittivity, water content and matric potential. An eddy covariance tower provides precipitation, net radiation, soil heat flux in addition to water vapor and CO₂ flux, as well as wind speed and direction. A cosmic ray neutron probe provides areal averaged soil moisture covering the entire study area. The USU Doc Daniel Snetel site is adjacent to the TWDEF instrumented site, with data available at <http://danielforest.usu.edu/>.

¹ Coauthored by: Ling Lv, Scott B. Jones, Jonathan Carlisle

2.1 Introduction

Climate studies suggest Western United States has been experiencing a warming trend since the late 1940s (Cayan et al., 2001). Environmental warming has important consequences for the hydrological cycle in the North American Intermountain Western (IMW), where 50% - 80% of water supply for human activities and agricultural production rely on snow melt water (Wang et al., 2009). The hydrological cycle includes processes of snow-accumulation, -sublimation and -ablation as well as melt-water infiltration, soil water storage, soil evaporation and plant transpiration. In warmer weather, less winter precipitation falls as snow and the melting of winter snow occurs earlier in the spring. Both effects lead to earlier stream peak flow, and possible drought in summer and autumn. Historical climate data also suggest that episodic events of extreme drought would increase water demand in this region (Wang and Gillies, 2012). In addition, the climate warming will directly impact the function of ecosystems such as plant physiology, frequency and duration of wildfires and distribution of species (Thomas et al., 2004; Westerling et al., 2006). To be able to analyze the climate and climate-proxy data and understand the ecological and hydrological response to climate change in Utah and the IMW, instrumentation at the T.W. Daniel Experimental Forest (TWDEF) was installed in the Wasatch Mountains of Northern Utah. The T.W. Daniel Experimental Forest was named after Professor Ted W. Daniel in August of 1996 and has a long history of research from a variety of disciplines.

The following aspects of the TWDEF site make it unique among existing sites in the IMW region (Table 2-1): (1) Geographical characteristics: TWDEF lies on a

mountaintops at 2600 m in the Wasatch Mountains, and a transition zone of different climate regimes in both seasonal and inter-annual time scales. Climate models yield poor climate predictions for this region because of the shortage of measured observations on the surface boundary. These parameters can be derived from the TWDEF measurements;

(2) Multiple plant types are represented, namely: aspen, conifer, grass and sagebrush, which are the dominant vegetation in the IMW. These vegetation types are expressed in patchworks, which is likely the result of frequent fires during the settlement period (1870-1891) and subsequent suppression since 1910 (Long, 1996). An closure fence was established in 2005 around the study site where vegetation plots were located in order to exclude nonnative grazers. Instrumentation planning and installation began in 2006 with environmental parameters measured within four vegetation types beginning in 2008. Although there are a number of published watershed-based ecological sites Table 2-1, few of them are able to address comparison studies regarding the effects of vegetation type on environment;

(3) Replicated experimental design: Triplicate plots containing each vegetation type were randomly selected three subplots were located within each plot area to capture the heterogeneous soil and plant conditions;

(4) co-located with other experimental stations: In 2007, USDA installed a SNOTEL site adjacent to the fenced enclosure. The University Novstar Consortium, (UNAVCO), a non-profit university-governed consortium funded installation of a Global Positioning System (GPS), that acts as a snow and soil moisture sensors in an adjacent meadow to the instrumentation at the TWDEF. In 2011, Arizona State University established a cosmic-ray neutron probe (CRNP) station within the study area., A comparison of TWDEF in situ soil moisture

sensor network measurements with the CRNP and GPS measurements will be discussed later. (5) High-density of environmental measurements: Instrumentation includes four automated micrometeorological towers (AMT), 108 soil moisture and matric potential sensors, an eddy covariance tower, a CRNP for areal soil moisture, the USU Doc Daniel SNOTEL site, and a GPS-based snow depth sensor.

2.2 Site Descriptions

Location: The T.W. Daniel Experimental Forest (TWDEF) site is located at the Bear River Range of the Wasatch Cache National Forest in Northern Utah, USA (41.86°N, 111.50°W), about 15 km south of the Utah-Idaho border. It ranges over an elevation of approximately 2550-2750 m (Figure 2-1). The site is a gently sloping (<10%), northeast to southeast trending ridge top, at the head of a contributing watershed to the Logan River and Bear River basin. The TWDEF is accessed by a seasonally maintained US Forest Service road, approximately 8 km from paved Utah highway 89 and 30 km from Logan, UT. Because of the remote ridge-top location, the TWDEF site contains no lakes or permanent streams and it lacks electrical power (i.e., other than solar power) and a water supply.

History: The experimental forest site was established in 1936 with an area of 1036 ha, as a part of the newly created Utah State University Forestry program. In the past decades, the forest was used for teaching and demonstrations (Long, 1996). Early research efforts were aimed understanding the fundamental principles of silviculture and disturbance ecology and ecosystem properties in relation to succession (Anhold et al., 1996; Ballard and Long, 1988; Clayton, 2003; Dean and Long, 1992). The site also has a

long history of timber harvest, livestock grazing, and dispersed recreation since the late 1800s. While there is a history of frequent fires prior to 1910, there is no evidence the site has burned since (Schimpf et al., 1980).

Climate: Climate at the TWDEF is typical of the montane semi-arid Intermountain West with large diurnal temperatures swings and seasonally cool and dry summers with cold winters accompanied by significant snow accumulation. The mean January and August temperature is -11 and 17 °C, respectively. December through March temperatures average -5 °C, while the growing season months of May to September average 12 °C. Annual precipitation averages 950 mm yr⁻¹, 80% of which falls as snow. Accumulation is variable due to drifting but typically peaks between 150 and 350 cm in depth. Snowmelt typically occurs between mid-May and mid-June. Figure 2-2 shows that the air temperatures from January through August of 2012 were higher than other years. The highest annual reference ET (ET₀) was 958.1 mm, and occurred in water year 2012. Vapor pressure deficit increases rapidly with increasing air temperature, which results in high ET₀.

Soil: A historical soil pedon survey was conducted during 1970s, and the latest survey happened in 2004. Soils throughout the site are derived from the knight formation of the Wasatch group, a Tertiary red conglomerate of quartzite, sandstone, and shale (Long, 1996; Schimpf et al., 1980). Most soils are fine, mixed, superactive typic haplocryalf (Boettinger et al., 2004). These soils have an organic matter- and base- rich surface soil or mollic epipedon characteristic of “prairie soils” (Schimpf et al., 1980). This trait is likely due to the base rich subsoil, slow decomposition rate, good distribution

of fine roots in the upper 50 cm of soil, and the high degree of mixing by orthopods and mammals such as pocket gophers (Andersen et al., 1980).

Vegetation: The vegetation succession represents a meadow →aspen→fir→spruce→sere in the middle rocky mountains (West and Reese, 1991). The principal vegetation types are aspen (*Populus trembloides*) (Gifford, 1966), conifer (*Picea engelmannii* and *Abies lasiocarpa*) and grass/forbs (*Agropyron trachycaulum* and *Bromus inermis leys.*) and sagebrush (*Artemisia tridentata*) (McArthur, 1981). *Picea engelmannii* and *Abies lasiocarpa* are the dominant late succession species throughout most of the forest (Reese et al., 1980). The predominant tree stands ages range from 80 to 120 years (Schimpf et al., 1980).

Instruments: A representative montane patchwork of the four predominant vegetation types was fenced in 2005 within TWDEF site. A solar-powered environmental observatory network was gradually constructed and began to collect data in August 2008. The site includes an eddy covariance tower, a Snotel station and twelve instrument clusters. The twelve instrument clusters are arranged with a primary and 2 secondary sensor towers in each of the 4 vegetative types for continuous environmental monitoring (Figure 2-1). Each tower is instrumented with a suite of above and below ground sensors, recorded with a data logger (CR10X or CR1000 or CR3000, Campbell Scientific, Inc, Logan, UT). The power supply is from a solar panel/battery system mounted on/under each tower. The data are wirelessly transmitted via a 2.4 GHz mesh radio modem (Digi/Maxtream, Xbee Pro modem), connected via low-loss antenna cables (Times LMR400) to antennas (Pacific Wireless) aimed at the summit radio station tower, which

transmits all data collected from the network to a repeater radio on Logan Peak, near Logan, UT. This monitoring network and transmission methodology has significantly reduced the time and cost for maintaining the instrumentation and database from the TWDEF instrumentation.

2.3 Instruments and Environmental Measurements

2.3.1 Meteorological Measurements

The locations of instrumented plots at the TWDEF were selected based on vegetation and soil study plots established prior to plans for instrumentation. The locations were selected to meet the long-term research goals of TWDEF. The four primary automated micrometeorological towers (ATMs) were assigned to one vegetation plot each with a pair of secondary towers (snow depth and air temperature only) assigned to the remaining 2 plots in each vegetation domain. Tower and soil instrumentation provide measurements every 30 minutes for air temperature, air vapor pressure, saturation vapor pressure, wind speed, net radiation, snow depth and summer-time precipitation (Table 2-2). In Figure 2-3, a 5-day example set of data illustrate the variations in air temperature and air vapor pressure among the 4 ATMs while contrasting the differences in net radiation and wind speed for the open (grass, sage) plots relative to the tree (aspen, conifer) covered plots. Tree canopies moderated wind speeds and change diurnal range of net radiation. Figure 2-4 shows mean vegetation type-dependent snow depth for the 2011 water year. Snow depth was deeper in the open areas (i.e. grass and sage plots) than plots within tree canopies. This effect is a result of tree canopy

interception as well as the western directional wind scouring and drifting snow in open areas (Meyer et al., 2012).

A novel measurement method for snow depth using GPS was proposed and the instrument was installed in a meadow 400 m southeast from the SNOTEL Site (Figure 2-1). The GPS signal fluctuations caused by surface reflections (GPS multipath reflectometry) are used to measure snow depth within a fairly large sensing region (circle radius of 10 to 20 m) (Nievinski and Larson, 2014a, 2014b). In Figure 2-5, we compared the temporally varying snow depths measured by the GPS estimates with SNOTEL snow depth measurements, finding good correlation but with an offset due to the sheltered environment of the SNOTEL site. This comparison highlights one of the challenges of snow monitoring, where there can be significant differences in snow cover for sites that are close together depending on exposure to solar radiation (e.g., slopes and aspect, tree shading).

Precipitation is the main water input for montane ecosystems in the IMW, therefore measurement of precipitation is fundamental to our understanding of hydrological processes (Goodrich et al., 2008). In the western high elevations of the IMW, 50-80% of the water supply is in the form of snowfall. Data on snow pack provide critical information to decision makers and water managers throughout the West. Although there is limited precipitation during the growing season, its measurement plays an important role in studying and understanding ecological processes in semiarid ecosystem (Ivans et al., 2006). The Natural Resources Conservation Service (NRCS) installed, operates, and maintains the USU Doc Daniel SNOTEL, located approximately

50 m away outside the southeast fence of the TWDEF (Figure 2-1). The USU Doc Daniel SNOTEL station is located within a wind-sheltered clearing in a conifer grove where data collection began in July 2007. Two distinct precipitation devices are installed as part of the SNOTEL station, one that measures snow water equivalent (SWE) based on a pressure sensing snow pillow and another that measures accumulative precipitation (AP) within a weighing precipitation gage. The SWE and AP values are corrected and reset to zero on October 1st of each year, the beginning of a water year. Figure 2-6 illustrates the significant variation in monthly precipitation and SWE over the 5 years data. This natural variation in water supply should be of concern to water managers and the public in general, and emphasizes the need to understand the regional and global climate mechanisms regulating precipitation in the IMW (Wang et al., 2009).

2.3.2 Soil Moisture Measurement

2.3.2.1 *TWDEF TDT Sensors Network System*

Direct soil water moisture monitoring facilitates understanding of the soil water status and temporal changes indicate water uptake rates. Time domain transmissometry (TDT) sensors were selected for monitoring purposes at the TWDEF site yielding soil dielectric permittivity, soil moisture, electrical conductivity and soil temperature. The logger and radio mesh network facilitates the wireless data transfer for automated, seamless, and near real-time data collection. The TDT sensor offers the advantage of the pulse generating and sampling electronics being mounted in the head of the probe, which allows the TDT sensor to be used with long cables and multiplexed through SDI-12

addressing. Another important advantage of the TDT sensor is the low cost, small size, high accuracy and stable operation at Gigahertz frequency (Blonquist et al., 2005b).

Adjacent to each primary or secondary weather station tower are three 3 m × 3 m sub-plots (36 sub-plots total). Each subplot has an external 2 m buffer protection perimeter zone space. Time-domain transmissometry (TDT) soil moisture sensors were placed horizontally at 10, 25 and 50 cm depths within this buffer zone. Co-located matric potential sensors at each depth are separated by at least 15 cm to minimize interference. Depth locations are offset by 40 cm to minimize vertical water and thermal interference. The TDT sensors measure dielectric permittivity directly using travel-time analysis for estimation of water content and provides independent measurements of soil temperature and estimated electrical conductivity. Detailed operation principles can be found elsewhere (Blonquist et al., 2005a; Jones et al., 2005; Robinson et al., 2003). The TDT sensors were calibrated in our lab based on the method of Seyfried et al. (2005). Figure 2-7 illustrates soil moisture and temperature values from one subplot in each vegetation type over the 2010 water year. The expected pattern is clearly seen of increased soil water content in the Fall, followed by relatively stable readings through the winter, with a significant increase during snow melt followed by dry down over the summer. Comparing different vegetation plots, it is clear that the timing of snowmelt is expressed in the timing of soil moisture increase. For example the grass plot leads the other 3 plots suggesting this particular grass plot melted out earlier than the other 3 vegetation plots, which is consistent with visual observations on a yearly basis. The temperature responses are much more consistent in comparison where each shows similar timing of spring snow

melt. The soil warming is more associated with net radiation than with snowmelt water warming the soil, where melt water temperature is likely near 0 °C.

2.3.2.2 *Cosmic-ray Neutron Probe (CRNP) soil moisture measurement*

Soil scientists have suggested that the intermediate-scale soil moisture measurement was a key unresolved need. The application of the Cosmic-ray Neutron Probe (CRNP, Hydroinnova, Albuquerque, NM) is a novel technique to provides estimates of average soil moisture to an effective depth within a footprint on the order of hundreds of meters in size (Jury et al., 2011; Robinson et al., 2008). The footprint diameter is 670 m at sea level, and increases with elevation (Zreda et al., 2011), while the effective depth varies with soil water content. The basic working principle of the CRNP lies in an inversely correlated soil moisture level with fast neutron intensity (neutron count) above the soil surface (Seyfried et al., 2005), which can be moderated by all sources of hydrogen within and near the soil, such as atmospheric water vapor, lattice water, snow cover and vegetation. Correction of the effects from soil lattice water, soil organic matter and atmospheric water vapor have been worked out, but effects of vegetation and snow on CRNP output require further investigation. The shape of the relationship between soil moisture content and fast neutron count rate is largely insensitive to the nature of the soil, but the offset in the relationship has some sensitivity to soil chemistry (Shuttleworth et al., 2010). Therefore, calibration is critical during installation (refer to Zreda et al. (2012) for more detail). A CRNP probe was first installed at the TWDEF on Aug. 13th, 2011 as part of the COSMOS network. Calibration was carried on the same day. Volumetric soil moisture samples were collected at 18

locations (along transects directed N, NE, SE, S, SW, and NW extending to radial distances from the CRNP of 25 m, 75 m, and 200 m. At each location soil samples were taken at 6 depths from 0-0.05 m, 0.05-0.1 m, 0.1-0.15 m, 0.15-0.2 m, 0.2-0.25 m, 0.25-0.3 m totaling 108 volumetric soil samples in all. The mean soil moisture was 0.155 ± 0.005 m³m⁻³. The mean count between 16:00 to 22:00 on Aug. 13th was 1352 ± 20 counts hr⁻¹. In Figure 2-8, we compared the temporal TDT network soil moisture measurements at 10 cm with CRNP soil moisture by the method of Franz et al. (2012), and found the same limitation of TDT sensors installed at 10 cm below soil surface, which is insensitive to shallow rain events the CRNP sees. When the TWDEF site is covered by snow, the CRNP signal is correlated to SWE, but accurate estimates need further study (Desilets et al., 2010).

2.3.3 Eddy Covariance

An eddy covariance (EC) tower was installed in the instrumentation meadow at the TWDEF site, within the vegetation domain of grass and sagebrush based on the predominant wind direction. The footprint of EC tower varies with the stability of atmosphere. Figure 2-9 shows that largest footprint is with a radius of approximately 500 m in a stable condition, and the smallest one is with a radius of around 85 m in an unstable condition. Sensors included: a CSAT3 three-dimensional sonic anemometer (Campbell Scientific, Inc, Logan, UT), a LiCor 7500 open-path water vapor and CO₂ sensor analyzer. Sampling frequency of 20Hz was used with 1 hour average fluxes determined. Sensors were managed and recorded with a CR3000 dataloggers (Campbell Scientific, Inc, Logan, UT). Instruments were mounted 2.64 m above the ground surface.

Solar radiation was measured using an NR01 4-way radiometer (HuksefluxUSA, Inc, Manorville, NY) mounted at 3.5 m above the soil surface. Air temperature and relative humidity were measured using an HMP 45 (Vaisala Inc, Finland) mounted 2.5 m above the soil surface. Soil heat flux was determined with Radiation Energy Balance Systems HFT3 heat flux plate in 2008 and until August 2009, after which the HFP01 (HuksefluxUSA, Inc, Manorville, NY) has been used. The soil heat flux plates were buried at 8 cm and the thermocouples were placed to determine the average soil temperature gradient between the plates and the surface. The Hydra probe 2 (Stevens Water Monitoring Systems) was buried at 3 cm and 8 cm depths to measure the soil moisture and soil temperatures in these two layers. Precipitation was measured with a Hach 8-inch diameter tipping bucket rain gauge (Hach Co., Loveland, CO). The sonic snow depth sensor (Judd Communications LLC, Salt Lake City, UT) was mounted at 3.3 m above the soil surface.

One-hour average fluxes of sensible and latent heat were calculated from the time series of 3D winds, temperature and water vapor density. Because of the heterogenous landscape, only the wind direction between 257° and 330° is determined to be effective measurements. The procedures for this were developed by another investigator at Utah State University. Thus, the procedure of energy balance closure check is necessary to retrieve latent heat flux (LE) and sensible heat flux (H). Based on the law of energy conservation, the value of $(LE+H)/(R_n-G)$ is equal to 1. Where R_n is net radiation and G is ground heat flux. However, at most flux measurement sites, this value is less than 1, and is considered as a very good value in the range of 0.8-0.9 (Cellier and Olioso, 1993).

Otherwise, energy was force close. Hourly energy balance closure values were calculated in the TWDEF site. Figure 2-10 shows a 5-day sample period that includes measurement of solar radiation, net radiation, soil heat flux, sensible heat flux, and latent heat flux. The value of sensible heat flux and latent heat flux is corrected by energy balance closure check.

2.3.4 Other Data

Dielectric-based soil matric potential sensors were installed parallel to the TDT water content sensors. These electromagnetic sensors measure the apparent dielectric of Ceramic Disks (Decagon Devices, MPS-1) (Figure 2-1) to directly monitor the soil water potential and the matric potential indirectly via the water retention relationship. Its temperature operating environment ranges from -40 °C to 50 °C. The measurement range of the MPS-1 sensor is -10 to -500 kPa. The resolution is 1 kPa from -10 to -100 kPa, and 4 kPa from -100 to -500 kPa. Because the MPS-1 measures the dielectric of the wet disk, it is unable to accurately detect the matric potential of frozen soil conditions.

2.3.5 Data Availability

Data from the TWDEF and the corresponding metadata are available for download at the Instrumented T.W. Daniel Experimental Forest website: <http://danielforest.usu.edu>, which is maintained by the Department of plants, soils, and Climate at Utah State University, Logan, UT, USA.

2.3.6 Example of Data Application

These data may be used for a variety of applications related to the description and modeling of the spatial and temporal dynamics of snow accumulation, snow sublimation, snow melting, infiltration, soil water content, soil water storage, evaporation and transpiration. Mahat (2011) has examined ways to improve snowmelt modeling capability to better account for vegetation canopy effects on snowmelt and has evaluated his model against the field data collected at the TWDEF site. That model enhanced the transmission of radiation through the canopy, meliorated the heat and water vapor exchange process between snow ground and atmosphere, and improved the process of canopy snow interception and unloading. Van Miegroet et al. (2005) studied soil organic carbon (SOC) pools among vegetation types with consideration for future climate change scenarios. They found vegetation type may influence SOC retention capacity under future climate projections by affecting potential SOC losses via leaching and decomposition.

References

- Andersen, D.C., MacMahon, J.A., Wolfe, M.L., 1980. Herbivorous Mammals along a Montane Sere: Community Structure and Energetics. *J. Mammal.* 61(3): 500-519.
- Anhold, J.A., Jenkins, M.J., Long, J.N., 1996. Management of lodgepole pine stand density to reduce susceptibility to mountain pine beetle attack. *West. J. Appl. For.* 11(2): 50-53.
- Ballard, L.A., Long, J.N., 1988. Influence of stand density on log quality of lodgepole pine. *Can. J. For. Res.* 18: 911-916.
- Blonquist, J.M.J., Jones, S.B., Robinson, D.A., 2005a. Standardizing characterization of electromagnetic water content sensors. *Vadose Zone J.* 4(4): 1059-1069.
- Blonquist, J.M.J., Jones, S.B., Robinson, D.A., 2005b. A time domain transmission sensor with TDR performance characteristics. *J. Hydrol.* 314(1-4): 235-245.

- Boettinger, J.L., Lawley, J.R., Van Miegroet, H., 2004. Morphology of soils in the aspen, conifer, grass/forbs, and sagebrush environmental monitoring sites, TW Daniel Experimental Forest, Logan, UT.
- Cayan, D.R., Kammerdiener, S.A., Bettnger, M.D., Caprio, J.M., Peterson, D.H., 2001. Changes in the onset of spring in the western united states. *Bull. Am. Meteorol. Soc.* 82(3): 399-415.
- Cellier, P., Olioso, A., 1993. A simple system for automated long-term Bowen ratio measurement. *Agric. For. Meteorol.* 66(1-2): 81-92.
- Clayton, J.C., 2003. Effects of clearcutting and wildfire on shrews(Soricidae: Sorex) in a Utah coniferous forest. *West. N. Am. Naturalist* 63(22): 264-267.
- Dean, T.J., Long, J.N., 1992. Influence of leaf area and canopy structure on size-density relations in even-aged lodgepole pine stands. *For. Ecol. Manage.* 49: 109-117.
- Desilets, D., Zreda, M., Ferré, T.P.A., 2010. Nature's neutron probe: Land surface hydrology at an elusive scale with cosmic rays. *Water Resour. Res.* 46(11): W11505.
- Franz, T., Mreda, M., Rosolem, R., Ferre, T.P.A., 2012. Field validation of a cosmic-ray neutron sensor using a distributed sensor network, *Vadose zone J.* 11, 4, doi:10.2136/vzj2012.0046.
- Gifford, G.F., 1966. Aspen Root Studies on Three Sites in Northern Utah. *Am. Midl. Nat.* 75(1): 132-141.
- Goodrich, D., Keefer, T., Unkrich, C., Nichols, M., Osborn, H., Stone, J., Smith, J., 2008. Long-term precipitation database, Walnut Gulch Experimental Watershed, Arizona, United States. *Water Resour. Res.* 44: 1-5.
- Ivans, S., Hipps, L., Leffler, A.J., Ivans, C.Y., 2006. Response of water vapor and CO2 fluxes in semiarid lands to seasonal and intermittent precipitation pulses. *J. Hydrometeorol.* 7(5): 995-1010.
- Jones, S.B., Blonquist, J.M., Robinson, D.A., Rasmussen, V.P., Or, D., 2005. Standardizing characterization of electromagnetic water content sensors. *Vadose Zone J.* 4(4): 1048-1058.
- Jury, W.A., Or, D., Pachepsky, Y., Vereecken, H., Hopmans, J.W., Ahuja, L.R., Clothier, B.E., Bristow, K.L., Kluitenberg, G.J., Moldrup, P., Simunek, J., van Genuchten, M. Th., Horton, R., 2011. Kirkham's legacy and contemporary challenges in soil physics research. *Soil Sci. Soc. Am. J.* 75(5): 1589-1601.

- Long, J.N., 1996. T.W. Daniel Experimental Forest. In: W.C. Schmidt and J.L. Friede (Ed.), *Experimental forests, ranges, and watersheds in the Northern Rocky Mountains: A compendium of Outdoor Laboratories in Utah, Idaho, and Montana*. USDA Forest Service Gen. Tech. Rep. INT-GTR-334., pp. 31-36.
- Mahat, V., 2011. *Effect of vegetation on the accumulation and melting of snow at the TW Daniels Experimental Forest*, Utah State University, Logan, 182 pp.
- McArthur, E.D., 1981. Taxonomy, origin, and distribution of big sagebrush (*Artemisia tridentata*) and allies (subgenus *Tridentatae*). In: K.L. Johnson (Ed.), *Proceedings of the First Utah Shrub Ecology Workshop*, Ephraim, Utah.
- Meyer, J.D.D., Jin, J., Wang, S.-Y., 2012. Systematic Patterns of the Inconsistency between Snow Water Equivalent and Accumulated Precipitation as Reported by the Snowpack Telemetry Network. *J. Hydrometeorol.* 13(6): 1970-1976.
- Nievinski, F.G., Larson, K.M., 2014a. Inverse Modeling of GPS Multipath for Snow Depth Estimation - Part I: Formulation and Simulations. *IEEE Trans. Geosci. Remote Sens.* PP(99): 1-9.
- Nievinski, F.G., Larson, K.M., 2014b. Inverse Modeling of GPS Multipath for Snow Depth Estimation - Part II: Application and Validation., *IEEE Trans. Geosci. Remote Sens.* PP(99): 1-10.
- Reese, G.A., Bayn, R.L., West, N.E., 1980. Evaluation of double-sampling estimators of subalpine herbage production. *J. Range Manage.* 33(4): 300-306.
- Robinson, D.A. Campbell, C.S., Hopmans, J.W., Hornbuckle, B.K., Jones, S.B., Knight, R., Ogden, F., Selker, J., Wendroth, O., 2008. Soil moisture measurement for ecological and hydrological watershed-scale observatories: a review. *Vadose Zone J.* 7(1): 358-389.
- Robinson, D.A., Jones, S.B., Wraith, J.M., Or, D., Friedman, S.P., 2003. A review of advances in dielectric and electrical conductivity measurement in soils using time domain reflectometry. *Vadose Zone J.* 2(4): 444-475.
- Schimpf, D.J., Henderson, J.A., MacMahon, J.A., 1980. Some aspects of succession in the spruce-fir forest zone of northern Utah. *Great Basin Nat.* 40: 1-26.
- Seyfried, M.S., Grant, L.E., Du, E., Humes, K., 2005. Dielectric Loss and Calibration of the Hydra Probe Soil Water Sensor. *Vadose Zone J.* 4(4): 1070-1079.
- Shuttleworth, W.J., Zreda, M., Zeng, X., Zweck, C., Ferre, P.A., 2010. The cosmic-ray Soil Moisture Observing System (COSMOS): a non-invasive, intermediate scale soil moisture measurement network, *Proceedings of the British Hydrological*

Society's Third International Symposium: 'Role of hydrology in managing consequences of a changing global environment, Newcastle University.

- Thomas, C.D., Cameron, A., Green, R.E., Bakkenes, M., Beaumont, L.J., Collingham, Y.C., Erasmus, B.F.N., de Siqueira, M.F., Grainger, A., Hannah, L. Hughes, L., Huntley, B., van Jaarsveld, A.S., Midgley, G.F., Miles, L., Ortega-Huerta, M.A., Phillips, O.L., Williams, S.E., 2004. Extinction risk from climate change. *Nature* 427(6970): 145-148.
- Van Miegroet, H., Boettinger, J.L., Baker, M.A., Nielsen, J., Evans, D., Stum, A., 2005. Soil carbon distribution and quality in a montane rangeland-forest mosaic in northern Utah. *For. Ecol. Manage.* 220(1-3): 284-299.
- Wang, S.-Y., Gillies, R., 2012. *Climatology of the U.S. Inter-Mountain West, Modern Climatology*, Dr Shih-Yu Wang (Ed.), ISBN: 978-953-51-0095-9, In Tech, Available from: <http://www.intechopen.com/books/modern-climatology/climatology-of-the-u-s-intermountain-west>.
- Wang, S.-Y., Gillies, R.R., Takle, E.S., Gutowski, W.J., Jr., 2009. Evaluation of precipitation in the Intermountain Region as simulated by the NARCCAP regional climate models. *Geophys. Res. Lett.* 36(11): L11704.
- West, N.E., Reese, G.A., 1991. Comparison of some methods for collecting and analyzing data on aboveground net production and diversity of herbaceous vegetation in a Northern Utah subalpine context. *Vegetatio* 96(2): 145-163.
- Westerling, A.L., Hidalgo, H.G., Cayan, D.R., Swetnam, T.W., 2006. Warming and earlier spring increase western U.S. forest wildfire activity. *Science* 313(5789): 940-3.
- Zreda, M., Shuttleworth, W.J., Zeng, X., Zweck, C., Desilets, D., Franz, T., Rosolem, R., 2012. COSMOS: The COsmic-ray Soil Moisture Observing System. *Hydrol. Earth Syst. Sci. Discuss.* 9(4): 4505-4551.
- Zreda, M., Zeng, X., Shuttleworth, J., Zweck, C., Ferre, T., Franz, T., Rosolem, R., Desilets, D., Desilets, S., Womack, G., 2011. Cosmic-Ray Neutrons, An Innovative Method for Measuring Area-Average Soil Moisture. *GEWEX News* 21(3): 6-10.

Table 2-1. Instrumented Experimental sites of nature ecosystems in the Western US

| Site* | TWDEF | AND | NR-C1 | Betasso | GLV | JRB | SCM | RCEW | NevCAN |
|---------------------|---|---|---|---|---|---|---|---|---|
| Funding | USDA | NSF | NSF | NSF | NSF | NSF | NSF | USDA | NSF EPSCoR |
| Spatial scale | Ridge-top | watershed | Ridge-top | foothill | watershed | watershed | watershed | watershed | Slope transect |
| Elevation, m | 2550-2750 | 410-1630 | 3021 | 1810-2024 | 3567-4024 | 2500-3050 | 1160-2340 | 1145-2244 | 900-3015 |
| State | UT | OR | CO | CO | CO | NM | AZ | ID | NV |
| Ecosystem | Aspen, conifer, grass, sage | Conifer | conifer | Conifer | Conifer | conifer | Desert | Aspen, conifer, grass, sage | salt desert, sage, subalpine |
| Resolution | 30 min | Daily | Daily | Hourly | Daily | 30 min/daily | 10 min | daily/hourly/15min | 10min |
| Replication | 3 | NA | NA | NA | NA | NA | NA | NA | NA |
| T _{air} | 2008- | 1958- | 1952- | 2009-(2&10 m) | 1986- | 2007- | 2009- | 1962-(daily) 1996-(15min) | 2011--(2&10 m) |
| RH | 2008- | 1958- | 1952- | 2009-(2&10 m) | 2000- | 2007- | 2009- | 1981- (hourly) | 2011-(2&10 m) |
| R _s | 2008- | 1972- | 1952- | 2009- | 1986- | 2007- | | 1981-(hourly) | 2011-(2&10 m) |
| P _B | NA | | 1952- | 2009- | 2000- | 2007- | 2009- | 1981-(hourly) | 2011-(2&10 m) |
| Δ | 2008- | 1988- | 2000- | NA | | 2007- | 2009- | 1981-(hourly) | 2011-(2&10 m) |
| Wind | 2011- | 1973- | 1952- | 2009-(2&10 m) | 2000- | 2007- | NA | 1981-(hourly) | 2011-(2&10 m) |
| SNOTEL | 2007-(hourly) | NA | 1981(monthly) | NA | NA | NA | NA | NA | NA |
| SD /SWE | 2008- | 1987-2010 | 2000- | 2010-(10min) | NA | 2007- | NA | 1961(biweekly)- | 2011- |
| P | 2008- | 1958- | 2000- | 2009- | NA | 2007- | NA | 1962-1996- | 2011- |
| SML | 2008- | 1990- | NA | | NA | NA | NA | 1976-1991 (hourly) | NA |
| θ | 2008- | 1998- | 1992- | 2009- | 2000- | 2007- | NA | 1970(biweekly)- | 2011- |
| T _{soil} | 2008- | 1987- | 2000- | 2009- | 2000- | 2007- | NA | 1981-1996 (15min) | 2011- |
| □ | 2008- | 1988-1994 | NA | NA | NA | NA | NA | NA | 2011- |
| EC | 2008- | NA | 1998- | NA | NA | 2007- | NA | 1996- | NA |
| Stream | NA | 1968- | 1981- | NA | 1985- | 2007-(daily) | 2009- | 1963- | NA |
| T _{stream} | NA | 1957-1983 | NA | NA | NA | 2007-(daily) | 2009- | NA | NA |
| T _{GW} | NA | 1989-1993 | NA | 2011- | NA | NA | NA | 1963- | NA |
| Reference | http://danielfor.est.usu.edu/Home.aspx | http://www.internet.edu/sites/and | http://culter.colrado.edu/NW/T/ | http://czo.colorado.edu/ | http://czo.colrado.edu/ | http://criticalzone.org | http://criticalzone.org | ftp.nwrc.ars.usda.gov | http://sensor.nevada.edu/NCCP/Default.aspx |

* TWDEF: T.W. Daniel Experimental Forest; AND: Andrews Forest Long Term Ecological Research site (LTER); Betasso: Betasso Critical Zone Observatory (CZO); GLV: Green Lake Valley CZO; JRB: Jemez River Basin CZO; SCM: Santa Catalina Mountains CZO; NR-C1: C1 in the Niwot Ridge LTER site; RCEW: Reynolds Creek Experimental Watershed; NevCAN: Nevada climate-ecohydrological assessment network. T_{air}, air temperature; RH, relative humidity; R_s, solar radiation; P_B, Barometric pressure; Δ, water vapor pressure deficit; SD /SWE, snow depth/snow water equivalent; P, precipitation; SML, snowmelt lysimeter; θ, soil moisture; T_{soil}, soil temperature; □, soil matric potential; EC, eddy covariance tower; Stream, stream flux; T_{stream}, temperature of Stream water; T_{GW}, temperature of Groundwater.

Table 2-2. Summary of instrumentation installed at the T.W. Daniel Experimental Forest (TWDEF) site

| Parameter | Method | Sensor height (cm) | Sensor maker and model | Sensor location |
|--|------------------------------------|-------------------------|--|--------------------------|
| Air temperature | platinum resistance detector (PRT) | 150* | Vaisala, HMP50 & HMP45 | Primary towers |
| Air temperature | thermistor | 150* | Judd Communications LLC, ultrasonic depth sensor | Primary/secondary towers |
| Atmospheric water vapor | capacitive polymer chip | 150* | Vaisala, HMP50 & HMP45 | Primary towers |
| Solar radiation - net radiation | thermopile | 150* | Kipp & Zoen, NR-Lite | Primary towers |
| Solar radiation - 4 - component | thermopile | 150* | Hukseflux Thermal Sensors B.V., NR01 | Sage A |
| Snow water equivalent | hyalon pillow | 0 | Campbell Scientific | Snotel |
| Snow depth | Sonic | 200* | Judd Communications LLC, ultrasonic depth sensor | All towers |
| Snow depth | Global Positioning System (GPS) | 300 | | Big meadow |
| Wind - speed | 3-cup anemometer - photochopper | 150* | Met One Instruments, Inc. 014A | Primary towers |
| Wind - direction | vane with potentiometer | 150* | Met One Instruments, Inc. 024A | Primary towers |
| Wind - speed & direction | sonic transducer | 265 | Campbell Scientific, Inc. CSAT3 sonic anemometer | EC tower |
| Atmospheric CO ₂ and H ₂ O | open path infrared gas absorption | 265 | Li-Cor Biosciences, LI-7500 | EC tower |
| Precipitation - wet | tipping bucket | variable | Texas Electronics, Inc. 525I | Primary towers |
| Precipitation - wet | tipping bucket | variable | Hach Company, 2149 | EC tower |
| Precipitation - all | 30cm diameter wet catchment | 366 | | Snotel |
| Surface temperature | thermocouple infrared detection | 150* | Apogee Instruments, Inc. IRR-PN | EC tower |
| Soil moisture, temperature, ECa | time domain transmissometry | (-10,-25,-50) | Acclima, Inc. ALL-SEN-TDT | 36 plots |
| Soil moisture | wave reflection | (-3-5,-10,-20,-50,-100) | Stevens Water Monitoring Systems, Hydra Probe 2 | EC tower |
| Soil temperature | thermocouple | (-2,-6) | Campbell Scientific, TCAV averaging probes | EC tower |
| Soil heat flux | thermopile | (-8) | Radiation Energy Balance Systems, Inc. HFT3 | EC tower |
| Soil heat flux | thermopile | (-8) | Hukseflux Thermal Sensors B.V., HFP01 | EC tower |
| Soil water potential | frequency domain w/ceramic disks | (-10,-25,-50) | Decagon Devices, Inc. MPS-1 | 36 plots |
| Snowmelt lysimeter | Pressure transducer | 0 | USU soil physics lab | GA, AC |
| CNPR | Cosmic-ray | 300 | Hydroinnova, Albuquerque, NM | GC |

* Approximate height above maximum snow depth. Primary tower include Aspen B (AB), Conifer A (CA), Grass C (GC) and SageB (SB). The other weather stations were included in secondary towers. All towers represent all the weather stations in the Figure 2-1.

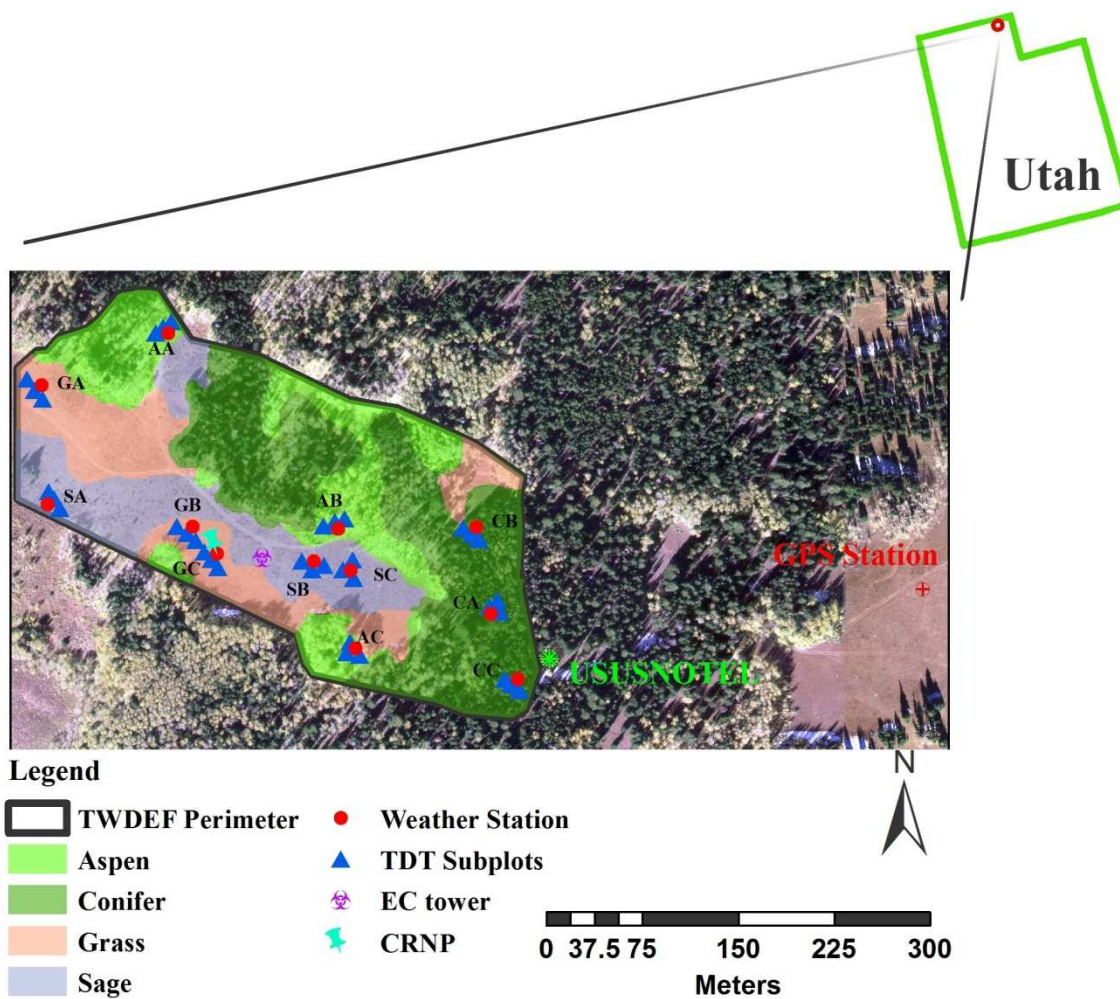


Figure 2-1. The over view of the TWDEF study site in Northern Utah and the layout of the data collection network contained within the fenced perimeter. A Cosmic-Ray Neutron Probe (CRNP), USU Doc Daniel Snotel site, and GPS station are also shown. The labels indicated the plots in each vegetation type, where the first letter represents vegetation type (a=aspen, c=conifer, g=grass, and s=sage), the second letter stands for the plot A, B, and C. For example, AA stands for the plot A of aspen.

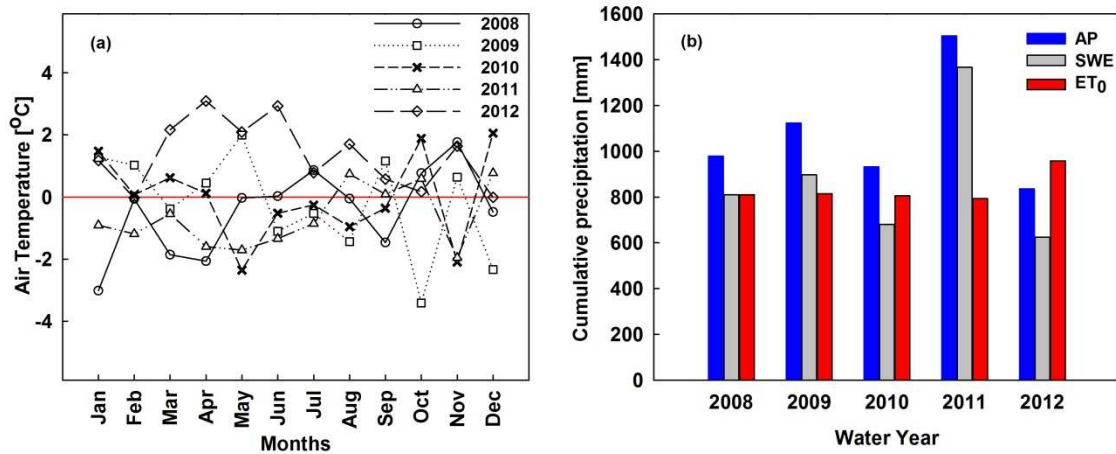


Figure 2-2. (a) Deviation of monthly air temperatures from 5-year average monthly air temperature during water years 2008-2012, and (b) annual accumulative precipitation (AP), annual snow water equivalent (SWE), and annual reference ET (ET₀) during water years 2008-2012 period at the USU Doc Daniel Snotel site, which is approximately 50 m away from the southwest edge of the TWDEF site. Reference ETs were estimated from the FAO-56 Penman-Monteith equation.

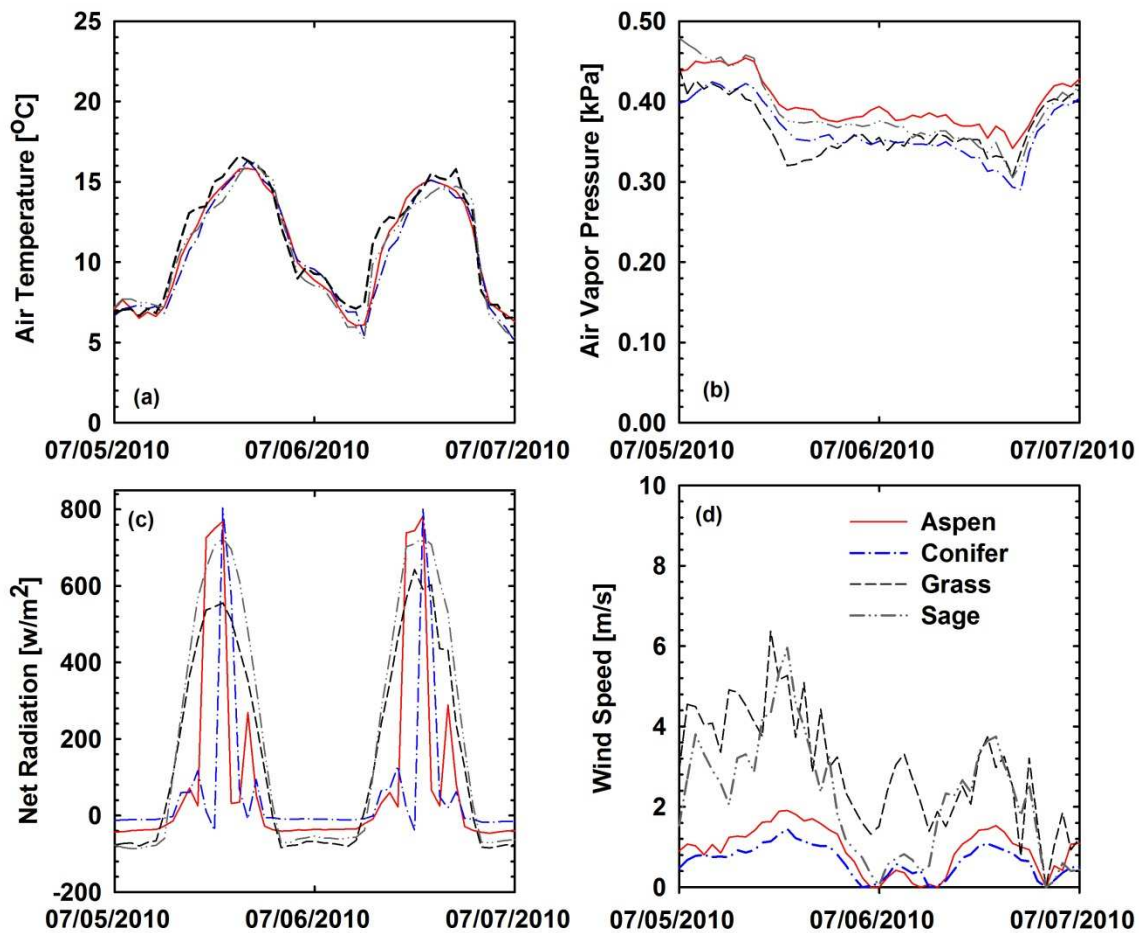


Figure 2-3. Sample data for comparison of the (a) air temperature, (b) air vapor pressure at dew point, (c) net radiation and (d) wind speed in the open areas (grass and sagebrush) and underneath the tree canopies (aspen and conifer) during the summer time when the vegetation canopy was fully developed.

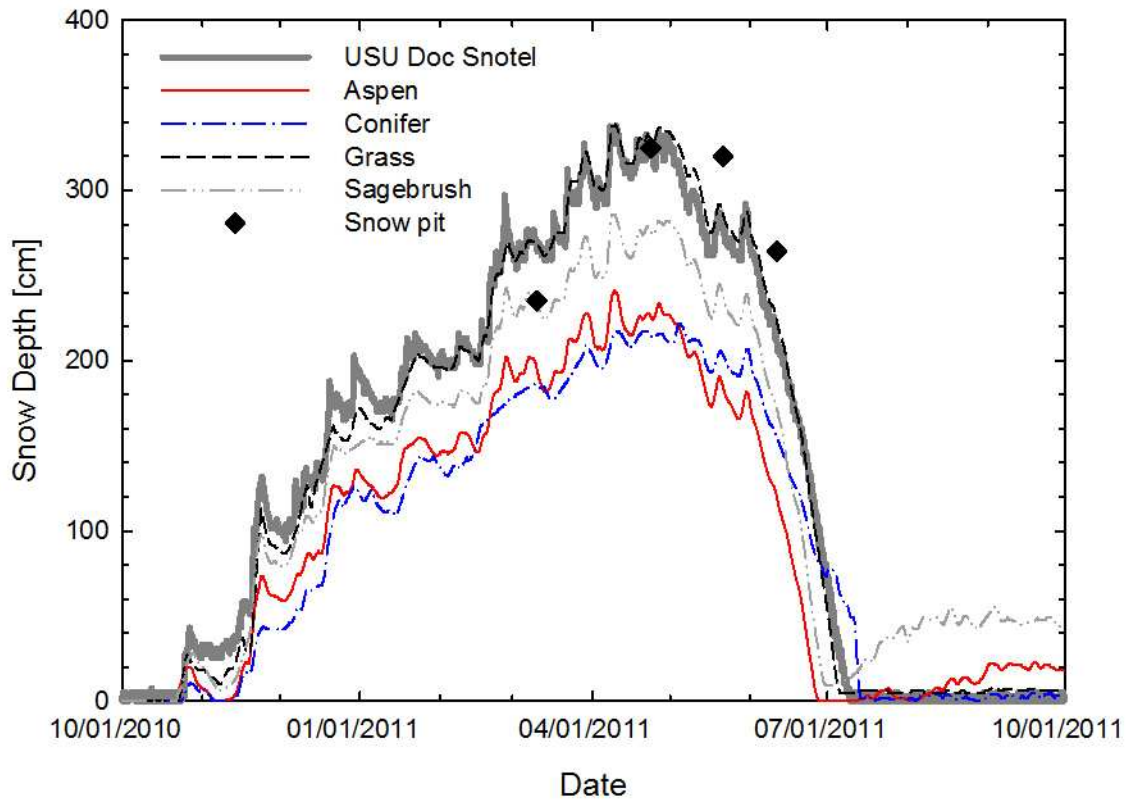


Figure 2-4. Sample data for Comparing of the effect of vegetation canopies on snow depth. Four snow pits were excavated near the grass plot. The offset in the snow depth sensor is because of vegetation growth after snow melt.

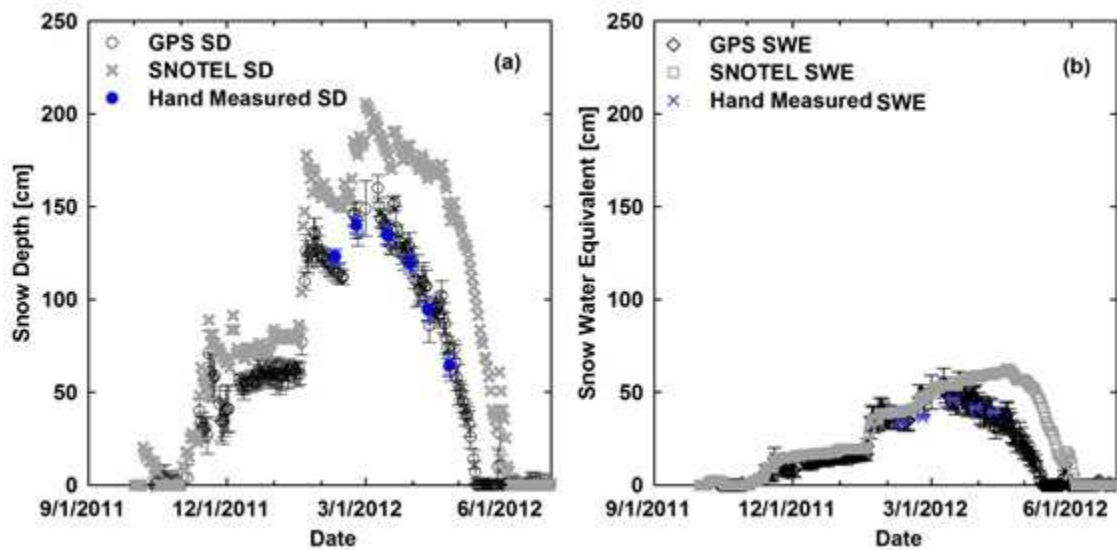


Figure 2-5. Sample data comparison of (a) GPS snow depth (SD) and (b) snow water equivalent (SWE) measurements with SNOTEL and hand measurements. Taking the GPS as the center location, the hand measurements transects were taken in four directions (45° , 135° , 180° , 225°) and at distances of 2.5 m, 5m, 7.5m, 10m, 15m, 20m and 25m.

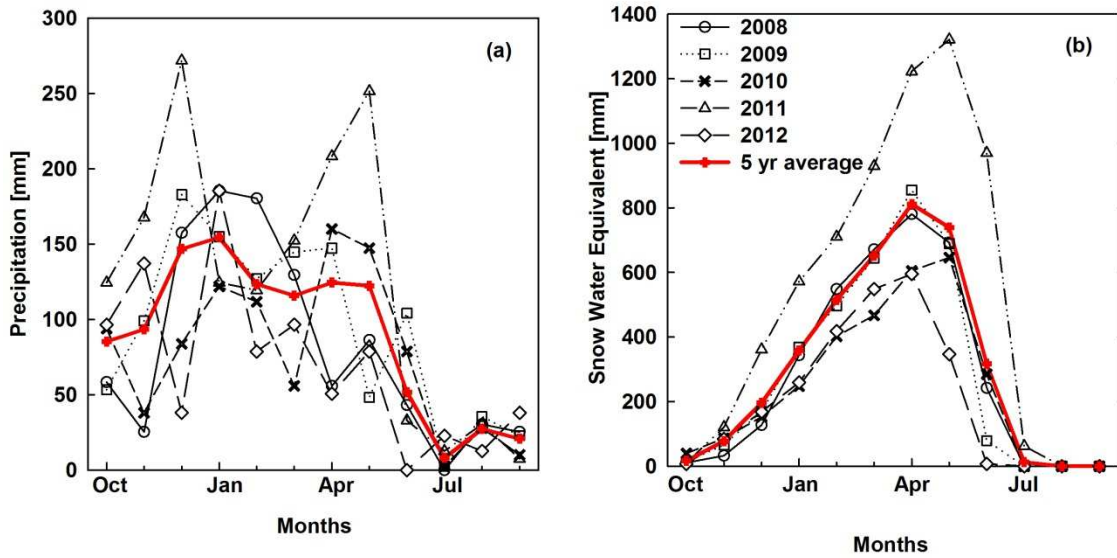


Figure 2-6. Monthly-precipitation (a) and -snow water equivalent (SWE) (b) during the 2008-2012 water years of measurement at the USU Doc Daniel Snotel site.

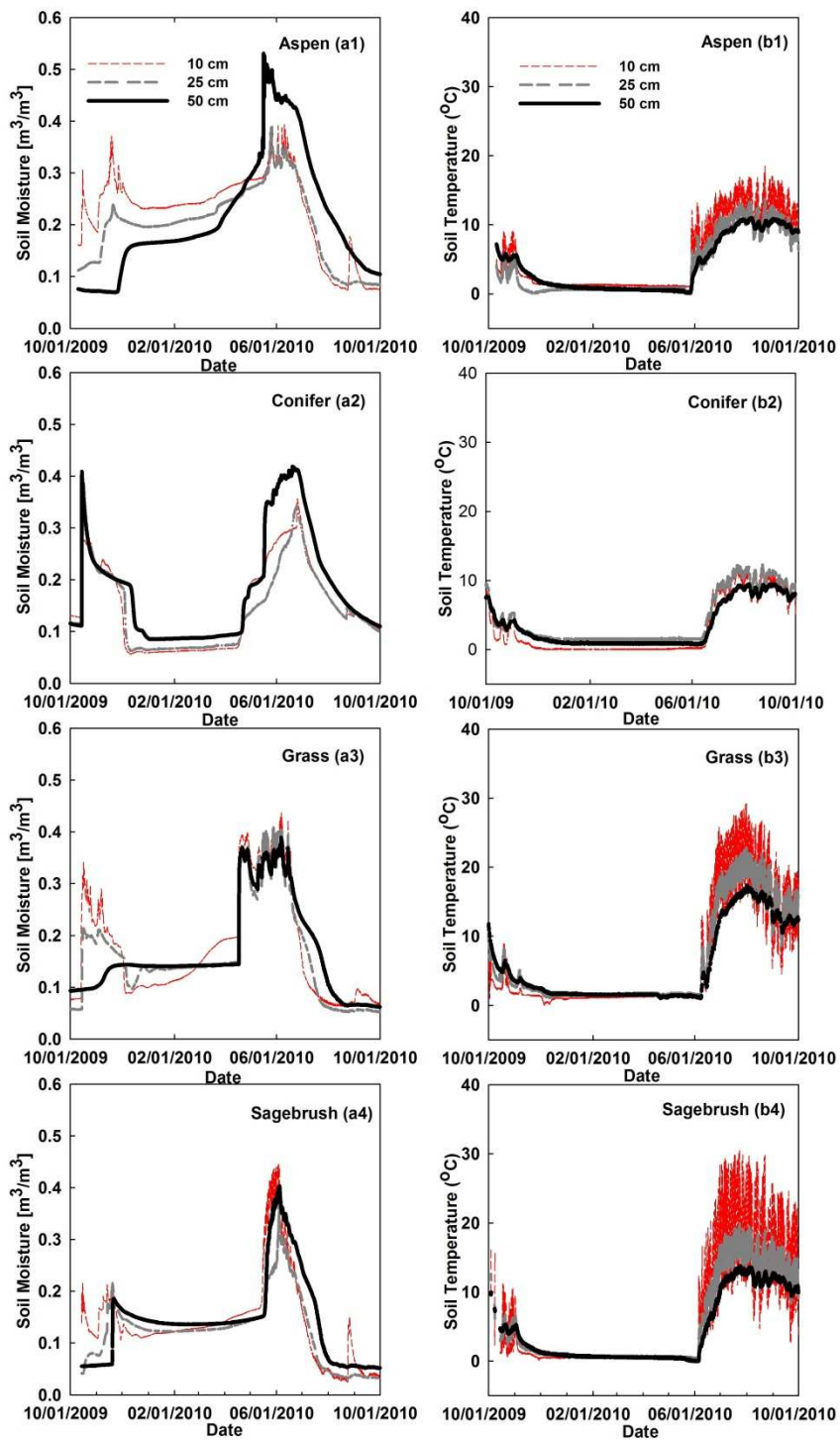


Figure 2-7. Thirty-minute averaged sample data of soil moisture (a1, a2, a3, and a4) and soil temperatures (b1, b2, b3, and b4) at depths of 10 cm, 25 cm, and 50 cm in one plot each of aspen, conifer, grass and sagebrush during the 2010 water year.

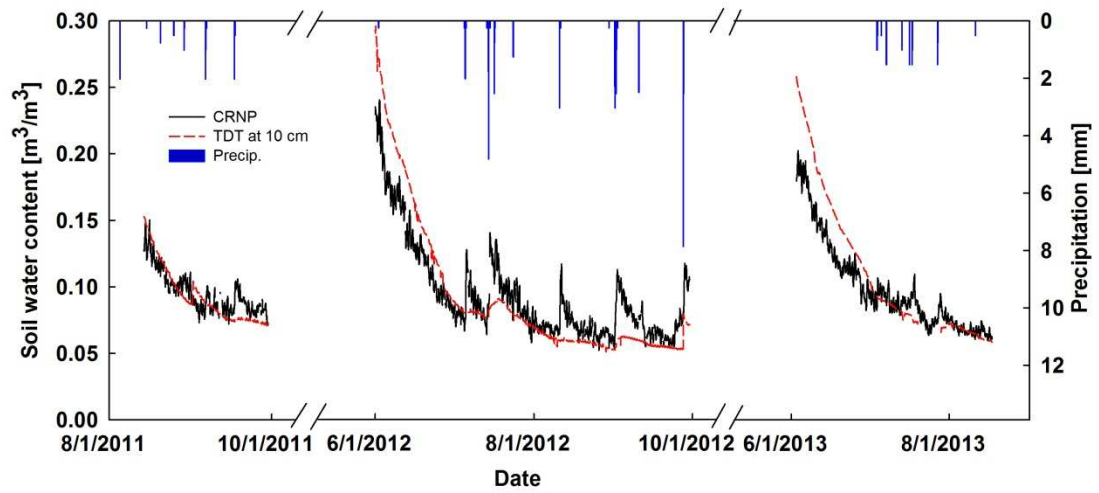


Figure 2-8. Comparison of areal soil moisture measured by the CRNP with aggregate estimates from the TDT-sensor network at the 10 cm depth. Each TDT soil moisture measurements was distance weighted from the CRNP sensor location as described in Chapter 4.

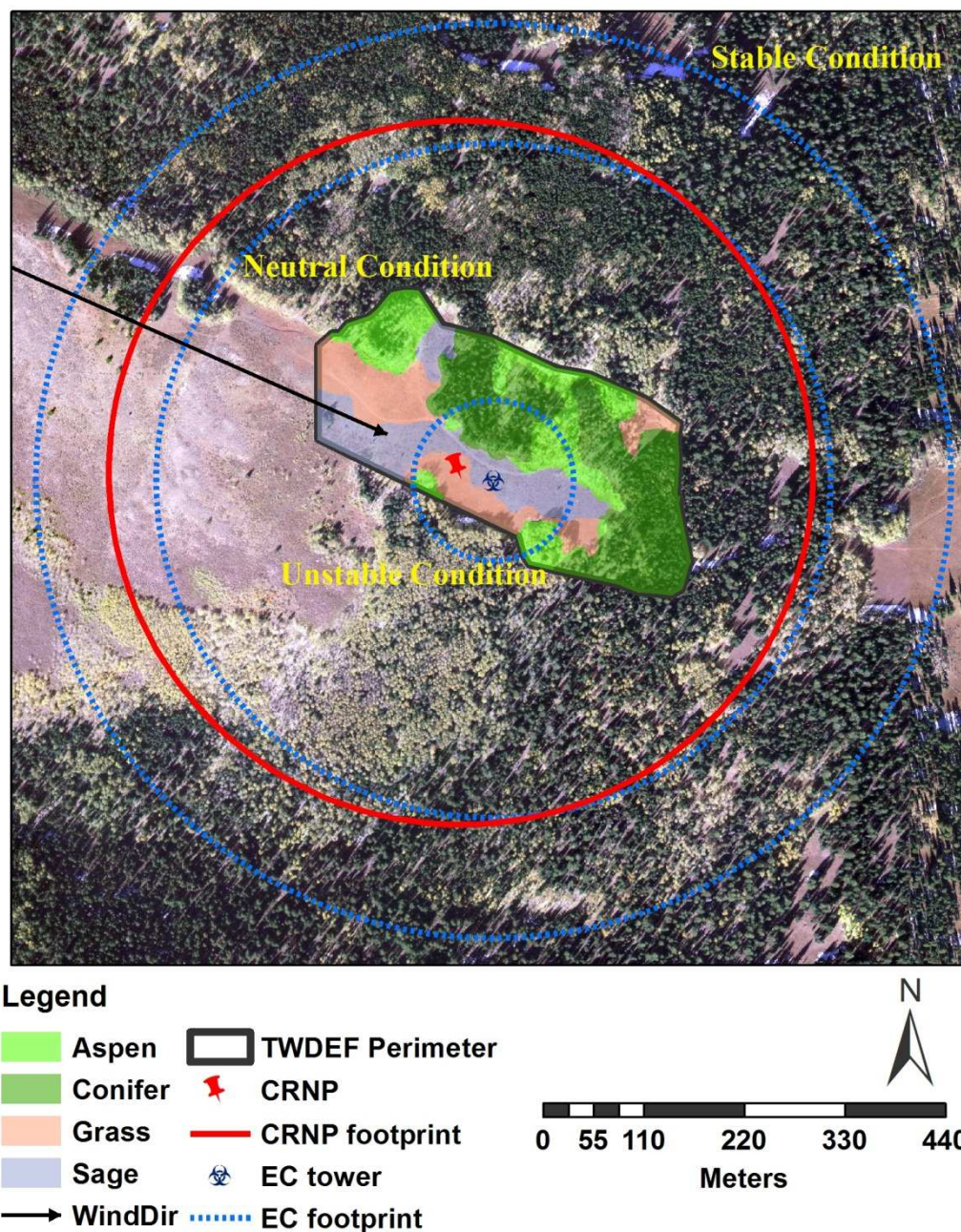


Figure 2-9. Illustration of footprint radius of Eddy covariance (EC) tower at TWDEF site under stable neutral and unstable weather conditions which are 500-, 370-, and 85 m, respectively. The EC footprint is calculation using the Method of Hsieh et al.(2000). Because of the heterogeneous landscape, only area enclosed within the EC footprint with a wind direction between 257° and 330° is considered acceptable data. The summer dominant wind direction is 294° (black arrow line in the graph). The footprint of Cosmic-Ray Neutron Probe (CRNP) is estimated at 385 m at the TWDEF elevation.

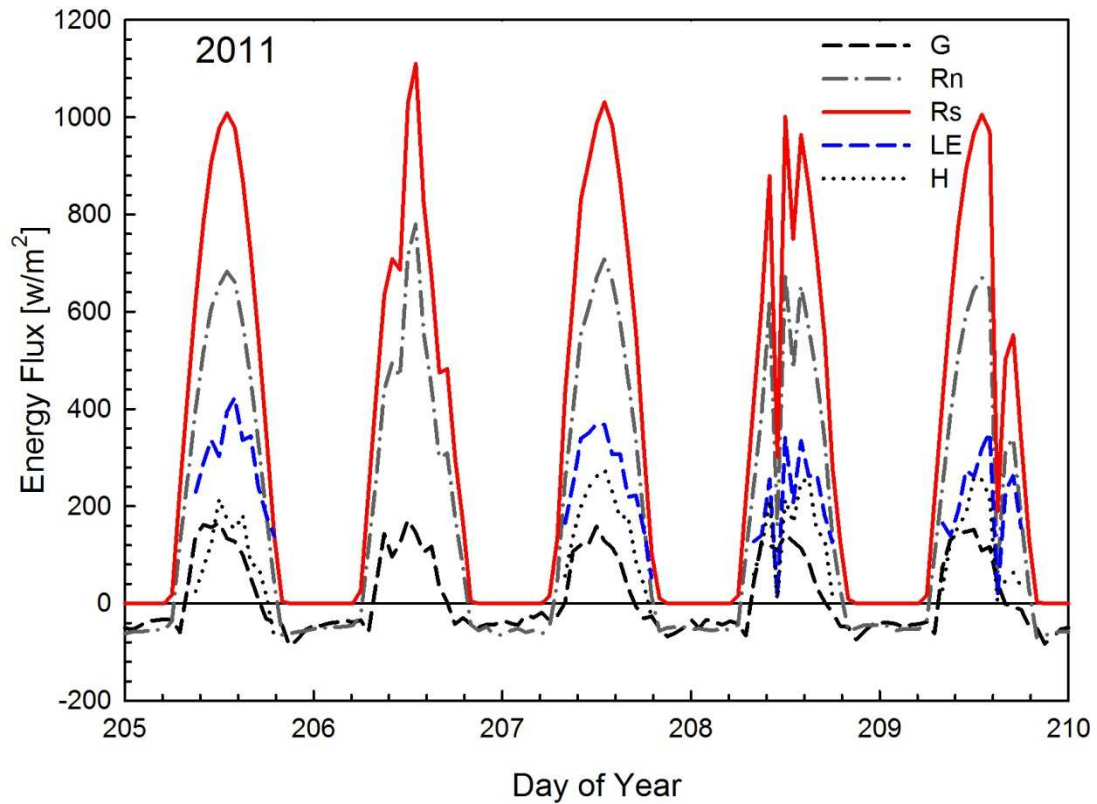


Figure 2-10. Sample eddy covariance measurements exhibiting the hourly energy flux including solar radiation (R_s), net radiation (R_n), soil heat flux (G), latent heat flux (LE), and sensible heat flux (H). The lack of LE and H on day 206 is because the wind direction was out of the acceptable range, i.e., 257° - 330° . The LE and H are estimated after energy balance closure check.

CHAPTER 3
EVAPOTRANSPIRATION IN A SEMI-ARID MOUNTAIN
ECOSYSTEM FROM INTEGRATED NUMERICAL
MODELING AND ENVIRONMENTAL DATA²

Abstract. Summertime evapotranspiration (ET) plays an important role in the annual water yield of montane ecosystems in the Intermountain West (IMW). Vegetation water use for four common species was numerically modeled using Hydrus-1D over four continuous growing seasons (2009 to 2012), informed by a network of soil water content measurements. The model simulated water transport within the soil and water loss from evaporation and transpiration processes. Simulations relied on Richard's equation for unsaturated flow while ET was guided by Feddes' root water uptake and soil evaporation functions. Simulations were compared with temporal dynamics of soil water content measurements at three depths (0.1 m, 0.25 m and 0.5 m) and with eddy covariance ET estimates. The simulations were able to effectively predict soil moisture and water uptake of montane plant communities during summer dry down. Results suggest a given vegetation type exhibited no significant difference (<5%) in ET comparing growing seasons, except where abnormally wet conditions occurred. Mean cumulative growing season ET estimates were 43.00 ± 4.65 , 40.16 ± 2.49 , 28.67 ± 1.88 , 26.14 ± 1.27 , and 28.78 ± 4.09 cm, for aspen, deep rooted conifer, shallow rooted conifer, grass and sage, respectively. A plot of normalized ET versus soil moisture suggested conifer transpiration

² Coauthored by: Ling Lv, Scott B. Jones, Lawrence E. Hipps.

rates fell below potential rates at much higher soil moisture values than aspen, grass and sage.

3.1 Introduction

Mountain ranges of the Intermountain West (IMW) are considered as the major water reservoir for the Western US. Most precipitation in the IMW comes in the form of wet winter storms that move from the Northern Pacific through most of the region, where 50-80% of the streams and rivers are fed by mountain snowpack (Wang and Gillies, 2012). Annual water yield for these mountain ecosystems is regulated by a variety of physical and biological water transfer processes including canopy interception of snow and rain, snowpack sublimation, soil water storage and evaporation and transpiration. The research of LaMalfa et al. (2007; LaMalfa and Ryle, 2006, 2008) revealed that net summertime ET played an important role in the annual water yield in the montane region of Northern Utah. Lacking a detailed understanding of these processes with sparsely distributed observation network data limit our ability to simulate and predict ET process in Western Mountains (Bales et al., 2006).

Techniques developed for direct ET measurements include soil and plant weighing lysimeters (Tian et al., 2011), catchment water budget (Wilson et al., 2001), Bowen ratio (Cellier and Olioso, 1993), and eddy covariance (EC) approaches. The lysimeter records weight changes. It is costly to install and maintain, and are limited to shallow-rooted and short vegetation ecosystems such as grassland. Catchment water budget uses the same dynamics as a lysimeter, but employs a single assessment of annual ET for a watershed and cannot be used at short temporal scales. The Bowen ratio method incorporates energy

budget and turbulent transfer assumptions with measurements of vertical gradients (Leo, 1965). The Bowen ratio neglects net horizontal advection of energy and assumes the vertical transport of heat and water vapor are equal (Angus and Watts, 1984). Under this assumption, the Bowen ratio method requires instruments installed in two different vertical levels above the plant canopy, which requires very accurate measurements (Tomlinson, 1996). Eddy covariance (EC) tower is used to measure and calculate vertical turbulent fluxes within atmospheric boundary layers. It was proven to have high accuracy in direct measurements of water vapor flux for long-term measurements (Goulden et al., 1996), and provides the average ET within its footprint. Complications of this technique is its footprint size changes with time due to wind direction (Shi et al., 2008), which requires the EC tower installed above a uniform terrain when ET measurements need to be taken for specific ecosystems. Moreover, if the land surface becomes decoupled from the atmosphere (e.g., light wind at night), it becomes difficult to interpret the EC measurements (Ivans et al., 2006; Spittlehouse and Black, 1980). In addition, EC instruments are somewhat expensive and expertise is required to analyze the data. Although hundreds of EC towers have been setup around the world, few of them are located in high elevation environments, especially above tree canopies.

A variety of analytical models are available for estimating ET for cases when no direct ET measurements are available. The most widely applied model is the Penman-Monteith (PM) equation. It is driven by observed meteorological data such as solar/net radiation, air temperature, humidity, and wind speed, but requires effects of turbulence and water status to be expressed as aerodynamic resistance and stomatal resistance. The

magnitude of ET estimated through the PM equation depends on not only the climatic conditions but also on the vegetation. The parameter of aerodynamic resistance and canopy resistance in the PM equation must be determined. Since the canopy resistance is difficult to determine, empirical models such as the Priestley-Taylor model are used or mechanistic models such as the Todorovic model, which was developed to enhance the simulation ability of PM equation. Good results with PM equation were obtained in several tree-stands and ecosystems such as Douglas Fir Stands on flat terrain in British Columbia (Black, 1979), Qinghai Spruce (*Picea crassifolia*) Forest of Qilian Mountains in China (Tian et al., 2011), a mixed conifer forest ecosystem in the Sierra Nevada Mountains of the western US (Fisher et al., 2005), a broad-leaf Korean Pine forest of the Changbai Mountains in China (Shi et al., 2008), a shrub ecosystem in Inner Mongolia, a shrub ecosystem in the northwestern Sierra Madre, Wyoming, USA (Wilske et al., 2010), a grassland ecosystem (Stannard, 1993; Sumner and Jacobs, 2005), an aspen forest (Blanken et al., 2001; Hogg et al., 1997) and so on. Reference ET (ET_0) is calculated from the PM equation under the assumption of a sufficiently large and well-watered, short green crop that fully shades ground, as has low stomatal resistance (Allen et al., 1998). The ET_0 is only affected by climatic parameters and does not consider vegetation characteristics and soil factors (e.g., drying soils) that may reduce the actual vegetation ET. In order to account for these factors, additional coefficients such as a vegetation coefficient or a stress coefficient are required to scale ET_0 to actual ET (Spano et al., 2009). Root uptake models assume the plant transpiration is constrained by the root uptake function.

An alternate approach to estimating actual ET through meteorological data and these coefficients is to directly measure soil root zone conditions such as soil matric potential or soil water content within the root zone. In this case a root uptake model (Feddes et al., 2001) can be solved as a sink term in the Richards equation, which is coupled within Soil-Plant-Atmosphere Continuum (SPAC) numerical models. These SPAC models have been used for up-scaling from the field- to the regional- and the global-scales (Feddes and Raats, 2004; Guswa, 2005; Raats, 2007). Some research on ET simulation coupling root water uptake show that these models can help us understand the ET process in natural vegetation and native ecosystems (El Maayar et al., 2009; Jarvis, 2011).

Despite the available ET modeling options, deployment and operation within a high-elevation mountainous location is challenging to operate and maintain as well as to obtain appropriate model input parameters. Considering the aforementioned disadvantages and deficiencies in applying direct measurement techniques in a mountainous area of the IMW as well as the limited availability of appropriate ET model input parameters relevant to our study area, we selected a well-developed, physically-based numerical modeling computer software package, Hydrus-1D (H1D), for simulating dynamics of ET. The simulation software couples a root water uptake model with the Penman-Monteith equation to inversely solve the Richards equation (Simunek et al., 2008). This requires little or no calibration when all required input parameters are experimentally determined (Simunek et al., 2012). More important is the ease with which H1D required input data can be determined. The H1D model has been successfully applied in numerous studies to

simulate ET processes in field and natural conditions (Simunek et al., 2012). The objectives of this study were to: (1) employ environmental data to fit parameters of the numerical model (H1D) and subsequently compare and validate simulations from the coupled PM equation and root water uptake model to estimate evaporation, transpiration and ET within each of the four common semi-arid montane vegetation types (aspen, conifer, grass/forbs and sagebrush); (2) compare and validate the numerically-simulated ET in the sage/grass meadow with measurements of ET from the EC tower, and (3) analyze, present and evaluate the different plant water use strategies to describe montane water demand for each of these vegetation types.

3.2 Theoretical Considerations

The Hydrus-1D (H1D) model (Simunek et al., 2008) was used to simulate the saturated-unsaturated water flow using a mass-lumped linear finite element scheme to numerically solve the one-dimensional Richards equation (Wöhling et al., 2008).

$$\frac{\partial \theta}{\partial t} = \frac{\partial}{\partial t} \left[K(h) \frac{\partial h}{\partial z} + 1 \right] - S \quad (3-1)$$

where, θ is the volumetric water content [cm^3/cm^3]; h is the soil pressure head [cm, negative for unsaturated conditions]; t is time [day]; and z is the spatial coordinate [cm]; positive downward; $K(h)$ is the soil pressure head-dependent unsaturated hydraulic conductivity [cm/day] and S is the sink term, accounting for plant water uptake. The soil water content θ is described using the van Genuchten-Mualen (VGM) model written (Mualem, 1976; van Genuchten, 1980).

$$K(S_e) = K_s S_e^{0.5} \left[1 - \left(1 - S_e^{1/m} \right)^m \right]^2 \quad (3-2)$$

where, S_e is effective saturation, defined as

$$\begin{cases} S_e = \frac{\theta - \theta_r}{\theta_s - \theta_r} = \frac{1}{[1 + |\alpha h|^n]^m}, h < 0 \\ S_e = 1, & h \geq 0 \end{cases} \quad (3-3)$$

and where, θ_r is the residual water content [cm^3/cm^3]; θ_s is the saturated water content [cm^3/cm^3]; K_s is the saturated hydraulic conductivity [cm/day] and α [cm^{-1}], n and m are empirical fitting parameters. The relationship between n and m is described by the assumption that $m = 1 - 1/n$, ($n > 1$). The initial hydraulic parameters were estimated based on the soil texture determined at each of the 12 TWDEF site plots (Olsen and Van Miegroet, 2010) with the Rosetta Lite v. 1.1, which is a module coupled into H1D.

3.2.1 Root Water Uptake

The actual transpiration rate, $T(t)$ is computed by integrating the sink term, $S(h)$, in Eq. 1 over the root zone:

$$T(t) = \int_{L_R}^0 S(h) dz = \int_{L_R}^0 \alpha(h) \cdot b(z) \cdot T_p dz \quad (3-4)$$

where, T is the actual transpiration rate (cm/day). L_R is the root depth (cm). T_p is the potential transpiration rate [cm/day] and $\alpha(h)$ is a reduction coefficient for root water uptake (Feddes et al., 1974, 2001). The reduction coefficients for each vegetation type are shown in Table 3-1. The function $b(z)$ is the normalized root density distribution [cm^{-1}], which was estimated from the 2004 soil pedon survey (Boettinger et al., 2004) and is illustrated in Figure 3-1.

3.2.2 Initial and Boundary Conditions

For the simulation initial conditions, we assumed the soil profiles were saturated with water content and the upper boundary condition (BC) was assumed as an atmospheric BC with surface runoff, with the bottom BC ($z=200$ cm) set as free drainage, suggesting in infinitely deep soil profile. The upper BC required specifying time-dependent precipitation [cm/d], interception [cm/d] and reference ET (ET_0) [cm/d]. The interception (I) of precipitation (P) was calculated as (Schwärzel et al., 2006):

$$I = a \cdot LAI \cdot \left(1 - \frac{1}{1 + \frac{SCF \cdot P}{a \cdot LAI}} \right) \quad (3-5)$$

where, a is an empirical coefficient [cm], LAI is leaf area index, and b is the soil cover fraction, with the term surface cover fraction, $SCF = 1 - \exp(-\kappa LAI)$, where κ is an extinction coefficient (Simunek et al., 2008) (Table 3-2).

To model the time dependence of LAI for Aspen, Grass/forbs and Sagebrush during the growing season, we used a logistic growth function (Yu et al., 2010).

$$LAI(t) = \frac{LAI_0 \cdot LAI_{\max}}{LAI_0 + (LAI_{\max} - LAI_0) \cdot \exp(-bt)} \quad (3-6)$$

where LAI_0 is the value of LAI at the beginning of the growing season ($t=0$), LAI_{\max} is the maximum LAI value, and b is an adjustable parameter. The relationship describing the physiological stages of aspen is given as

$$\sum D = \sum_{d_i}^{d_f} \max(T_a - 5, 0) \quad (3-7)$$

where d is the day of year, d_i and d_f are the initial and final values of d for each aspen physiological period of degree-day accumulation, and T_a is the daily air temperature. We identified d_i for each year when the daily mean soil temperature at the 25-cm depth exceeded $-0.2 \text{ }^\circ\text{C}$.

ET_0 , was calculated from Penman-Monteith equation (Allen et al., 1998), and then was partitioned into reference evaporation (E_0) and reference transpiration (T_0) using Beer's Law (Ritchie, 1972).

$$E_0(t) = ET_0 \cdot (1 - SCF) \quad (3-8)$$

$$T_0(t) = ET_0 \cdot SCF \quad (3-9)$$

3.2.3 Inverse Modeling Procedure

The aim of inverse modeling in our study was to find the optimized VGM soil hydraulic parameters for each monitored soil layer (10 cm, 25 cm and 50 cm) with the objective that the agreement between observed and simulated volumetric soil water contents can be optimized (Caldwell et al., 2013). The parameters are optimized by minimizing the objective function (Šimůnek and Hopmans, 2002) using Marquardt-Levenberg nonlinear minimization method (Marquardt, 1963). The goodness of the agreement is measured by the coefficient of determination (R^2), and root mean square error (RMSE). The closer the R-square is to 1, the more accurate the model parameter estimation is. The smaller the RMSE is, the more accurate the model parameter estimation is. In general, for paired simulations and observations, the simulation can be regarded as a good fit if the R-square is greater than 0.8 (Vrugt et al., 2001).

Šimůnek et al. (1998) found that independent measurement of the θ_r parameter could decrease the uncertainty of the soil hydraulic parameters. In our study, to reduce the number of parameters to be optimized and thus reduce the uncertainty of the parameter estimation, residual water contents for each depth in each subplot were fixed as the difference between mean of the minimum soil water content measurements of the year of 2009, 2010, 2011, and 2012 and two times of its standard deviation. Figure 3-3 shows the mean minimum soil moisture and the corresponding standard deviation of the depth of 10 cm, 25 cm and 50 cm in each subplot. The other four VGM hydraulic parameters (θ_s , α , n , K_s) were fitted in each layer.

3.3 Materials and Methods

3.3.1 Study Area and Experimental Data

The experimental data were collected from the T.W. Daniel Experimental Forest (TWDEF), located within the Bear River Range of the Wasatch Cache National Forest in Northern Utah, USA (41.86° N, 111.50° W). The instrumented part of the forest lies with an area 200 m × 400 m at an elevation of 2600 m (Figure 3-2). The climate is typical of the montane semi-arid IMW with a mid-growing season (July) mean air temperature of 14.4 °C, with an annual mean precipitation of 950 mm yr⁻¹, 80% of which falls as snow (Van Miegroet et al., 2005). The soil in the TWDEF is classified as fine, mixed, superactive typic haplocryalf. The top 50 cm of soil is disturbed by animals such as pocket gophers.

The vegetation cover across the TWDEF forms a patchwork of 4 cover types: aspen, conifer, grass/forbs and sagebrush (Andersen et al., 1980). The average height of aspen stand (*Populus tremuloides*) is 12 m and its understory is dominated by grass/forbs (*rudbeckia occidentalis*, *Bromus carinatus* and *Elymus trachycaulu*). The height of conifer stands is around 10~15 m, consisting primarily of Engelmann spruce (*Picea engelmannii*) or Rocky mountain Fir (*Abies lasiocarpa*), and its understory is predominantly bare ground or needle litter. Grass (dominated by *Bromus carinatus* and *Elymus trachycaulus*) height is around 0.5 m at full canopy. Sagebrush (*Artemisia tridentata*) has an approximate height of 0.8 m. The LAI of conifer was measured using Line Quantum Meter (MQ-301, Apogee) and it was 2.43. Table 3-3 shows the physiological stage of aspen, grass and sage. For grass/forbs and sage, we use the day when snow totally melted as the start day of the growing season and the LAI reached a maximum after 60 days. For aspen, we used the threshold values of cumulative degree days ($\sum D$) based on air temperature to determine the physiological stage. The aspen canopy started to green up at a $\sum D$ of 70 °C days, reached at 90% maximum LAI at $\sum D$ of 220 °C days and reached the end of green-up at $\sum D$ of 300 °C days (Barr et al., 2004). Figure 3-1 showed the layout of the TWDEF site. Three plots for each vegetation type and three subplots (triangles) within each plot were established in 2004, with one automated micrometeorological station (ATM) and two secondary towers for each vegetation type (solid circles). The TWDEF site began to have on-going data collection in 2008. In this study, we focus on the growing season data, which begins each

year with the end of snowmelt through the end of the water year (Sep 30th) in 2009, 2010, 2011 and 2012 (Table 3-4).

A significant part of the monitoring network, includes 108 time domain transmissometry sensors (TDT, Acclima, Inc, Meridian, Idaho, USA), used to estimate soil water content and soil temperature within each subplot. The TDT operation principle employs travel-time analysis for dielectric permittivity analysis, which is described in detail elsewhere (Blonquist et al., 2005; Jones et al., 2005; Robinson et al., 2003). In each of 36 subplots at the TWDEF site, the TDTs were inserted horizontally at depths of 0.10 m, 0.25 m, and 0.50 m by excavation, sieving and removal of larger stones and repacking of the soil profile. The data recording is by standard commercial data loggers (CR1000/CR10X dataloggers, Campbell Scientific, Logan UT, USA), with data telemetry to a storage computer on the USU campus every 30 min. There is one data collection and instrumentation system within each of 12 experimental plots.

Measured parameters at each ATM include air temperature and relative humidity, wind speed, net radiation and precipitation. Since the ATMs in Aspen and Conifer communities were located under the canopies, the measurements from these two towers reflect the understory conditions and are not appropriate for ET estimation of the canopy. For consistency of meteorological observations, measurements from the ATM above the grass/forbs plot with an elevation of 2631 m, was used to represent weather conditions at the TWDEF site. In case of instrument/sensor malfunctioned at the grass/forbs ATM, measurements from the sage ATM at an elevation of 2626 m was used to fill missing values. Year-round precipitation data from the USU Doc Daniel SNOTEL station, which

is just east of the perimeter of fenced study area, was used to validate or fill missing values of precipitation. Because the net radiation depends on vegetation and location, we chose to use solar radiation measurements at the EC tower, whose data were recorded using dataloggers, i.e., models CR3000 and CR10X dataloggers (Campbell Scientific, Logan, UT, USA).

3.3.2 Eddy Covariance Measurement

Instruments: An eddy covariance tower (EC-tower) was installed in the center of TWDEF instrumented site, where the domain vegetation coverage is a mixed grass and sagebrush meadow. The instruments included a CSAT3 three-dimensional sonic anemometer (Campbell Scientific, Inc, Logan, UT, USA) and a Li 7500A open-path water vapor and CO₂ analyzer (Li-Cor, Inc, Lincoln, NE, USA). Sensors were sampled at 20Hz. One-hour average fluxes of sensible and latent heat were calculated from the time series of 3D winds, temperature and water vapor density. Sensors were controlled and recorded with a CR3000X datalogger. Instruments were mounted 2.65 m above ground surface. Solar radiation was measured using NR01 4-way radiometer (HuksefluxUSA, Inc, Manorville, NY, USA) mounted at 3.5 m above the soil surface. Air temperature and relative humidity were measured using HMP 45 (Transcat, Inc, Rochester, NY, USA) mounted 2.5 m above the soil surface. Soil heat flux was determined with Radiation Energy Balance Systems HFT3 heat flux plate (Campbell Scientific, Logan, UT, USA) between 2008 and August 2009. An HFP01 (HuksefluxUSA, Inc, Manorville, NY, USA) has been used since then. The soil heat flux plates were buried at 8 cm and the thermocouples were placed to determine the average soil temperature gradient between the plates and the

surface. Two Hydraprobe II (Stevens Water Monitoring Systems, Inc, Portland, OR, USA) water content sensors were buried at 0.03 m in grass and sage patches and one sensor at 10 cm in the west side of EC tower to measure the soil moisture and soil temperatures in these two layers. Summertime precipitation was measured with a Hach 8-inch diameter tipping bucket rain gauge. The sonic snow depth sensor (Judd Communications LLC, Salt Lake City, UT, USA) was mounted at 3.3 m above the soil surface to measure snow depth and air temperature.

Energy balance closure check: Examining closure of the energy balance is a very useful check on the overall consistency of latent heat flux and sensible heat flux measurements using the eddy covariance method. The energy balance closure is defined as $(H+LE)/(R_n-G)$, where, H is sensible heat flux, LE is latent heat flux, R_n is net radiation, and G is soil heat flux. Perfect measurements would result in a value of 1.0, however, in practice, values are typically lower, in the range of 0.8-0.9 is considered a very good value (Twine et al., 2000). We partitioned the missing energy into LE and H using the measured ratio of H/LE (Angus and Watts, 1984) when H/LE was out of the range of 0.8-0.9. During the nighttime, eddy covariance does not work well (De Bruin and Holtslag, 1982; Law et al., 2000; Stannard, 1993). But since ET value was close to zero at night, we did not include the nighttime (from 1900 MST to 0500 MST next day) EC measurements, comparing only the daily measured ET with the simulated ET by numerical modeling in the grass and sage site.

3.4 Statistical Analysis

To assess annual variability of water use and the effect of vegetation type on water use, the evaporation, transpiration and ET values were regressed on clay content for each vegetation type over 2009, 2010, 2011, and 2012. This study was arranged in a completely randomized design. The PROC MIX function (Ver. 9.3, SAS Inc, Raleigh, NC, USA) was used to analyze the simulated evaporation, transpiration and ET.

3.5 Results and Discussions

3.5.1 Precipitation

The TWDEF experiences hot, dry summers and cold winters, with most of the annual precipitation falling in the form of snow. Intermittent rain events occur in the spring and summer. Figure 3-4 shows the annual precipitation at the TWDEF being 1122.7 mm in the 2009 (2008-2009) water year, 932.2 mm in 2010, 1503.7 mm in 2011 and 835.7 mm in 2012. The snow melt-out date varied with years, vegetation, location, etc. With the deepest snow in water year 2011, snow depletion extended until the beginning of July, 2011. Wind drifted snow deposits in the open areas of the upper slope at the TWDEF instrumented meadow significantly delaying final melt-out (e.g. at the Grass A site) (Meyer et al., 2012). Because of radiation interception within conifer, snow in those plots usually melts later than in the other vegetation.

3.5.2 Soil Moisture and Water Transport Calibration

The H1D numerical model optimizes the van Genuchten soil hydraulic parameters in order to match simulated soil moisture with TDT-measured soil moisture to an acceptable

accuracy ($R^2 \geq 0.8$). Model calibration, or parameter optimization, is an indirect approach for estimating soil hydraulic parameters from soil water transport data. In this study, the observed soil moisture at 3 different depths in each individual vegetation subplot over the 4 growing seasons (water years) of 2009, 2010, 2011, and 2012 was used to calibrate the model by optimizing the van Genuchten hydraulic parameters.

The Figure 3-5 shows simulated and observed soil moisture values at 10 cm, 25 cm, and 50 cm for four vegetation types over three years. Simulated and observed water contents are well matched in most instances, indicating that the model was able to simulate time-series boundary flux, suggesting a good fit between the simulated water contents and observed water content at different depths. Correlations were also developed for simulated and observed soil moisture at 10 cm, 25 cm, and 50 cm for four vegetation types. All r-squared values were above 0.8. The means of correlation and root mean square error (RMSE) values were around 0.95 and $0.005 \text{ m}^3/\text{m}^3$, respectively, indicating a very good fit for model simulations. The optimized hydraulic properties (θ_s , α , n , K_s) including their 95% confidence interval were calculated by the Hydrus-1D for each simulation. Example of soil water retention curve and hydraulic conductivity curve with 95% confidence intervals were shown in Figure 3-6. The smaller confidence intervals were obtained, and the highest uncertainty occurred when the soil is close to saturation.

On Sep 14th, 2011, a Giddings soil hydraulic rig was used to extract soil core samples to 2 m depth where possible, in the vicinity of each plot. High rock content common in areas of the TWDEF site led to varied sample extraction depths (Figure 3-7). Sample length and bore hole depth were compared to account for compaction effect on

soil water content determinations from oven drying. Soil samples were cut into 10 cm sections and placed in labeled containers, then oven dried in the soil physics lab at Utah State University. Volumetric soil moisture was calculated and compared with simulated values on the same day. Variation of soil moisture in space is widely recognized. Both observed and simulated volumetric soil water contents showed increased trends with depth. The absolute difference between observed and averaged simulated soil water contents (mean of 3 subplots) along whole soil profiles varied between $0 \text{ m}^3/\text{m}^3$ and $0.06 \text{ m}^3/\text{m}^3$, indicating the simulated and observed water contents followed a similar trend.

3.5.3 Comparison of Simulated and Measured ET

The availability of eddy covariance estimates of ET within the grass/sage dominated footprint provides a means to compare the simulated values of ET for the grass and sage vegetation plots. The only useful, though not ideal, fetch around the EC-tower is limited to a swath based on wind direction between 257° and 330° passing over grass and sagebrush meadow northwest of the EC instrumental tower. These limitations stem from the height of EC tower, surrounding vegetation and topographical constraints in the instrumented domain. We compared the H1D simulated ET to a processed set of EC-tower estimated ET daily values when possible (Figure 3-8). For example, in the 2009 growing season data, only 10 days could be checked for good daytime ET measurements. The reason for this is the soil heat flux plates and soil moisture sensors failed due to rodent damage, excluding much of the annual data. Based only on a minimum R-squared value of 0.74 in 2012, the model performed reasonably well in simulating ET. The RMSEs were 0.33 mm/day in 2009, 0.59 mm/day in 2010,

0.50 mm/day in 2011, and 0.74 mm/day in 2012. The H1D model slightly underestimated ET compared to the EC-tower measurements. The reason for the ET difference between H1D simulation and EC-tower measurements may result from: (1) the imperfect representation of reality in the H1D model where only 3 soil layers were used in the inverse fitting of soil hydraulic parameters above the 50 cm depth. In the forward simulations, the soil profiles were divided into more than 6 layers in the top 2 m. Additionally, although root branching pattern are genetically determined, environmental factors modify the characteristics of root systems (Johnson and Aguirre, 1991; Zobel, 2011). Therefore, root distribution and density varies considerably in terms of the spatial distribution and among species and even among individuals within a species (Webster, 1978). In our simulation, the root density distribution for each plot was assumed to be static in both space and time. (2) The incompatibility of the horizontal scales for EC instruments: the typical horizontal scale of EC system is 10 m for the net radiation measurement, 0.1 m for the soil heat flux measurement, and 100 m for the latent heat flux and sensible heat flux (Foken, 2008). In our study site, the EC tower was located at the center of the meadow, which was surrounded by tall trees (Figure 3-2). Part of the meadow fell into the shadow of trees due to the change of the solar zenith angle, which resulted from variations in the incident solar radiation and soil heat flux across the footprint of the EC tower. (3) The measurement uncertainty of soil heat flux (G): Several potentially significant errors can occur when using flux plates to measure G, including heat flow distortion near the plate, liquid water and vapor flow divergence and poor contact between the plate and soil matrix (Cobos and Baker, 2003; Sauer et al., 2003).

Soil heat flux measured by soil heat flux plates consisted of two components: The heat flux density through the plate (G_m) and the soil heat storage (S). Studies (Heusinkveld et al., 2004; Sauer et al., 2007) showed that the heat distortion effect of soil heat plates would consistently underestimate G_m by 20% to 25% in dry sand due to heat flow distortion. Novel sensors or correction techniques are required to minimize the heat and water flow distortion. There may also have been potential errors in the soil storage component due to variation in soil moisture content and /or large spatial and temporal heterogeneity in soil heat flux across the study site (Leuning et al., 2012).

Although we have no direct ET measurements for aspen and conifer in our study, compiled ET estimates from studies in similar environments give confidence in our estimates shown in Table 3-5. LaMalfa and Ryle (2008) applied the water balance equation to study the summer water use of aspen and conifer in a high-elevation montane watershed also in the Northern Wasatch Mountains of UT. The results showed that the measured total ET was 451 mm for aspen and 343 mm for conifer in 2006. Among our four-year simulations, the model estimated total ET for was about 430 mm for aspen, 402 mm for the conifer site with root depths extending 110 cm (drC), and ET was 287 mm for the conifer sites with rooting depths less than 65 cm (srC).

3.5.4 Plant Water Use Characteristics

Conifer may transpire on favorable days even in wintertime (Sanna et al., 2006), for example the two-year paired study of (LaMalfa and Ryle, 2008) in aspen and conifer stands showed the total transpiration of conifer was less than 28 mm/yr during spring snow melt prior to aspen leaf flush and in the Fall after aspen leaf senescence. Our

statistical analysis of the simulated ET results shown in Table 3-6 demonstrate that in any year aspen exhibit the highest ET, followed by deep rooted conifer, shallow rooted conifer and sage and grass. This agrees with the results from other studies (Flerchinger et al., 1996; Johnston, 1969; LaMalfa and Ryle, 2008). Aspen and deep rooted conifer have significantly higher ($p < 0.05$) water use than shallow rooted conifer, grass and sage. Conifer with shallow rooting depth showed similar water use compared to grass and sage. The total of ET for the same vegetation varies from one growing seasons to another, but without any significant differences (Table 3-7) except for aspen and sage in the growing season of 2009. Generally for most of the year, TWDEF experiences a wet winter and dry summer, and water from snow melt at the TWDEF site easily recharges the entire soil profile to saturated water content at the beginning of each growing season. Likewise, the vegetation regularly use up most of that water by the end of the growing season each year. An additional note that June 2009 was an abnormally wet month, which may have contributed to significantly higher water use by aspen and sage in 2009 (Wang et al., 2010).

Several observations can be drawn from Figure 3-9 regarding the variations in daily evaporation rates, transpiration rates and ET rates during the four growing seasons studied. First, the start date of transpiration varies from year to year and among species. The spring of 2011 was cool and unusually wet, and the vegetation started actively transpiring much later than in the other three years. By contrast, temperatures in 2012 were record-breakingly high, and the vegetation exhibited earlier start of transpiration compared to the other years (Harris, 2012). The transpiration rates and ET rates of aspen,

grass, and sage showed a parabola-shaped variation, where the highest ET rates for the aspen, grass and sage occurred after leaf flush each year. Conifer employed a different water use strategy where the initial rise in water use was less than Aspen and transpiration rates diminished during the remainder of the growing season. The transpiration pattern of conifer can be explained by the nearly constant LAI and the seasonal soil moisture depletion, which essentially is consistent with the precipitation characteristics in the IMW. Precipitation in the IMW exhibits a cold season regime from the wettest month of May to the driest month of July (Wang et al., 2009). Soil evaporation rate throughout the growing seasons is low, and ranges from 0 to 4 mm/day (Figure 3-9). For aspen, grass and sage, the variations of soil evaporation rate and transpiration rate are antipodal due to the canopy development and soil moisture decline (Or et al., 2013). The average soil evaporation rate under the conifer canopy was approximately 0.67 mm/day, and exhibited a nearly constant trend throughout the study period.

3.5.5 ET and Soil Moisture

Soil moisture is the key variable which synthesizes the atmosphere forcing, vegetation response and surface evaporation through ET. In a water-limited condition, ET undergoes a transition from near potential rates toward a state of water stress where rates are significantly reduced as seen in Figure 3-9. To study the water stress, we quantified the relationship between daily-integrated ET rate and soil moisture in the near surface for the four vegetation communities. The daily-integrated ET rates were normalized by the associated reference ET values, which were simulated in the numerical model using the

Penman-Monteith equation. The actual soil moisture dynamics were measured at the 10 cm depth using the TDT sensors.

Figure 3-10 shows normalized ET rates from the aspen, conifer, grass and sage. The aspen, grass and sage transpired at potential rates during each study year until a repeatable soil moisture threshold was reached. The soil moisture thresholds were approximately $0.25 \text{ m}^3/\text{m}^3$ for aspen and $0.1 \text{ m}^3/\text{m}^3$ for both grass and sage. Below these thresholds daily ET rates of grass and sage dropped precipitously and approached zero. The daily ET rate of aspen was 90% of reference ET when soil moisture reached $0.25 \text{ m}^3/\text{m}^3$, and it declined precipitously and approached zero when soil moisture was below a second threshold, $0.12 \text{ m}^3/\text{m}^3$. In comparison, conifer exhibited a nearly continuously decreasing pattern with soil moisture reduction. In other words, conifer exhibited more sensitivity to soil moisture than the other vegetation types, especially when it had a shallow rooted system. Research on the physiological response of plants to drying soil and subsequent water stress has grouped plant behaviors as isohydric (having tight stomatal control and a minimum threshold of water potential that cause stomata to close) and anisohydric (having loose stomatal control and no discernable threshold of water potential maintenance) (Tardieu and Simonneau, 1998). Conifer exhibited an isohydric behavior. In contrast, aspen, grass and sage showed an anisohydric behavior, which does not depend on soil moisture status until plants were stressed (Tardieu and Simonneau, 1998). The same behavior was also observed in other studies (Pataki et al., 2000; Ponton et al., 2006).

3.6 Conclusions

The focus of this paper was on ET estimation in four common vegetation types found in Montane ecosystems of the IMW. The approach employed the Hydrus-1D numerical model, which employed conventional meteorological data and additional measurements of soil moisture as inputs. The goodness of hydraulic parameter inverse fitting was evaluated by TDT measured soil moisture at depths of -10 cm, -25 cm, and -50 cm in addition to independent soil moisture profile comparisons. The modeled ET values in the study area for the growing seasons of 2009, 2010, 2011, and 2012 were consistent with the directly measured ET by the eddy covariance system and with studies carried out in similar ecosystems. The consistency implies that the numerically simulated estimates show potential as a method to estimate ET in high elevation mountainous areas yielding high temporal resolution, depending on the availability of monitoring sites.

Our modeled results found that for each growing season, the aspen showed significantly higher total ET than grass and sage, followed by the deep rooted conifer. For the same vegetation type, the total ET had no significant difference among growing seasons except for deviations during an abnormally wet growing season. The mean ET rates were 4.1 mm/day, 3.9 mm/day, 2.6 mm/day, 2.3 mm/day and 2.3 mm/day for aspen, deep root conifer, shallow root conifer, and grass and sage, respectively. Regardless of the differential snowpack accumulation, the growing-season ET removed at least 50.8%, 42.5%, 32.8% and 33.3% of the total annual precipitation for aspen, conifer, grass, and sage, respectively, for the driest year of 2012, compared to 30.3%, 23.1%, 16.9% and 17.7%, respectively, of total precipitation for the wettest year of 2011.

By comparing the relative ET with diminishing soil moisture we concluded that conifer showed more sensitivity to soil moisture than the other vegetation types. Aspen, grass and sage roots ceased water uptake from the soil when soil moisture dropped below about $0.1 \text{ m}^3/\text{m}^3$ at the 10 cm depth, while conifer, on the other hand, was able to continue to transpire at low rates under very dry conditions.

References

- Allen, R.G., Pereira, L.S., Raes, D., Smith, M., 1998. Crop evapotranspiration - Guidelines for computing crop water requirements-FAO Irrigation and drainage paper 56. FAO - Food and Agriculture Organization of the United Nations, Rome.
- Andersen, D.C., MacMahon, J.A., Wolfe, M.L., 1980. Herbivorous Mammals along a Montane Sere: Community Structure and Energetics. *J. Mammal.* 61(3): 500-519.
- Angus, D.E., Watts, P.J., 1984. Evapotranspiration — How good is the Bowen ratio method? *Agric. Water Manage.* 8(1-3): 133-150.
- Bales, R.C., Molotch, N.P., Painter, T.H., Bettinger, M.D., Rice, R., Dozier, J., 2006. Mountain hydrology of the western United States. *Water Resour. Res.* 42(8).
- Barr, A.G., Black, T.A., Hogg, E.H., Kljun, N., Morgenstern, K., Nesic, Z., 2004. Inter-annual variability in the leaf area index of a boreal aspen-hazelnut forest in relation to net ecosystem production. *Agric. For. Meteorol.* 126(3-4): 237-255.
- Betts, A.K., Ball, J.H., 1997. Albedo over the boreal forest. *J. Geophys. Res. D: Atmos.* 102(D24): 28901-28909.
- Black, T.A., 1979. Evapotranspiration from Douglas fir stands exposed to soil water deficits. *Water Resour. Res.* 15(1): 164-170.
- Black, T.A., Chen, J.-M., Lee, X., Sagar, R.M., 1991. Characteristics of shortwave and longwave irradiances under a Douglas-fir forest stand. *Can. J. For. Res.* 21(7): 1020-1028.
- Blanken, P.D., Black, T.A., Neumann, H.H., den Hartog, G., Yang, P.C., Nesic, Z., Lee, X., 2001. The seasonal water and energy exchange above and within a boreal aspen forest. *J. Hydrol.* 245(1-4): 118-136.
- Blonquist, J.M.J., Jones, S.B., Robinson, D.A., 2005. Standardizing characterization of electromagnetic water content sensors. *Vadose Zone J.* 4(4): 1059-1069.

- Boettinger, J.L., Lawley, J.R., Van Miegroet, H., 2004. Morphology of soils in the aspen, conifer, grass/forbs, and sagebrush environmental monitoring sites, TW Daniel Experimental Forest, Logan, UT.
- Brantley, S.T., Young, D.R., 2007. Leaf-area index and light attenuation in rapidly expanding shrub thickets. *Ecology* 88(2): 524-530.
- Caldwell, T.G., Wöhling, T., Young, M.H., Boyle, D.P., McDonald, E.V., 2013. Characterizing Disturbed Desert Soils Using Multiobjective Parameter Optimization. *Vadose Zone J.* 12(1), 1-23, doi: 10.2136/vzj2012.0083.
- Cellier, P., Olioso, A., 1993. A simple system for automated long-term Bowen ratio measurement. *Agric. For. Meteorol.* 66(1-2): 81-92.
- Clark, P.E., Seyfried, M.S., 2001. Point Sampling for Leaf Area Index in Sagebrush Steppe Communities. *J. Range Manage.* 54(5): 589-594.
- Cobos, D.R., Baker, J.M., 2003. In Situ measurement of soil heat flux with the gradient method. *Vadose Zone J.* 2, 589-594.
- Chen, J.M., Blanken, P.D., Black, T.A., Guilbeault, M., Chen, S., 1997. Radiation regime and canopy architecture in a boreal aspen forest. *Agric. For. Meteorol.* 86(1-2): 107-125.
- De Bruin, H.A.R., Holtslag, A.A.M., 1982. A Simple Parameterization of the Surface Fluxes of Sensible and Latent Heat During Daytime Compared with the Penman-Monteith Concept. *J. Appl. Meteorol.* 21(11): 1610-1621.
- El Maayar, M., Price, D.T., Chen, J.M., 2009. Simulating daily, monthly and annual water balances in a land surface model using alternative root water uptake schemes. *Adv. Water Resour.* 32(9): 1444-1459.
- Feddes, R.A., Brester, E., P., N.S., 1974. Field Test of a Modified Numerical Model for Water Uptake by Root Systems. *Water Resour. Res.* 10(6): 1199-1206.
- Feddes, R.A., Hoff, H., Bruen, M., Dawson, T., Rosnay, P. de, Dirmeyer, P. Jockson, R.B., Kabat, P. Kleidon, A., Lilly, A., Pitman, A., 2001. Modeling root water uptake in hydrological and climate models. *Bull. Am. Meteorol. Soc.* 82(12): 2797-2809.
- Feddes, R.A., Raats, P.A.C., 2004. Parameterizing the soil - water - plant root system. In: Workshop (Editor), *Unsaturated-zone modeling; progress, challenges and applications*, pp. 95-141.

- Fisher, J.B., DeBiase, T.A., Qi, Y., Xu, M., Goldstein, A.H., 2005. Evapotranspiration models compared on a Sierra Nevada forest ecosystem. *Environ. Modell. Softw.* 20(6): 783-796.
- Flerchinger, G.N., Hanson, C.L., Wight, J.R., 1996. Modeling evapotranspiration and surface energy budgets across a watershed. *Water resour. Res.* 32(8): 2539-2548.
- Foken, T., 2008. The energy balance closure problem: an overview. *Ecol. Appl.* 18(6): 1351-1367.
- Gifford, G.F., Humphries, W., Jaynes, R.A., 1984. A preliminary quantification of the impacts of aspen to conifer succession on water yield- II. modeling results. *J. Am. Water Resour. Assoc.* 20(2): 181-186.
- Goulden, M.L., Munger, J.W., Fan, S.M., Daube, B.C., Wofsy, S.C., 1996. Measurements of carbon sequestration by long-term eddy covariance: methods and a critical evaluation of accuracy. *Glob. Change Biol.* 2: 169-182.
- Guswa, A.J., 2005. Soil-moisture limits on plant uptake: An upscaled relationship for water-limited ecosystems. *Adv. Water Resour.* 28(6): 543-552.
- Harris, L., 2012. Modeling our climate's future, Utah Science. Utah Agricultural Experiment Station, Utah State University, Logan, Utah pp. 3-5.
- Havranek, W., Benecke, U., 1978. The influence of soil moisture on water potential, transpiration and photosynthesis of conifer seedlings. *Plant Soil*, 49(1): 91-103.
- Heusinkveld, B.G., Jacobs, A.F.G., Holtslag, A.A.M., Berkowicz, S.M., 2004. Surface energy balance closure in an arid region: role of soil heat flux. *Agric. For. Meteorol.* 122(1-2): 21-37.
- Hogg, E.H., Black, T.A., Hartog, G., Neumann, H.H., Zimmermann, R., Hurdle, P.A., Blanken, P.D., Nesic, Z., Yang, P.C., Staebler, R.M., McDonald, K.C., Oren, R., 1997. A comparison of sap flow and eddy fluxes of water vapor from a boreal deciduous forest. *J. Geophys. Res.* 102(24): 28,929-28,937.
- Hsieh, C.I., Katul, G., Chi, T.W., 2000. An approximate analytical model for footprint estimation of scalar fluxes in thermally stratified atmospheric flows. *Adv. Water Res.*, 23(7): 765-772.
- Evans, S., Hipps, L., Leffler, A.J., Evans, C.Y., 2006. Response of water vapor and CO₂ fluxes in semiarid lands to seasonal and intermittent precipitation pulses. *J. Hydrometeorol.* 7(5): 995-1010.

- Jarvis, N.J., 2011. Simple physics-based models of compensatory plant water uptake: concepts and eco-hydrological consequences. *Hydrol. Earth Syst. Sci. Discuss.* 8: 6789-6831.
- Johnson, D.A., Aguirre, L., 1991. Effect of water on morphological development in seedlings of three range grasses: root branching patterns. *J. Range Manage.* 44(4): 355-360.
- Johnston, R., 1969. Soil moisture depletion and estimated evapotranspiration on Utah mountain watersheds. *USDA For. Service Res. Paper* 67: 1-13.
- Johnston, R.S., 1970. Evapotranspiration from bare, herbaceous, and aspen plots: A check on a former study. *Water Resour. Res.* 6(1): 324-327.
- Jones, S.B., Blonquist, J.M., Robinson, D.A., Rasmussen, V.P., Or, D., 2005. Standardizing characterization of electromagnetic water content sensors. *Vadose Zone J.* 4(4): 1048-1058.
- Kelliher, F.M., Leuning, R., Schulze, E.D., 1993. Evaporation and canopy characteristics of coniferous forests and grasslands. *Oecologia* 95(2): 153-163.
- Kiniry, J., Johnson, M.-V., Mitchell, R., Vogel, K., Kaiser, J., Bruckerhoff, S. Cordsiemon, R., 2011. Switchgrass leaf area index and Light Extinction Coefficients. *Agron. J.* 103(1): 119-122.
- Kolb, K.J., Sperry, J.S., 1999. Transport constraints on water use by the Great Basin shrub, *Artemisia tridentata*. *Plant Cell Environ.* 22(8): 925-935.
- LaMalfa, E., Leffler, A.J., Ryle, R., 2007. Differential snowpack accumulation and soil water dynamics in aspen and conifer communities: implications for water yield. In: B. McGurk, R. Decker and G. Freeman (Editors), *Western snow conference*, Kailua-Kona, Hawaii, pp. 117-174.
- LaMalfa, E., Ryle, R., 2006. Differences in water balance between aspen and conifer communities: the fate of spring snow melt in a northern rocky mountain watershed. In: R. Julander and M. Bruce (Editors), *Western Snow Conference*, Las Cruces, New Mexico, pp. 17-27.
- LaMalfa, E., Ryle, R., 2008. Differential snowpack accumulation and water dynamics in aspen and conifer communities: implications for water yield and ecosystem function. *Ecosystems* 11(4): 569-581.
- Law, B.E., Williams, M., Anthoni, P.M., Baldocchi, D.D., Unsworth, M.H., 2000. Measuring and modelling seasonal variation of carbon dioxide and water vapour exchange of a *Pinus ponderosa* forest subject to soil water deficit. *Global Change Biol.* 6(6): 613-630.

- Lecain, D.R., Morgan, J.A., Schuman, G.E., Reeder, J.D., Hart, R.H., 2000. Carbon Exchange Rates in Grazed and Ungrazed Pastures of Wyoming. *J. Range Manage.* 53(2): 199-206.
- Leo, J.F., 1965. Accuracy of Evapotranspiration determinations by the bowen ration method. *Int. Assoc. Sci. Hydrol.: Bull.* 10(2): 38-48.
- Leuning, R., van Gorsel, E., Massman, W.J., Isaac, P.R., 2012. Reflections on the surface energy imbalance problem. *Agric. For. Meteorol.* 156(0): 65-74.
- Marquardt, D.W., 1963. An algorithm for least-squares estimation of nonlinear parameters. *J. Soc. Ind. Appl. Math.* 11(2): 431-441.
- Meyer, J.D.D., Jin, J., Wang, S.-Y., 2012. Systematic Patterns of the Inconsistency between Snow Water Equivalent and Accumulated Precipitation as Reported by the Snowpack Telemetry Network. *J. Hydrometeorol.* 13(6): 1970-1976.
- Mualem, Y., 1976. A new model for predicting the hydraulic conductivity of unsaturated porous media. *Water Resour. Res.*, 12(3): 513-522.
- Olsen, H.R., Van Miegroet, H., 2010. Factors affecting carbon dioxide release from forest and rangeland soils in Northern Utah. *Soil Sci. Soc. Am. J.*, 74(1): 282-291.
- Or, D., Lehmann, P., Shahraeeni, E., Shokri, N., 2013. Advances in Soil Evaporation Physics—A Review. *Vadose Zone J.* 12(4), doi: 10.2136/vzj2012.0163.
- Pataki, D.E., Oren, R., Smith, W.K., 2000. Sap flux of co-occurring species in a Western subalpine forest during seasonal soil drought. *Ecology* 81(9): 2557-2566.
- Ponton, S., Flanagan, L.B., Alstad, K.P., Johnson, B.G., Morgenstern, K., Kljun, N., Black, T.A., Barr, A.G., 2006. Comparison of ecosystem water-use efficiency among Douglas-fir forest, aspen forest and grassland using eddy covariance and carbon isotope techniques. *Global Change Biol.* 12(2): 294-310.
- Raats, P., 2007. Uptake of water from soils by plant roots. *Transp. Porous Med.* 68(1): 5-28, doi: 10.1007/s11242-006-9055-6.
- Ritchie, J.T., 1972. Model for predicting evaporation from a row crop with incomplete cover. *Water Resour. Res.* 8(5): 1204-1213.
- Robinson, D.A., Jones, S.B., Wraith, J.M., Or, D., Friedman, S.P., 2003. A review of advances in dielectric and electrical conductivity measurement in soils using time domain reflectometry. *Vadose Zone J.* 2(4): 444-475.
- Running, S.W., 1976. Environmental control of leaf water conductance in conifers. *Can. J. For. Res.* 6(1): 104-112.

- Ryel, R., Caldwell, M., Yoder, C., Or, D., Leffler, A., 2002. Hydraulic redistribution in a stand of *Artemisia tridentata*: evaluation of benefits to transpiration assessed with a simulation model. *Oecologia* 130(2): 173-184.
- Ryel, R.J., Leffler, A.J., Ivans, C., Peek, M.S., Caldwell, M.M., 2010. Functional differences in water-use patterns of contrasting life forms in Great Basin Steppelands. *Vadose Zone J.* 9(3): 548-560.
- Sanna, S., Suni, T., Pumpanen, J., Gronholm T., Kolari P., Nikinmaa, E., Hari, P., Vesala, T., 2006. Wintertime photosynthesis and water uptake in a boreal forest. *Tree Physiol.* 26(6): 749-757.
- Sauer, T.J., Meek, D.W., Ochsner, T.E., Harris, A.R., Horton, R., 2003. Errors in heat flux measurement by flux plates of contrasting design and thermal conductivity. *Vadose Zone J.* 2, 580-588, doi: 10.2136/vzj2003.5800.
- Sauer, T.J., Ochsner, T.E., Horton, R., 2007. Soil heat flux plates. *Agron. J.*, 99(1): 304-310.
- Schwärzel, K., Šimůnek, J., van Genuchten, M.T., Wessolek, G., 2006. Measurement and modeling of soil-water dynamics and evapotranspiration of drained peatland soils. *J. Plant Nutr. Soil Sci.* 169(6): 762-774.
- Shi, T., Guan, D., Wang, A., Wu, J., Jin, C., Han, S., 2008. Comparison of three models to estimate evapotranspiration for a temperate mixed forest. *Hydrol. Processes* 22(17): 3431-3443.
- Šimůnek, J., Hopmans, J.W., 2002. Parameter Optimization and Nonlinear Fitting. In: J.H. Dane and G.C. Topp (Ed.), *Methods of Soil Analysis, Part 4, Physical methods*. SSSA, Madison, WI, pp. 139-157.
- Simunek, J., Sejna, M., Saito, H., Sakai, M., van Genuchten, M.T., 2008. The HYDRUS-1D software package for simulating the one-dimensional movement of water, heat, and multiple solutes in Variably-saturated Media. Department of environmental sciences university of California riverside, California.
- Simunek, J., van Genuchten, M.T., Sejna, M., 2012. HYDRUS: model use, calibration and validation. Special issue on Standard/Engineering Procedures for Model Calibration and Validation, *Trans. ASABE* 55(4): 1261-1274.
- Šimůnek, J., van Genuchten, M.T., Wendroth, O., 1998. Parameter Estimation Analysis of the Evaporation Method for Determining Soil Hydraulic Properties. *Soil Sci. Soc. Am. J.* 62(4): 894-905.
- Spano, D., Snyder, R.L., Sirca, C., Duce, P., 2009. ECOWAT—A model for ecosystem evapotranspiration estimation. *Agric. For. Meteorol.* 149(10): 1584-1596.

- Spittlehouse, D.L., Black, T.A., 1980. Evaluation of the Bowen ratio/energy balance method for determining forest evapotranspiration. *Atmos. Ocean* 18(2): 98-116.
- Stannard, D.I., 1993. Comparison of Penman-Monteith, Shuttleworth-Wallace, and Modified Priestley-Taylor Evapotranspiration Models for wildland vegetation in semiarid rangeland. *Water Resour. Res.* 29(5): 1379-1392.
- Sumner, D.M., Jacobs, J.M., 2005. Utility of Penman-Monteith, Priestley-Taylor, reference evapotranspiration, and pan evaporation methods to estimate pasture evapotranspiration. *J. Hydrol.* 308(1-4): 81-104.
- Tardieu, F., Simonneau, T., 1998. Variability among species of stomatal control under fluctuating soil water status and evaporative demand: modelling isohydric and anisohydric behaviours. *J. Exp. Bot.* 49(Special Issue): 419-432.
- Taylor, S.T., Ashcroft, G.L., 1972. *Physical edaphology: the physics of irrigated and nonirrigated soils.* W.H. Freeman (Ed.), San Francisco, California.
- Tian, F.X., Zhao, C.Y., Feng, Z.D., 2011. Simulating evapotranspiration of Qinghai spruce (*Picea crassifolia*) forest in the Qilian Mountains, northwestern China. *J. Arid. Environ.* 75(7): 648-655.
- Tomlinson, S.A., 1996. Comparison of Bowen-ratios, eddy correlation, and weighing lysimeter evapotranspiration for two sparse canopy sites in eastern Washington. In: U.S. Geological Survey. *Water-Resources Investigations Report 96-4081*, Tacoma, WA.
- Twine, T.E., Kustas, W.P., Norman, J.M., Cook, D.R., Houser, P.R., Meyers, T.P., Prueger, J.H., Starks, P.J., Wesely, M.L., 2000. Correcting eddy-covariance flux underestimates over a grassland. *Agric. For. Meteorol.* 103(3): 279-300.
- van Genuchten, M.T., 1980. A Closed-form Equation for Predicting the Hydraulic Conductivity of Unsaturated Soils. *Soil Sci. Soc. Am. J.* 44(5): 892-898.
- Van Miegroet, H., Boettinger, J.L., Baker, M.A., Nielsen, J., Evans, D., Stum, A., 2005. Soil carbon distribution and quality in a montane rangeland-forest mosaic in northern Utah. *For. Ecol. Manage.* 220(1-3): 284-299.
- Vrugt, J.A., Hopmans, J.W., Šimunek, J., 2001. Calibration of a Two-Dimensional Root Water Uptake Model. *Soil Sci. Soc. Am. J.* 65(4): 1027-1037.
- Wang, S.-Y., Gillies, R., 2012. *Climatology of the U.S. Inter-Mountain West, Modern Climatology*, Dr Shih-Yu Wang (Ed.), ISBN: 978-953-51-0095-9, In Tech, Available from: <http://www.intechopen.com/books/modern-climatology/climatology-of-the-u-s-intermountain-west>.

- Wang, S.-Y., Gillies, R.R., Jin, J., Hipps, L.E., 2009. Recent rainfall cycle in the Intermountain Region as a quadrature amplitude modulation from the Pacific decadal oscillation. *Geophys. Res. Lett.* 36(2): L02705.
- Wang, S.-Y., Hipps, L., Gillies, R., Jiang, X., Moller, A., 2010. Circumglobal teleconnection and early summer rainfall in the US Intermountain West. *Theor. Appl. Climatol.* 102(3): 245-252.
- Webster, C.C., 1978. Plant Root Systems: Their Function and Interaction with the Soil. *Exp. Agric.* 14(03): 291-291.
- Wilske, B., Kwon, H., Wei, L., Chen, S., Lu, N., Lin, G., Xie, J., Guan, W., Pendall, E., Ewers, B.E., Chen, J., 2010. Evapotranspiration (ET) and regulating mechanisms in two semiarid *Artemisia*-dominated shrub steppes at opposite sides of the globe. *J. Arid. Environ.* 74(11): 1461-1470.
- Wilson, K.B., Hanson, P.J., Mulholland, P.J., Baldocchi, D.D., Wullschleger, S.D., 2001. A comparison of methods for determining forest evapotranspiration and its components: sap-flow, soil water budget, eddy covariance and catchment water balance. *Agric. For. Meteorol.* 106(2): 153-168.
- Wöhling, T., Vrugt, J.A., Barkle, G.F., 2008. Comparison of Three Multiobjective Optimization Algorithms for Inverse Modeling of Vadose Zone. *Soil Sci. Soc. Am. J.* 72(2): 305-319.
- Yu, Z., Lü, H., Zhu, Y., Drake, S., Liang, C., 2010. Long-term effects of revegetation on soil hydrological processes in vegetation-stabilized desert ecosystems. *Hydrol. Processes* 24(1): 87-95.
- Zobel, R.W., 2011. A Developmental Genetic Basis for Defining Root Classes. *Crop Sci.* 51(4): 1410-1413.

Table 3-1. Feddes Parameters defining root water uptake reduction coefficient, $\alpha(h)$ for studied vegetation types (Havranek and Benecke, 1978; Kelliher et al., 1993; Kolb and Sperry, 1999; Running, 1976; Ryel et al., 2002; Ryel et al., 2010; Taylor and Ashcroft, 1972)

| Vegetation | h1 [cm] | h2 [cm] | h3h [cm] | h3l [cm] | h4 [cm] | T _{Plow} [cm/d] | T _{Phigh} [cm/d] |
|-------------|---------|---------|----------|----------|---------|-----------------------------|------------------------------|
| Aspen | 0 | 0 | -330 | -2000 | -15000 | 0.5 | 0.1 |
| Conifer | 0 | 0 | -5100 | -12800 | -21500 | 0.5 | 0.1 |
| Grass/forbs | 0 | 0 | -300 | -1000 | -15000 | 0.5 | 0.1 |
| sagebrush | 0 | 0 | -400 | -5100 | -33000 | 0.95 | 0.1 |

Table 3-2. Albedos and extinction coefficients of TWDEF plants types (Betts and Ball, 1997; Black et al., 1991; Brantley and Young, 2007; Chen et al., 1997; Kiniry et al., 2011)

| Parameters | Aspen | Conifer | Grass | Sagebrush |
|------------------------|-------|---------|-------|-----------|
| albedo | 0.15 | 0.13 | 0.21 | 0.18 |
| Extinction coefficient | 0.42 | 0.52 | 0.38 | 0.52 |

Table 3-3. Vegetation physiological stages for plant types at the TWDEF. The LAI₀ and LAI_{max} were from previous studies (Barr et al., 2004; Clark and Seyfried, 2001; Gifford et al., 1984; Lecain et al., 2000)

| | | Date of the vegetation phonological stages | | | LAI ₀ | LAI _{max} * |
|-------------|------|--|---------------------------|--------------------|------------------|----------------------|
| | | Green up | 90% of LAI _{max} | LAI _{max} | | |
| Aspen | 2009 | May-29 | Jul-3 | Jul-12 | 0.01 | 5.6 |
| | 2010 | Jun-24 | Jul-9 | Jul-17 | | |
| | 2011 | Jun-24 | Jul-10 | Jul-18 | | |
| | 2012 | Jun-01 | Jun-24 | Jul-1 | | |
| Grass/Forbs | 2009 | Jun-05/Jun-16 | Jul-20/Jul-31 | Aug-01/Aug-15 | 0.01 | 2.3 |
| | 2010 | Jun-14 | Jul-29 | Aug-13 | | |
| | 2011 | Jul-09 | Aug-23 | Sep-07 | | |
| | 2012 | May-15/Jun-01 | Jul-01/Jul-15 | Jul-14/Jul-31 | | |
| Sage | 2009 | May-25 | Jul-09 | Jul-24 | 0.01 | 2.3 |
| | 2010 | Jun-14 | Jul-29 | Aug-13 | | |
| | 2011 | Jul-09 | Aug-23 | Sep-07 | | |
| | 2012 | May-15/Jun-01 | Jul-01/Jul-15 | Jul-14/Jul-31 | | |

* LAI_{max} is the total LAI of overstory and understory.

Table 3-4. The snow ablation date for different vegetation sites in water year of 2009, 2010, 2011, and 2012. Drifted and accumulated snow generally builds up on grass A and sage A plots resulting in later snowmelt compared to grass and sage plots

| | 2009 | 2010 | 2011 | 2012 |
|-------------|-----------------|--------|-----------------|---------------|
| Aspen | Jun-01 | Jun-14 | Jun-28 | Jun-01 |
| Conifer | Jun-12 | Jun-27 | Jul-06 | Jun-01 |
| Grass/Forbs | Jun -05/ Jun-16 | Jun-14 | Jun -28/ Jul-09 | May-15/May-30 |
| Sagebrush | May-25 | Jun-01 | Jun-28/ Jul-09 | May-15/May-30 |

Table 3-5. The total ET (averaged from 4-year simulation) of aspen and conifer as compiled from the literature

| Site | Lat (°) | Lon. (°) | h [#] (m) | Averaged total ET(cm) | | Citation |
|------------------------|---------|----------|--------------------|-----------------------|--|----------------------------|
| | | | | Aspen | Conifer | |
| Reynolds creek | 43.20 | -116.75 | 1840-2036 | 45.60 | | (Flerchinger et al., 1996) |
| Bear river mountain | 41.34 | -111.43 | 2515 | 45.10 | 34.30 | (LaMalfa and Ryle, 2008) |
| Northern Utah mountain | | | 2750 | 40.1±0.74 | 33.00±0.23 | (Johnston, 1969; 1970) |
| TWDEF | 41.87 | -111.51 | 2650 | 43.00±4.65 | 40.16±2.49 (drC*) 28.67±1.88 (srC*) | This study |

h is elevation.

* drC: conifer has deep rooted at plot CA and CB; srC: conifer is shallow rooted plot CC.

Table 3-6. Significance testing of total evaporation, transpiration, and ET for each vegetation type compared for the same growing seasons (confidence level of $\alpha=0.05$). Units are in cm of water loss

| Vegetation | 2009 | | | 2010 | | | 2011 | | | 2012 | | |
|------------|-------|--------|--------|-------|--------|--------|-------|--------|--------|-------|--------|---------|
| | E | T | ET | E | T | ET | E | T | ET | E | T | ET |
| Aspen | 6.48b | 43.36a | 49.84a | 4.95a | 34.97a | 39.92a | 4.83b | 37.06a | 41.89a | 5.36a | 34.95a | 40.31a |
| drC* | 7.60b | 35.77b | 43.37b | 7.51a | 33.31a | 40.82a | 8.12a | 29.70b | 37.82a | 7.41a | 31.23a | 38.64ab |
| srC* | 7.39b | 21.93c | 29.32c | 4.39a | 22.25b | 26.65b | 4.44b | 23.30c | 27.73b | 5.61a | 25.35b | 30.96b |
| Grass | 6.72b | 20.30c | 27.02c | 6.73a | 18.37b | 25.10b | 6.34a | 18.66c | 24.99b | 7.73a | 19.71b | 27.44b |
| Sage | 7.86a | 26.93c | 34.79c | 5.73a | 20.51b | 26.24b | 8.67a | 17.45c | 26.12b | 6.50a | 21.47b | 27.97b |

* drC: conifer has deep rooted at plot CA and CB; srC: conifer is shallow rooted plot CC.

Table 3-7. Significance testing for each vegetation type during the four simulated growing seasons of 2009, 2010, 2011, and 2012 (confidence level of $\alpha=0.05$). Units are in cm of water loss

| Year | Vegetation | | | | | | | | | | | | | | |
|--------------|------------|--------|--------|-------|--------|--------|-------|--------|--------|-------|--------|--------|-------|--------|--------|
| | Aspen | | | drC* | | | srC* | | | Grass | | | Sage | | |
| | E | T | ET | E | T | ET | E | T | ET | E | T | ET | E | T | ET |
| 2009 | 6.48a | 43.36a | 49.84a | 7.60a | 35.77a | 43.37a | 7.39a | 21.93a | 29.32a | 6.72a | 20.30a | 27.02a | 7.86a | 26.93a | 34.79a |
| 2010 | 4.95a | 34.97b | 39.92b | 7.51a | 33.31a | 40.82a | 4.39a | 22.25a | 26.65a | 6.73a | 18.37a | 25.10a | 5.73a | 20.51b | 26.24b |
| 2011 | 4.83a | 37.06b | 41.89b | 8.12a | 29.70a | 37.82a | 4.44a | 23.30a | 27.73a | 6.34a | 18.66a | 24.99a | 8.67a | 17.45b | 26.12b |
| 2012 | 5.36a | 34.95b | 40.31b | 7.41a | 31.23a | 38.64a | 5.61a | 25.35a | 30.96a | 7.73a | 19.71a | 27.44a | 6.50a | 21.47b | 27.97b |
| 4-yr average | 5.41 | 37.585 | 42.99 | 7.66 | 32.50 | 40.16 | 5.46 | 23.21 | 28.67 | 6.88 | 19.26 | 26.14 | 7.19 | 21.59 | 28.78 |

* drC: conifer has deep rooted at plot CA and CB; srC: conifer is shallow rooted plot CC.

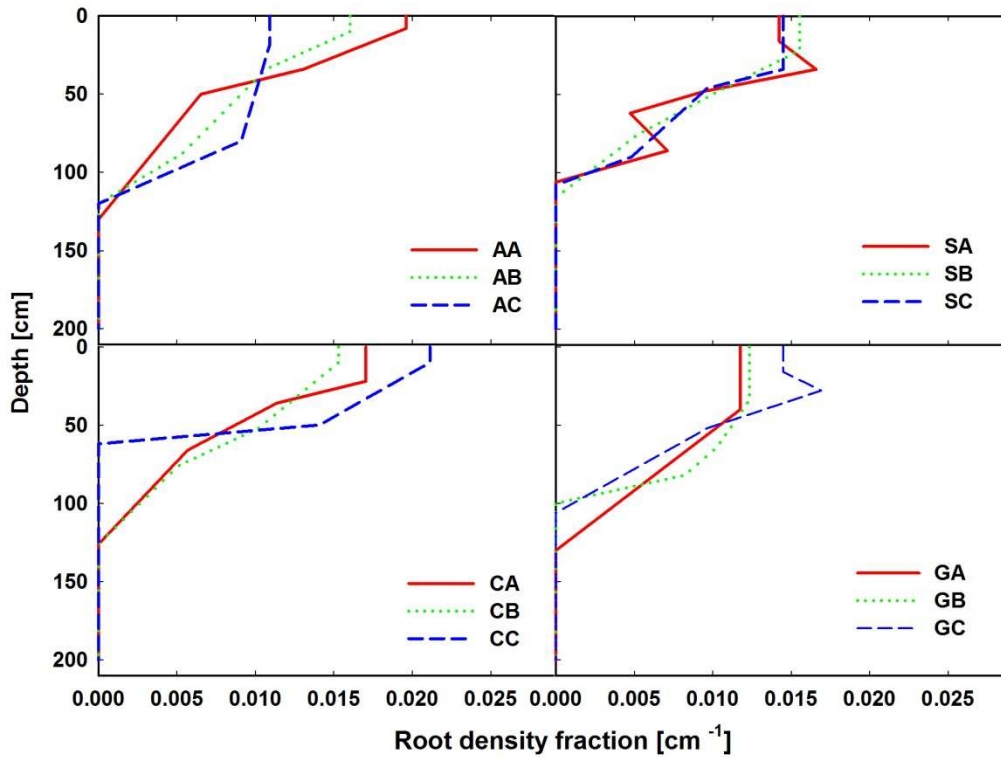


Figure 3-1. Root distribution density in the vegetation, aspen = A, conifer = C, sage = S, and grass = G for plots A, B, and C. Root density as a function of depth was interpreted from the 2004 soil pedon surveys. Because the root depth of the conifer plot C did not extend below 62 cm while the other two went beyond 1.2 m., we separated the analyses to shallow and deep rooted plots.

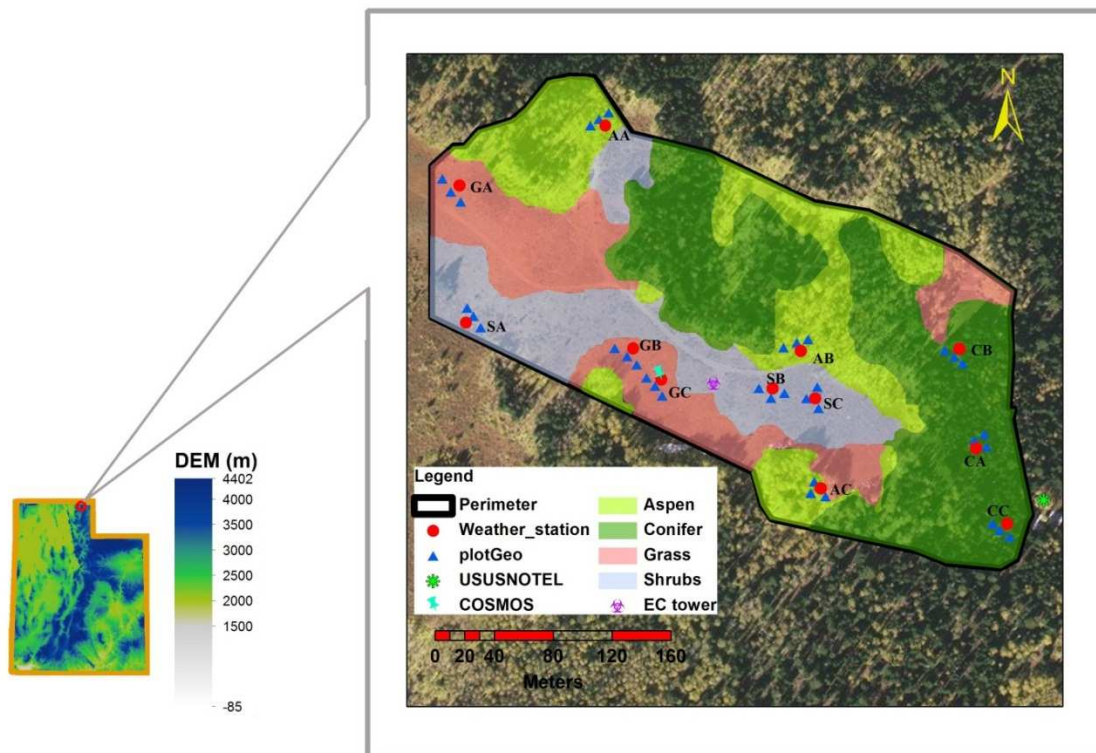


Figure 3-2. The T.W. Daniel Experimental Forest (TWDEF) site located in Northern Utah, illustrating the data collection network distributed within the study site. The site is surrounded by a perimeter fence with 12 primary/secondary weather stations and associated subplots. The Doc Daniel Snotel site is located at the Eastern edge of the TEDEF enclosure. The source of the DEM was from the U.S. Geological Survey (USGS) in spatial resolutions of 1 arc-second (30 m).

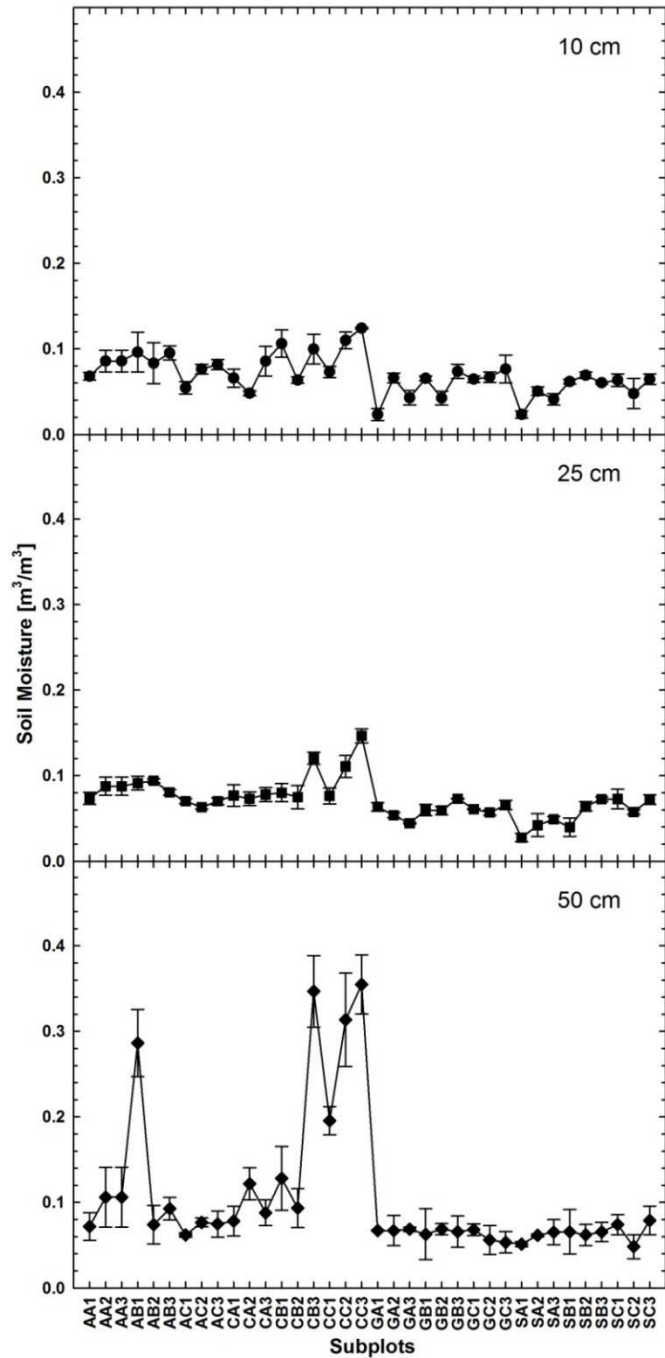


Figure 3-3. The mean and standard deviation of minimum soil moisture measured by TDT sensor in water years 2009, 2010, 2011, and 2012 for each subplot at 10-, 25-, and 50 cm depths. The x-axis designates each subplot, where the first letter represents vegetation type (a=aspen, c=conifer, g=grass, and s=sage), the second letter stands for the plot A, B, and C, and the last number represents the subplots number, i.e. 1 through 3.

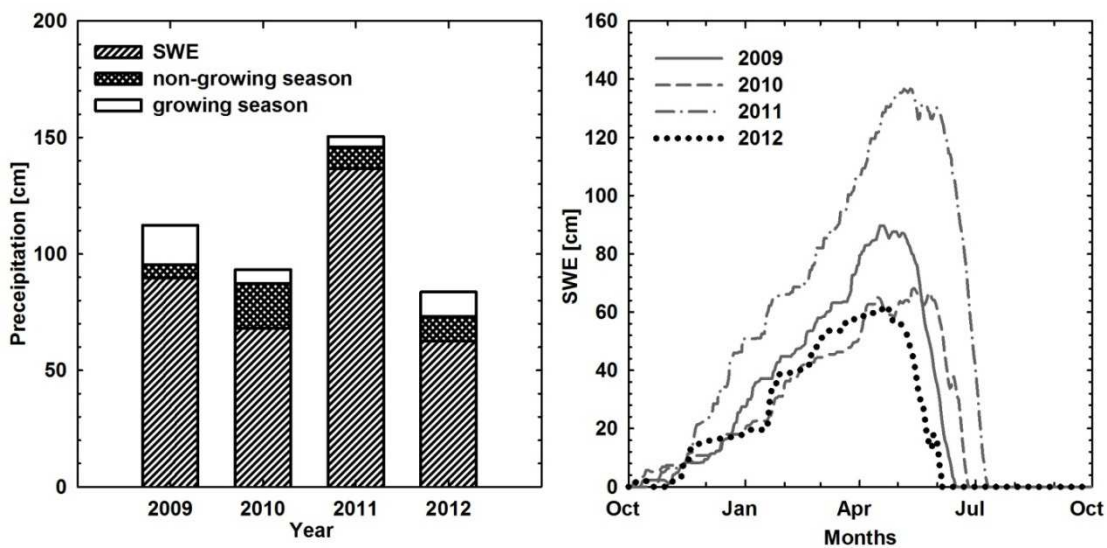


Figure 3-4. Total precipitation for grass (left), and temporal variation in snow water equivalent (SWE) at the USU Doc Daniel Snotel site (right) for water years 2009, 2010, 2011, and 2012.

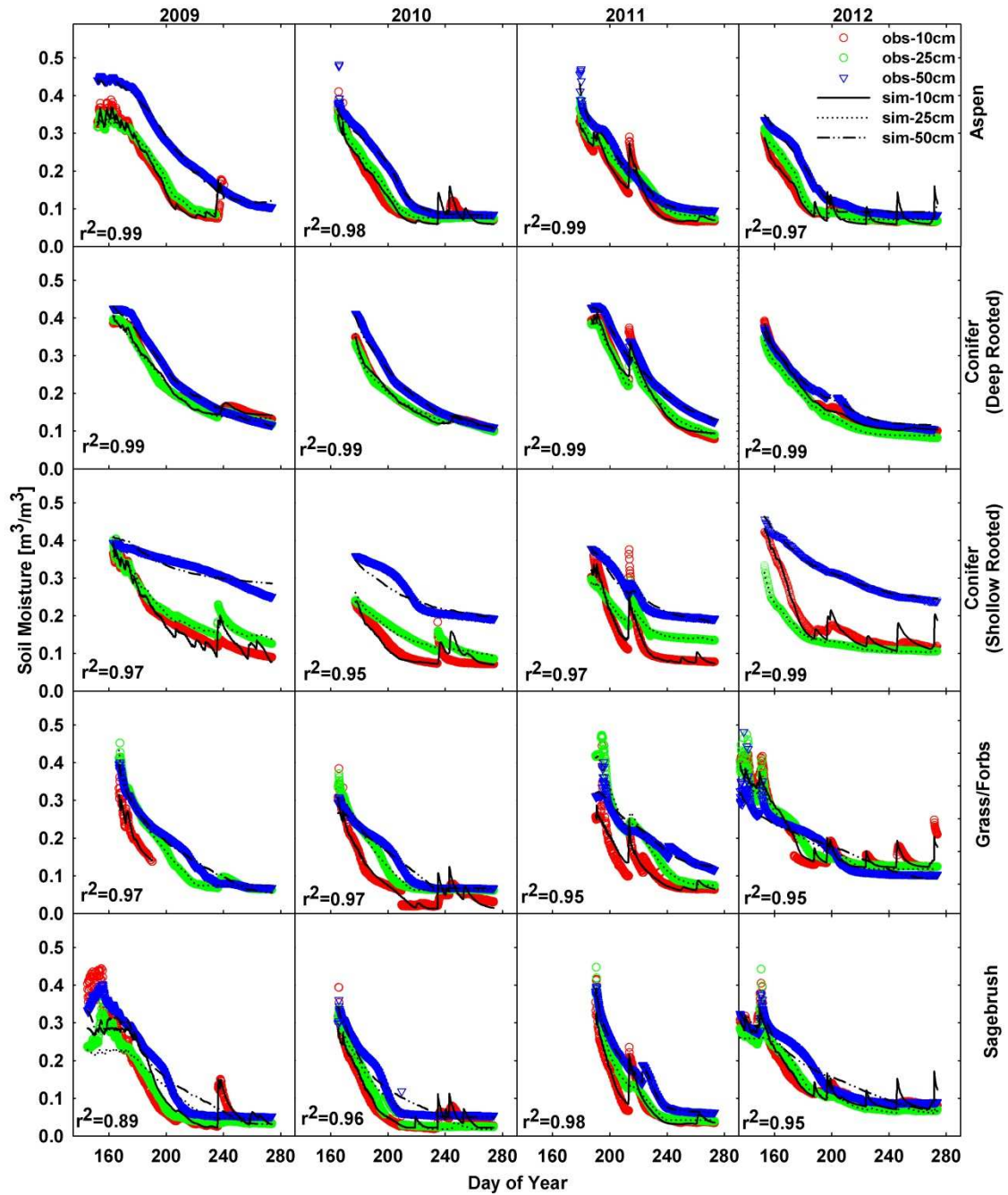


Figure 3-5. Example simulated soil moisture calibrations from measured values at 10-, 25-, and 50- cm depths in Aspen, Conifer, Grass/Forbs and sagebrush sites during the study periods of 2009, 2010, 2011, and 2012.

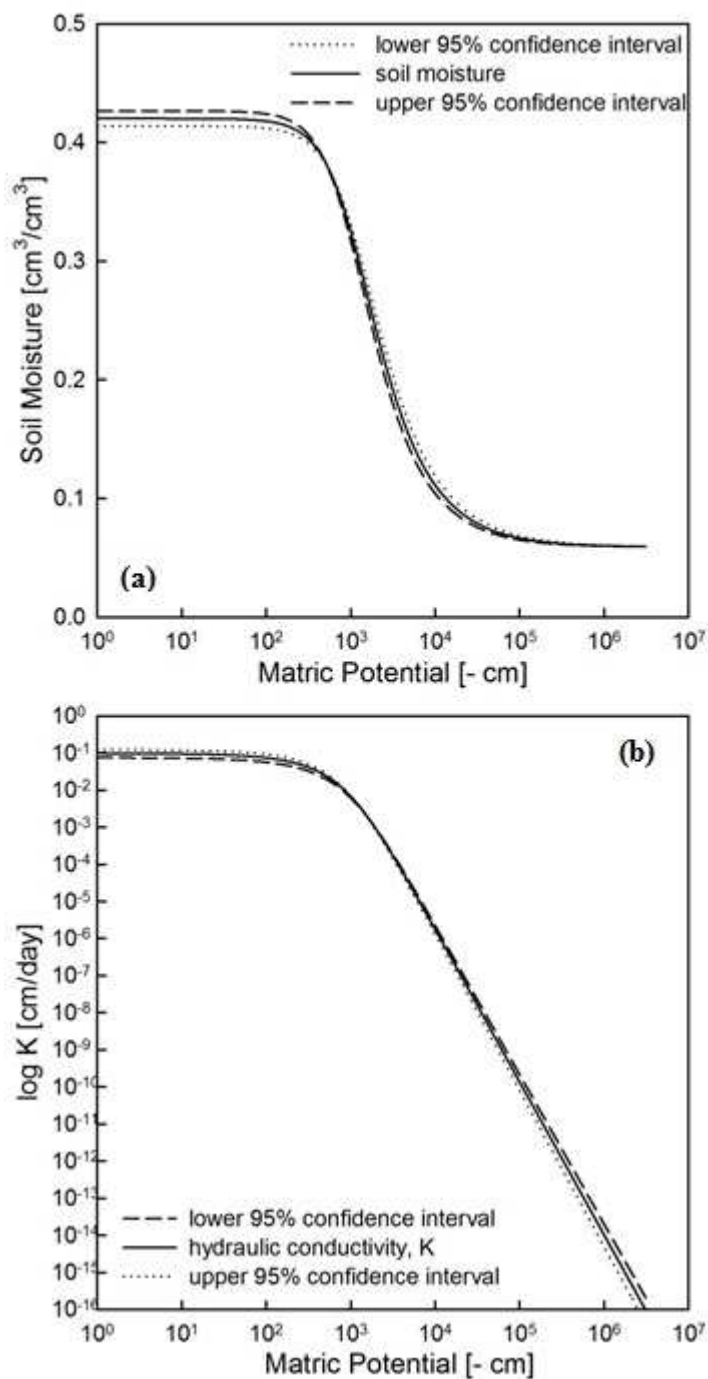


Figure 3-6. Example of simulated hydraulic properties and corresponding 95% confidence intervals for (a) soil moisture and (b) hydraulic conductivity (K) for the top layer of AA1, which is subplot one of plot A in aspen.

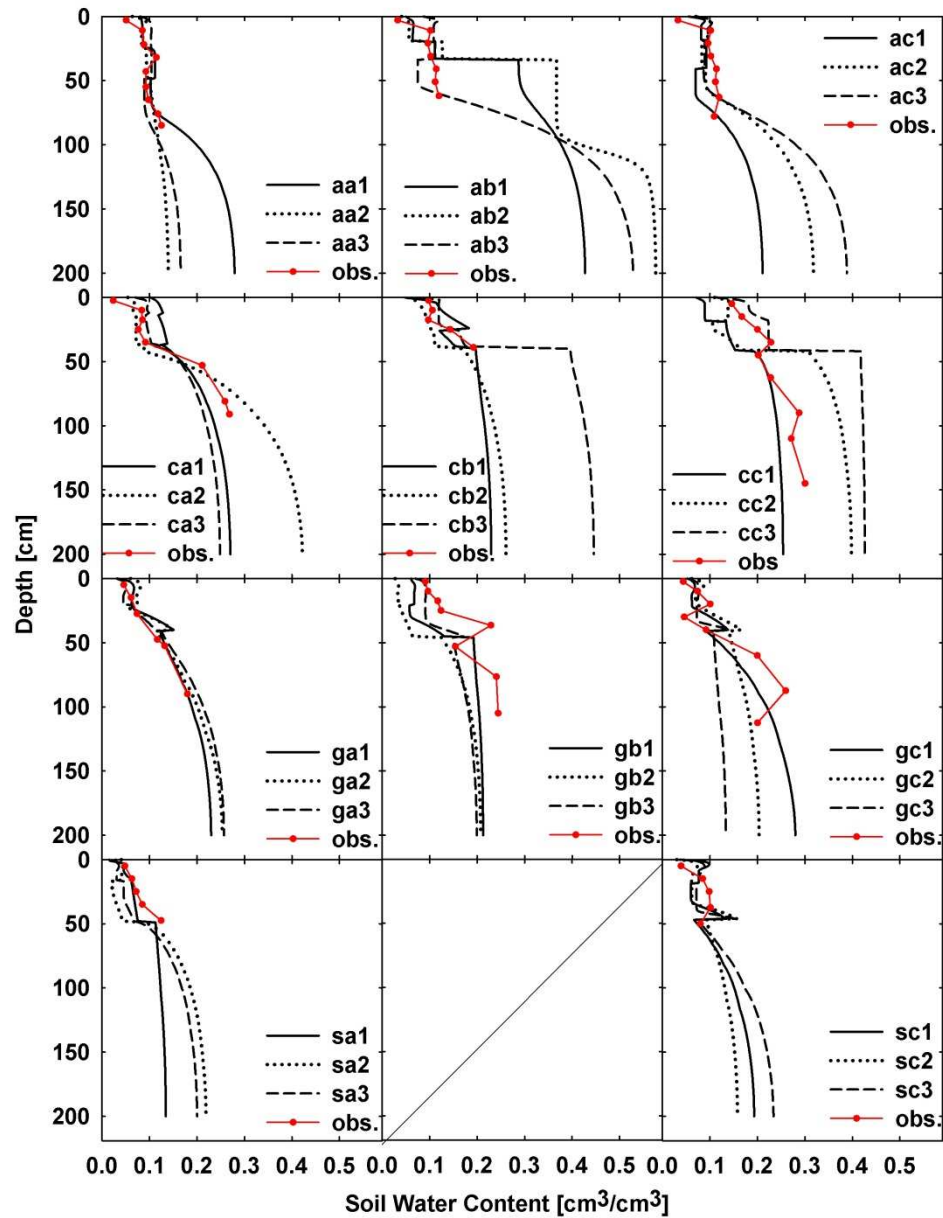


Figure 3-7. Comparison of soil core sampled with Hydrus-1D simulated soil moisture distribution profiles among the four vegetation types plots (aspen, conifer, grass/forbs, and sagebrush) on Sep. 14th, 2011. The first letter of legend represents vegetation type (a=aspen, c=conifer, g=grass, and s=sage), the second letter stands for the plot A, B, and C, and the last number represents the subplots number, i.e. 1 through 3. Sage B simulation was unavailable due to failure of the TDT soil moisture sensors.

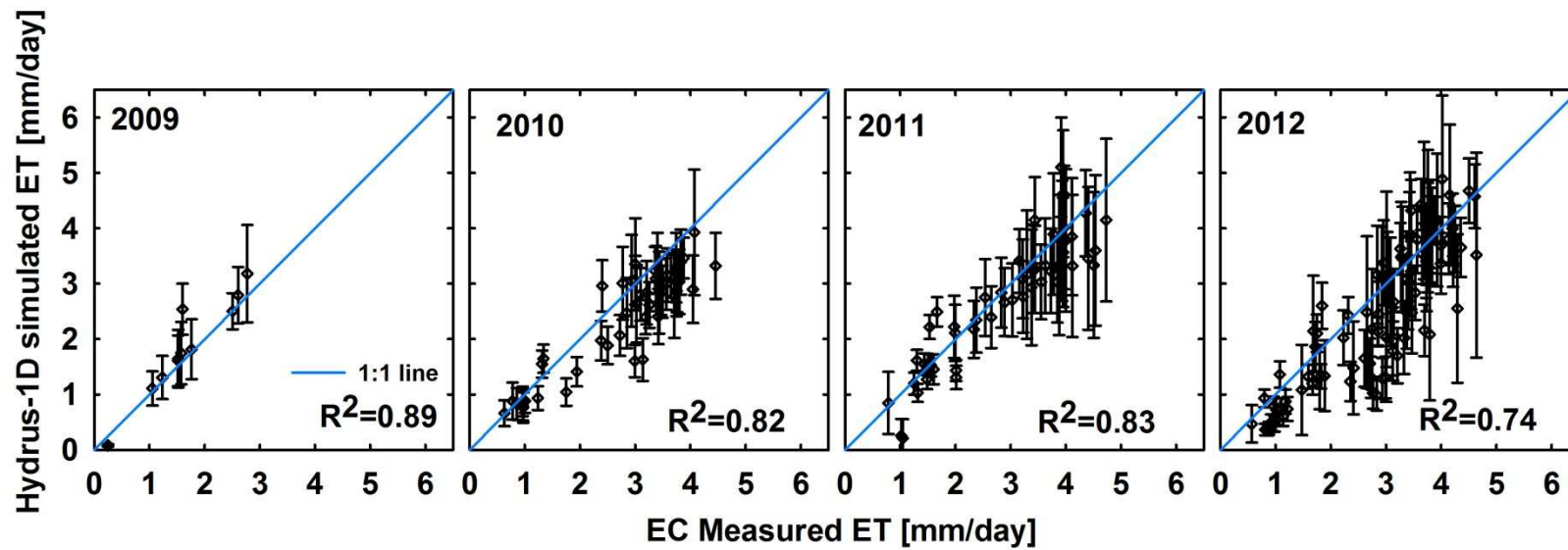


Figure 3-8. Comparison between the calculated ET from eddy covariance tower and the numerically simulated ET (mean±1 standard deviation). The mean numerically simulated ET was computed from 18 subplots, 9 in grass and 9 in sagebrush, with error bars representing one standard deviation from the means.

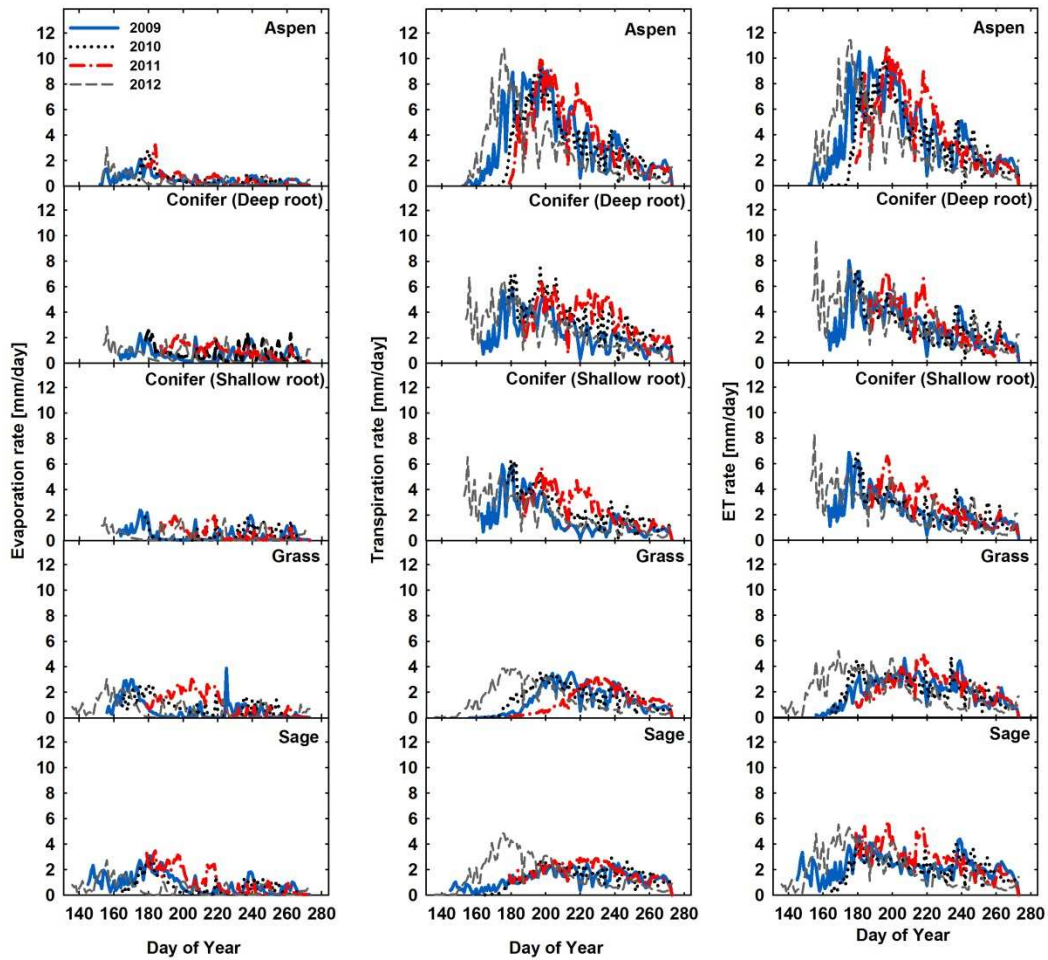


Figure 3-9. Numerically simulated (Hydrus-1D) average daily evaporation rates, transpiration rates, and evapotranspiration (ET) rates for aspen, conifer, grass and sage during the growing seasons of 2009, 2010, 2011, and 2012.

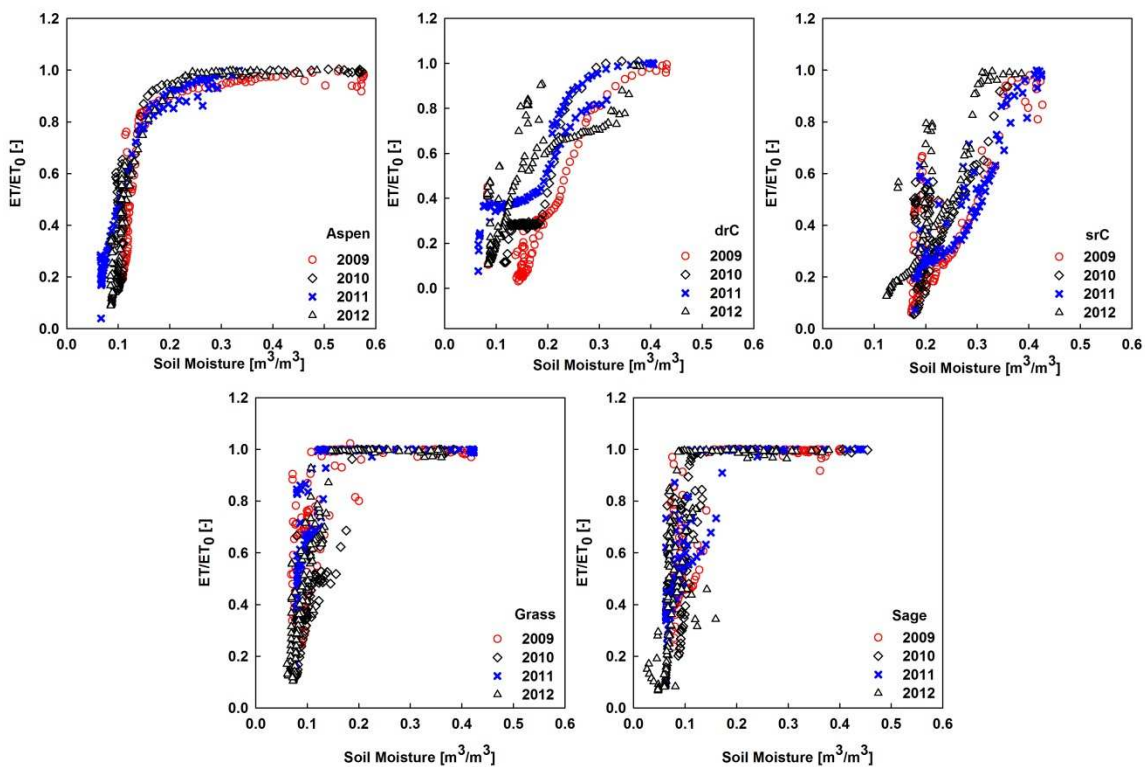


Figure 3-10. Normalized daily ET rate (ratio of daily ET rate to reference ET rate) as a function of soil moisture in the near surface layer (10 cm depth) for aspen, conifer (deep-rooted conifer = drC, shallow-rooted conifer = srC), grass and sage during the growing seasons of 2009, 2010, 2011, and 2012.

CHAPTER 4
MEASURED AND MODELED SOIL MOISTURE COMPARED
WITH COSMIC-RAY NEUTRON PROBE
ESTIMATES IN A MIXED FOREST³

Abstract. Soil moisture is a key variable in most environmental processes and the Cosmic-ray neutron probe (CRNP) fills a niche need for intermediate-scale soil moisture measurements. In this paper, the CRNP estimated soil moisture was compared with a soil moisture measurement network including 108 time-domain transmissometry (TDT) probes. We also employed a Hydrus-1D numerical simulation of the vertical soil moisture profile at targeted locations. The results showed that near-surface soil moisture estimated by the numerical simulation improved the correlation between the sensor network and the CRNP estimation during rainfall events. The CRNP estimates of soil moisture exhibited a dry bias at the beginning of the snow-free period because of a distinctly different seasonal soil moisture distribution, being nearly binary when wet in the early summer and nearly Gaussian under dry conditions. Using a combination of soil moisture measurements and near-surface simulations the CRNP output was recalibrated to capture the wetter conditions, resulting in a RMSE ($0.012 \text{ m}^3/\text{m}^3$) of less than half the original calibration RMSE ($0.025 \text{ m}^3/\text{m}^3$).

4.1. Introduction

Soil moisture is an important variable impacting most ecological and environmental processes. It significantly affects the ongoing exchange of water and

³ Coauthored by: Ling Lv, Trenton E. Franz, David A. Robinson, Scott B. Jones

energy between the land and atmosphere (Wang et al., 2005; Seneviratne et al., 2010). Antecedent soil moisture governs the generation of runoff and resulting flooding due to its effect on infiltration capacities (Minet et al., 2011). Reliable simulations of these processes require areal averages of soil moisture measured at intermediate or larger scales (Ochsner et al., 2013; Robinson et al., 2008). Therefore the compatibility of soil moisture model- and measurement-scales dictates the quality of the resulting simulations (Scipal et al., 2005). The degree of soil moisture variability not only depends on the static factors such as soil texture, soil organic matter, soil structure etc., but also on dynamic factors such as vegetation, weather conditions, etc. (Reynolds, 1970). Due to greater variation in topography and vegetation cover, non-uniform litter input, and less uniform soil mixing inherent in plowing (i.e., as opposed to bioturbation), the soil moisture distribution in a natural ecosystem exhibits more heterogeneity compared to an agriculture system (Flinn and Marks, 2007; Hawley et al., 1983), requiring larger sampling size. Regarding the scale of soil moisture determination, the point-scale has made major advances with a broad selection of precise, affordable in situ sensors available (Blonquist et al., 2005a, 2005b; Bogaen et al., 2007; Jones et al., 2005; Robinson et al., 2003a; Rosenbaum et al., 2010; Vereecken et al., 2008), while at the larger remote sensing scales, capabilities continue to improve, though presently with less accuracy at regional and continental scales. A glaring intermediate-scale gap for soil moisture assessment remains (Ochsner et al., 2013; Robinson et al., 2008). But the development of the Cosmic-ray Neutron Probe (CRNP, Hydroinnova, Albuquerque, NM) offers abilities to assess scales of hundreds of meters.

The CRNP is a novel non-invasive technique (Shuttleworth et al., 2010; Zreda et al., 2008;) to measure the areal averaged soil moisture of an effective depth on the order of decimeters within a radial footprint on the order of several hundred meters (Zreda et al., 2008; Zreda et al., 2012). This technique is analogous to the neutron probe used for down-hole soil moisture measurements (Kramer et al., 1992), but the equilibrium intensity of fast neutrons are measured with the CRNP instead of thermalized neutrons as with the down-hole method. This causes the response to be inversely, instead of directly correlated. It is known that secondary cosmic-rays interact with nuclei of atoms in the atmosphere, water, vegetation and soil, leading to the emission of fast neutrons in the atmosphere, and fast neutrons mainly moderated by hydrogen atoms (Zreda et al., 2011). Franz et al. (2012) suggested the CRNP is highly sensitive to the shallow subsurface soil moisture, but a lack of shallow (< 10 cm) soil moisture measurements limited their conclusions in this regard. The radial footprint of the CRNP is over a surface diameter of about 600 m at sea level in dry air, but that sensing diameter increases with increasing elevation and decreases with increasing atmospheric humidity (Desilets and Zreda 2013).

The objectives of this research were to compare the summer-time CRNP soil moisture estimates using a horizontal and depth-weighted averaging approach with (1) measurements from a network of 108 time-domain transmissometry (TDT) soil moisture sensors, and (2) 36 numerically simulated soil water content profiles.

4.2. Theoretical Considerations

The CRNP measures the moderated neutron counts and records totals every hour. Using a neutron particle transport model, Desilets et al. (2010) found a theoretical

relationship between relative neutron counts and soil moisture in homogeneous sand (SiO₂):

$$\theta_g(N) = \left[\frac{a_0}{N/N_0 - a_1} - a_2 \right]. \quad (4-1)$$

where, $\theta_g(N)$ (g/g) is the average gravimetric soil moisture, and empirical fitting parameters are given by $a_0=0.0808$, $a_1=0.372$, and $a_2=0.115$. The neutron counting rate, N , is output from the CRNP in counts per hour (cph), which is presented on the COSMOS website under data level 2 (<http://cosmos.hwr.arizona.edu/>) and N_0 is the neutron counting rate over dry soil under the same reference conditions and needs to be estimated with at least one independent soil moisture calibration.

In natural ecosystems, the hourly neutron counting rate in equation 4-1 is influenced not only by soil moisture, but also by hydrogen in other water-related sources which include, soil lattice water, water in soil organic matter, atmospheric water vapor, and water in or on vegetation. Previous research (Zreda et al., 2012) suggests a methodology to correct for lattice water and water in soil organic matter by partitioning them from total moisture, and correct for atmospheric water vapor by assigning a correction factor to the hourly neutron counting rate

$$N' = N \cdot C_{wv}. \quad (4-2)$$

where, N' is water vapor corrected neutron count rate (count h⁻¹), C_{wv} is the atmospheric water vapor correction factor (Rosolem et al., 2013), and written as

$$C_{wv} = 1 + 0.0054 \cdot (\rho_v - \rho_v^{ref}). \quad (4-3)$$

where, ρ_v is the measured absolute water vapor (g/m^3), ρ_v^{ref} is the absolute water vapor (g/m^3) at a reference condition (here we use dry air, $\rho_v^{\text{ref}} = 0 \text{ g}/\text{m}^3$).

Finally, the soil moisture, θ_v (m^3/m^3), is written as

$$\theta_v = \left[\frac{a_0}{N'/N'_0 - a_1} - a_2 - (\rho_{\text{SOC}} + \rho_\tau) \right] \cdot \rho_b \cdot \quad (4-4)$$

where, ρ_τ is the weight fraction of lattice water in dry soil (g/g), ρ_{SOC} is the weight fraction of soil organic carbon water equivalent in dry soil (g/g), ρ_b is soil bulk density (g/cm^3) and N_0' is the corrected value of N_0 , $N_0' = N_0 \times C_{\text{wv}}$.

In the subsurface, we assume that the CRNP measurement support volume is a cylinder with a depth that varies with soil pore water (θ_v), lattice water (ρ_τ), soil organic carbon (ρ_{SOC}), and soil bulk density (ρ_b). Franz et al. (2013b) calculated the effective depth, $z^*(\theta_v)$, using the following equation

$$z^*(\theta_v) = \frac{0.058}{\rho_b \cdot (\rho_\tau + \rho_{\text{SOC}}) + \theta_v + 0.0829} \quad (4-5)$$

4.3. Materials and Methodologies

4.3.1. Study Area

The study area lies within the Utah State University T.W. Daniel Experimental Forest (TWDEF), located approximately 30 km Northeast of Logan, UT ($41.86^\circ \text{ N}, 111.50^\circ \text{ W}$) (Figure 4-1). The Climate there is typical of the montane semi-arid intermountain West with a mid-growing season (July) mean temperature of 14.4° C , and mean precipitation of 950 mm y^{-1} , 80% of which falls as snow. Snowmelt typically

occurs between mid-May and mid-June. The mean growing season occurs between May and September when mean rainfall totals are 277 mm, with July and August typically getting less than 20 mm (Van Miegroet et al., 2005). The site is a gently sloping (<10%) northeast to southeast trending ridge top at the head of a contributing watershed to the Logan River and Bear River basin. The study site has an area of 86,000 m² and an elevation around 2600 m. The soil is formed in aeolian deposits overlying residuum and colluvium from the Wasatch formation (Woldeselassie et al., 2012). The forest soils (aspen and conifer) were classified as fine to coarse-loamy to loamy-skeletal haplocryalfs, and the rangeland soils (sage and grass) were classified as fine-loamy to loamy-skeletal haploxeralfs (Olsen and Van Miegroet, 2010). Additionally, conifer forest soil had characteristic O horizons (less than 0.03 m), and aspen forest and non-forest soil lacked an O horizon (Olsen and Van Miegroet, 2010).

The landscape is a patchwork of four dominant vegetation communities common to the Intermountain Region. Forest communities include aspen (*Populus trembloides*) and conifer, predominantly Engelmann Spruce (*Picea engelmannii*), subalpine fir (*Abies lasiocarpa*). The tree size distribution in the site is shown in Table 4-1. Non-forest communities include grasses and forbs (dominated by *Bromus carinatus* and *Elymus trachycaulu*, et al.), and sagebrush (*Artemisia tridentata*) (McArthur, 1981; Olsen and Van Miegroet, 2010). The percentage of vegetation communities within the TWDEF site are: 21% aspen, 43% conifer, 18% grass, and 18 % sage. The percentages of aspen, conifer, grass, and sage within the CRNP footprint are 33%, 47%, and 9% and 11%,

respectively. All vegetation communities are characterized by similar elevation, aspect, climate, geomorphology, and geology (Van Miegroet et al., 2005).

4.3.2. TDT Soil Moisture Sensor Network

Time-domain transmissometry (TDT, Acclima, Inc, Meridian, Idaho, USA) sensors provided travel-time measurements of dielectric permittivity to estimate soil moisture, with soil temperature and electrical conductivity measurements also provided. The TDT operation principles can be found elsewhere (Blonquist et al., 2005a; Jones et al., 2005; Robinson et al., 2003a), and its calibration to moisture relies on the method of Topp et al. (1980). The TDT method offers the advantage of having the pulse generating and sampling electronics mounted in the head of the probe, which allows TDT to be used with longer cable lengths and without the need for multiplexers, relying instead on sensor addressing and SDI-12 communications. The most important benefits are that TDT has developed as a low cost, small size, high stability and accuracy for measuring permittivity (Blonquist et al., 2005b). The TDT instrument provides a reliable measurement of relative permittivity, similar to time domain reflectometry (TDR), and therefore of soil moisture with a resolution of $\pm 0.02 \text{ m}^3 \text{ m}^{-3}$ (Topp et al., 2001). In our study site, 3 plots (Figure 4-1) for each dominant vegetation type were randomly selected and 3 subplots (5m×5m) within each plot were setup for statistical measures. Within each subplot, TDT sensors were installed horizontally at depths of 0.10 m, 0.25 m, and 0.50 m, beginning measurements in September 2008. The TDT data is recorded with commercial data loggers (CR1000/CR10X dataloggers, Campbell Scientific, Logan, UT, USA) and

data is relayed via telemetry every 30 minutes back to a data storage computer at Utah State University.

4.3.3. Portable TDR Soil Moisture Measurements

The portable TDR consists of several components: TDR100 (Campbell scientific Inc, Logan, UT, USA), CR1000 data logger, two-rod steel detecting probe with 0.1 m length, LED screen with control button, and 12v battery. We first calibrated the portable TDR in water and in air (Robinson et al., 2003b) and then used it to measure soil moisture within the TWDEF site. Soil moisture was measured along five transects, which began near the CRNP and ended at the perimeter fence of the TWDEF site. The TDR-based soil moisture measurement campaigns were implemented during the growing season of 2012. The first field campaign was taken after snowmelt (June 07, 2012), when soil was expected to be wettest. Thereafter, the soil moisture was measured monthly, on July 06, August 01, and September 02, 2012. These TDR sampling events recorded the soil moisture status during relatively wet, medium, and dry conditions. A CR1000 datalogger recorded volumetric soil moisture and the corresponding GPS location during sampling.

4.3.4. Soil Texture Mapping

By following the method of Abdu et al. (2008), georeferenced apparent electrical conductivity (ECa) measurements were taken non-invasively using a DUALEM-1S (Dualem, Milton, ON, Canada) ground conductivity instrument coupled with a Trimble (Trimble, Sunnyvale, CA, USA) ProXT GPS unit. Electrical sensors are particularly suited to soil measurements because the electrical conductivity of soil is highly dependent

on the ECa of the clay percentage, soil solution and water content (Friedman, 2005). The EMI instrument was held approximately 40 cm above ground while traversing the instrumented area with an approximate penetration depth of 60 cm and measurement volume of about 0.6 m³. The ECa data was acquired using a handheld geographic information system (HGIS, StarPal Inc, Fort Collins, CO, USA) program within an Allegro CX handheld field computer (Juniper Systems, Logan, UT, USA). The EMI mapping process required a few hours with the ECa data being collected every second. The ECa data were subsequently checked for continuity and anomalous values using a time-series view of the data. Anomalous values, which can be caused by buried metal fragments, wires, pipes, etc., were identified and removed from the data set as a quality control measure.

The EMI data were subsequently corrected and analyzed using geostatistical analysis techniques (Abdu et al., 2008), including Kriging, normal score transformation, sequential Gaussian simulation. The spatial site selection algorithm in the ESAP software package (Lesch et al., 2000) was used in order to pick out twelve calibration sites where soil was sampled for subsequent lab analysis of soil texture and EC. The selection algorithm that uses response surface methodology (RSM) was developed by Lesch et al. (1995) to predict field scale soil salinity from ECa survey data using multiple linear regression (MLR) models and a limited quantity of calibration samples. We adopted the site-selection technique to predict field-scale clay percentage due to the high correlation between soil textural properties and ECa in low ECe soils such as those found in our study site.

4.3.5. CRNP Calibration

The CRNP probe (CRS 1000, hydroinnova, Albuquerque, NM, USA) was first installed at the TWDEF on Aug. 13th, 2011 as part of the national CRNP network. Calibration was carried out on the same day during which soil samples were collected at 18 locations along six compass transects (i.e., N, NE, SE, S, SW, and NW) at radial distances from the CRNP probe of 25-, 75-, and 200-m. Samples were collected at each location at 6 depths of 0 - 0.05-, 0.05 - 0.1-, 0.1 - 0.15-, 0.15 - 0.2-, 0.2 - 0.25-, and 0.25 - 0.3-m for a total of 108 soil samples. For each sample, soil-water content and -bulk density were determined by oven drying at 105 °C. Soil lattice water and soil organic matter content (SOC) measurements in 1g subsamples were taken from each of the 108 calibration samples. The 108 aggregate samples were sent to Actlabs in Canada (<http://www.actlabs.com>) to measure the lattice water and SOC. The mean count reading from CRNP between 16:00 to 22:00 on Aug. 13th was 1352 ± 20 counts hr⁻¹, and the mean absolute water vapor density was 6 g/m³ (Table 4-2).

The hourly fast neutron count of the CRNP automatically corrects the temporal changes in air pressure and incoming neutron flux, with data posted at <http://cosmos.hwr.arizona.edu/Probes/StationDat/046/index.php>. It is also important to consider correction for other hydrogen source effects such as atmospheric water vapor, lattice water, SOC and so on, to get an accurate estimation of the average areal soil moisture. With the installation date of the CRNP in August 2011, our study period was focused on the growing seasons of 2011 and 2012 with 2013 used as a validation year.

4.3.6. Numerical Model Simulation of Near Surface Soil Moisture

Franz et al. (2012) suggested the CRNP is highly sensitive to shallow subsurface soil moisture, but lack of soil moisture measurements down to 0.1 m limited their conclusions regarding near-surface correlation. Soil water content dynamics above 0.1 m were simulated using numerical simulation software, Hydrus-1D (H1D), which is a soil process modeling software package (Simunek et al., 2008). The code combines a root water uptake model, the Penman-Monteith equation and Richards Equation (Simunek et al., 2008) to simulate the soil water contents within the soil profile including the near surface for each subplot (36 subplots total). Based on soil surveys at the TWDEF site (Boettinger et al., 2004), vegetation rooting depths were determined down to 1.2 m with no ground water found within their 2 m sampling depth. Therefore, we set the H1D domain to be a 2 m vertical column with a resolution of 0.01 m. The soil profile was further discretized into three layers according to the soil Genetic horizon samples (Olsen and Van Miegroet, 2010) for each plot and ensuring that each layer included a soil moisture sensor. Due to the lack of a soil moisture sensor within the top 10 cm, e.g., the litter layer in conifer plots, we used the simulated soil moisture at 0.03 m to represent pore water of litter layers. The lower boundary condition was set as a free drainage boundary. The upper boundary condition was an atmospheric boundary condition with surface runoff possible when excess water built up on the surface. The meteorological measurements were monitored at each climate tower (dots in Figure 4-1) and used to compute the upper boundary condition. We used soil water content measured at 0.1 m, 0.25 m, and 0.5 m depth as inputs to inversely solve for soil hydraulic parameters at each

location and with these soil hydraulic parameters, simulated soil moisture at 0.03 m and 0.05 m depths over the growing seasons of 2011 and 2012.

4.3.7. Comparison of CRNP with Distributed Sensor Network

To compare the CRNP areal soil moisture with the TDT in situ distributed sensor network measurement, or with the numerically simulated soil moisture values, the point soil moisture measurements or simulations were computed with a horizontal and vertical averaging weight function given by (Franz et al., 2012)

$$\bar{\theta} = \sum wt(z) \cdot \left[\sum_{i=1}^n wt(r) \cdot \theta_i(z) \right] \quad (4-6)$$

where, $\bar{\theta}$ is average areal soil moisture measurement of the TDT network or the Hydrus-1D simulation for the TWDEF site, $wt(z)$ is a linear depth weight factor at a depth of z , which is proven to be have good agreement with non-linear (Bogena et al., 2003) method (Hawdon et al., 2014). $wt(r)$ is horizontal weight factor at a distance r from the CRNP, $\theta_i(z)$ is the measured/simulated soil water content at a depth of z in subplot i ; n is the total number of subplots (i.e. $n=36$).

Vertical weighting, $wt(z)$, is calculated using a linear depth weight function (Franz et al., 2012):

$$\begin{cases} wt(z) = \alpha_z(1 - z/z^*) & 0 \leq z \leq z^* \\ wt(z) = 0 & z > z^* \end{cases} \quad (4-7)$$

where, α_z is a function in which the weights sum to unity, defined as:

$$\int_0^{z^*} \alpha_z \left(1 - z/z^*\right) dz = 1 \quad (4-8)$$

Horizontal weighting was obtained from a relationship between the cumulative fraction of counts and the CRNP footprint radius (Zreda et al., 2008). This relationship is simplified as follows

$$\begin{cases} wt(r) = \alpha_r(1 - r/R) & 0 \leq r \leq R \\ wt(r) = 0 & r > R \end{cases} \quad (4-9)$$

where, α_r is a constant defined as before by the condition that the weights sum to unity

$$\int_0^R \alpha_r (1 - r/R) dr = 1 \quad (4-10)$$

where, R is the footprint radius of 385 m for the TWDEF site and $\alpha_r = 0.0052$.

4.4. Results and Discussions

In comparing the CRNP estimates of near surface soil moisture with the TDT-soil moisture sensor network, we had a brief analysis of the effect of vegetation structure and soil texture on heterogeneity of soil moisture within the instrumented domain. We also analyzed seasonal change of soil moisture field, which are included in the effect of horizontal heterogeneity on the CRNP output.

4.4.1. Soil Moisture Comparison of CRNP with the TDT Network

In order to compare soil moisture measurements from the TDT network with the estimated soil moisture (θ_v) from the CRNP using equation 4-4, we computed TDT weighed average areal soil moisture ($\bar{\theta}_{TDT}$) by assigning horizontal weight factors for each subplot and vertical weight factors to each sensor depth. The comparison was shown

in Figure 4-2 (a). The RSME and R^2 between $\bar{\theta}_{TDT}$ and θ_v were $0.011 \text{ m}^3/\text{m}^3$ and 0.74, respectively in 2011, and $0.023 \text{ m}^3/\text{m}^3$ and 0.81, respectively in 2012. The difference between $\bar{\theta}_{TDT}$ and θ_v was as high as $0.08 \text{ m}^3/\text{m}^3$ over the growing season of 2012. The CRNP averaged areal soil moisture response was highly sensitive to small rainfall events in the late summer, however, due to the 10 cm or deeper burial depth of the TDT soil moisture sensors, the TDT weighted soil moisture response was very insensitive to rainfall events at the TWDEF site (Figure 4-2 (a)).

Franz et al. (2012) concluded that the CRNP is more sensitive to soil moisture at shallow depths. To estimate soil moisture values in the near surface, we applied the Hydrus-1D (H1D) numerical model to predict the van-Genuchten soil hydraulic parameters in soil locations where TDT sensors were installed. Table 4-3 illustrates a few examples of the soil hydraulic parameters estimated using inverse simulation with the numerical model. Using these parameters, we extracted soil moisture estimates at 0.03 m and 0.05 m depths using forward numerical simulations. We then used the same methods to compute the areal averaged weighted soil moisture ($\bar{\theta}_{H1D}$) based on our simulations. Compared to $\bar{\theta}_{TDT}$, the $\bar{\theta}_{H1D}$ showed marked improvement in soil moisture estimates during rainfall events (Figure 4-2 (b)). The absolute difference between θ_v and $\bar{\theta}_{H1D}$ was less than $0.02 \text{ m}^3/\text{m}^3$ when rainfall occurred. The RSME and R^2 between θ_v and $\bar{\theta}_{H1D}$ is $0.021 \text{ m}^3/\text{m}^3$ and 0.84. The considerable high differences between θ_v and $\bar{\theta}_{H1D}$ at the beginning of the growing season of 2012 still exist.

As we noted, both $\bar{\theta}_{TDT}$ and $\bar{\theta}_{H1D}$ agreed well with θ_v during relatively dry periods. The RMSE was $0.009 \text{ m}^3/\text{m}^3$, and R^2 was 0.96, when the θ_v less than or equal to $0.1 \text{ m}^3/\text{m}^3$. For θ_v greater than $0.1 \text{ m}^3/\text{m}^3$ the CRNP estimate of soil moisture under predicts the independently determined methods. One possible explanation for this discrepancy may be a result of the timing and soil moisture distribution during the field calibration of the CRNP, yielding the constants used in equation 4-4 (i.e., $a_0 = 0.0808$, $a_1 = 0.372$, and $a_2 = 0.115$). We therefore felt it was necessary to re-examine the calibration and soil moisture impacting the CRNP at the TWDEF site.

4.4.2. Vegetation Related Soil Moisture Distribution Within the TWDEF Site

As stated previously, the TWDEF site is a patchwork of four dominant vegetation types. The CRNP was installed near the center of the meadow, which is surrounded by trees. To explore the spatial organization of soil moisture at the TWDEF site resulting from vegetation structure, soil moisture was measured by the portable TDR was divided into four groups based on the dominant vegetation coverage.

The seasonal evolution of the soil moisture for each vegetation type is shown in Figure 4-3. During the wet period (Jun 07), the mean and standard deviation (SD) of soil moisture for each vegetation type were $0.225 \pm 0.045 \text{ m}^3/\text{m}^3$, $0.245 \pm 0.062 \text{ m}^3/\text{m}^3$, $0.14 \pm 0.052 \text{ m}^3/\text{m}^3$, and $0.15 \pm 0.050 \text{ m}^3/\text{m}^3$ for aspen, conifer, grass, and sage, respectively. Through processes of evapotranspiration and deep drainage, the soil moisture gradually decreased to a minimum value. In the dry period (Aug 01), the mean and SD of soil moisture were $0.050 \pm 0.006 \text{ m}^3/\text{m}^3$, $0.052 \pm 0.007 \text{ m}^3/\text{m}^3$, $0.047 \pm 0.008 \text{ m}^3/\text{m}^3$, and

0.044±0.007 m³/m³ for aspen, conifer, grass, and sage, respectively. Mean soil moisture values underneath tree canopies were significantly higher (P<0.005) than values in grass and sage. One possible reason for this is the dominance of soil clay content associated with trees compared to grass and sage (Figure 4-4). The relationship between clay content and soil moisture is illustrated in Figure 4-5. We also looked at the relationship between TDT sensors installation location and soil clay content, where clay content was grouped into three categories: High clay content (>17%), medium clay content (≥10% and ≤17%), and low clay content (<10%). As expected, for a given sampling date, locations with a higher clay content exhibited higher soil water content. Soil moisture at locations with clay contents greater than 17%, showed significantly higher (P<0.05) soil moisture than the other two groups over time.

4.4.3. Seasonal Change of Soil Moisture Distribution

We used variograms of soil moisture distribution measured using a portable TDR to characterize the seasonal change of soil moisture in the TWDEF research site. The nugget, sill, range and ratio of nugget to sill (nugget contribution) are listed in Table 4-4. The range in June was more than 100 m. The apparent range decreased in July, and was virtually gone in August. In other words, soil moisture exhibited strong spatial structure in early summer when the soil profile was wet but that structure became random by August in agreement with observations of soil moisture patterns made by others (Western and Grayson, 1998). Rainfall in September brought back spatial structure of soil moisture, which had a longer range but was more random than August soil moisture because the nugget contribution was higher.

This evolution of the soil moisture's structure together with vegetation related soil moisture patterns implied that the spatial soil moisture surrounding the CRNP had a near binary (dry-wet strip-like) soil moisture distribution at the beginning of the study period. This soil moisture distribution evolved from binary toward a Gaussian distribution as the soil was getting drier. This suggested that the CRNP output was biased dry at the start of the growing season and those biases were minimized as the soil was drying (Franz et al., 2013a).

4.4.4. Recalibration of CRNP for the TWDEF Site

For specific site conditions, it is critical to establish local CRNP calibration functions. We attempted to re-fit parameters in equation 4-4 (a_0 , a_1 , and a_2) in order to improve the CRNP estimates for our site, given our measured and modeled seasonal soil moisture. Using the solver in Excel, an objective function was established to minimize the sum of squared errors (SSE) between the CRNP values and the numerical simulated values including the important near surface estimates. The RMSE and R^2 for this optimization was $0.012 \text{ m}^3/\text{m}^3$ and 0.95 between $\bar{\theta}_{H1D}$ during 2012 and the soil moisture, θ_v' , computed from recalibrated parameters of equation 4-4 with $a_0=0.012$, $a_1=0.367$, and $a_2=0.227$.

Compared to the parameters published by Desilets et al. (2010), the newly fitted parameters yield soil moisture estimates which are much better correlated as shown in Figure 4-6. To evaluate our recalibration, we calculated θ_v and $\bar{\theta}_{TDT}$ for the growing season in 2013 using the same procedures as 2011 and 2012, and compared them with θ_v'

during the same period of 2013 (Figure 4-7). In 2013, before recalibration the RMSE and R^2 between θ_v and $\bar{\theta}_{TDT}$ were $0.025 \text{ m}^3/\text{m}^3$ and 0.87, respectively. And after recalibration the RMSE and R^2 changed into $0.011 \text{ m}^3/\text{m}^3$ and 0.97, respectively. The results demonstrate the improved CRNP correlation with the measured soil moisture values, especially during the wet season with an R^2 value between θ_v and $\bar{\theta}_{TDT}$ of 0.95. This strengthens the case for checking calibration functions once seasonal data are available, whether through soil moisture array, modeling or manual measurements of soil moisture in the near surface.

4.5. Conclusions

In this study, we compared the CRNP soil moisture measurements and in situ distributed TDT sensor soil moisture network measurements. Lacking TDT water content measurements in the near-surface ($> 10 \text{ cm}$) we employed numerical simulations of soil moisture to provide estimates of shallow soil moisture. We evaluated the relationship between soil moisture distribution patterns and soil texture as well as vegetation structure within the study site. We found soil moisture underneath trees to be significantly higher than soil moisture beneath sage or grass, which showed correlation to soil texture as well. The CRNP location in the central portion of the meadow at the TWDEF site, turned out to be a relatively dry location (i.e., coarse-textured, sandy soil). We used manual sampling of soil moisture to characterize the seasonal change of soil moisture distribution with time revealing a nearly-binary distribution early in the growing season when the soil was wet and we saw a shift toward reduced structure and a Gaussian soil moisture distribution as the soil dried out. This leads to our observation that the original CRNP

calibration yielded an underestimate of soil moisture in wet conditions. A recalibrated CRNP function between neutron count and a combination of soil moisture measurements and near-surface simulations was established by fitting the parameters, $a_0 = 0.120$, $a_1 = 0.367$, and $a_2 = 0.227$. Compared to the RMSE and R^2 between $\bar{\theta}_{TDR}$ and θ_v in 2013, the recalibration reduced the RMSE from $0.025 \text{ m}^3/\text{m}^3$ to $0.012 \text{ m}^3/\text{m}^3$, and increased R^2 from 0.8 to 0.97. Our study implied that multiple calibrations attribute to improve the determination of the parameters involved in the calibration function. The timing distribution of each calibration was according to the change of soil moisture characteristics in a specific CRNP site.

References

- Abdu, H., Robinson, D.A., Seyfried, M., Jones, S.B., 2008. Geophysical imaging of watershed subsurface patterns and prediction of soil texture and water holding capacity. *Water Resour. Res.* 44(4): W00D18.
- Blonquist, J.M.J., Jones, S.B., Robinson, D.A., 2005a. Standardizing characterization of electromagnetic water content sensors. *Vadose Zone J.* 4(4): 1059-1069.
- Blonquist, J.M.J., Jones, S.B., Robinson, D.A., 2005b. A time domain transmission sensor with TDR performance characteristics. *J. Hydrol.* 314(1-4): 235-245.
- Boettinger, J.L., Lawley, J.R., Van Miegroet, H., 2004. Morphology of soils in the aspen, conifer, grass/forbs, and sagebrush environmental monitoring sites, TW Daniel Experimental Forest, Logan, UT.
- Bogena, H.R., Huisman, J.A., Baatz, R., Hendricks Franssen, H.J., Vereecken, H., 2013. Accuracy of the cosmic-ray soil water content probe in humid forest ecosystems: The worst case scenario. *Water Resour. Res.* 49, 5778-5791, doi: 10.1002/wrcr.20463.
- Bogena, H.R., Huisman, J.A., Oberdörster, C., Vereecken, H., 2007. Evaluation of a low-cost soil water content sensor for wireless network applications. *J. Hydrol.* 344(1-2): 32-42.

- Desilets, D., Zreda, M., 2013. Footprint diameter for a cosmic-ray soil moisture probe: Theory and Monte Carlo simulations. *Water Resour. Res.* 49(6): 3566-3575.
- Desilets, D., Zreda, M., Ferré, T.P.A., 2010. Nature's neutron probe: Land surface hydrology at an elusive scale with cosmic rays. *Water Resour. Res.* 46(11), W11505, doi: 10.1029/2009WR008726.
- Flinn, K.M., Marks, P.L., 2007. Agricultural legacies in forest environments: tree communities, soil properties, and light availability. *Ecol. Appl.* 17(2): 452-463.
- Franz, T., Mreda, M., Rosolem, R., Ferré, T.P.A., 2012. Field validation of a cosmic-ray neutron sensor using a distributed sensor network, *Vadose zone J.* 11, 4, doi:10.2136/vzj2012.0046.
- Franz, T.E., Zreda, M., Ferré, T.P.A., Rosolem, R., 2013a. An assessment of the effect of horizontal soil moisture heterogeneity on the area-average measurement of cosmic-ray neutrons. *Water Resour. Res.* 49(10): 6450-6458.
- Franz, T.E., Zreda, M., Rosolem, R., Hornbuckle, B.K., Irvin, S.L., Adams, H., Kolb, T.E., Zweg, C., Shuttleworth, W.J., 2013b. Ecosystem-scale measurements of biomass water using cosmic ray neutrons. *Geophys. Res. Lett.* 40(15): 3929-3933.
- Friedman, S.P., 2005. Soil properties influencing apparent electrical conductivity: a review. *Comput. Electron. Agric.* 46(1-3): 45-70.
- Hawdon, A., McJannet, D., Wallace, J., 2014. Calibration and correction procedures for cosmic-ray neutron soil moisture probes located across Australia. *Water Resour. Res.* 50, doi: 10.1002/2013WR015138.
- Hawley, M.E., Jackson, T.J., McCuen, R.H., 1983. Surface soil moisture variation on small agricultural watersheds. *J. Hydrol.* 62(1-4): 179-200.
- Jenkins, J.C., Chojnacky, D.C., Heath, L.S., Birdsey, R.A., 2003. National-Scale Biomass Estimators for United States Tree Species. *For. Sci.* 49(1): 12-35.
- Jones, S.B., Blonquist, J.M., Robinson, D.A., Rasmussen, V.P., Or, D., 2005. Standardizing characterization of electromagnetic water content sensors. *Vadose Zone J.* 4(4): 1048-1058.
- Wang, K., Wang, P., Liu, J., Sparrow, M., Haginoya, S., Zhou, X., 2005. Variation of surface albedo and soil thermal parameters with soil moisture content at a semi-desert site on the western Tibetan Plateau. *Boundary Layer Meteorol.* 116(1): 117-129.
- Kramer, J.H., Cullen, S.J., Everett, L.G., 1992. Vadose Zone Monitoring with the Neutron Moisture Probe. *Ground Water Monit. Rem.* 12(3): 177-187.

- Lesch, S.M., Rhoades, J.D., Corwin, D.L., 2000. The ESAP-95 version 2.01R user manual and tutorial guide. 146, USDA-ARS, George E. Brown, Jr., Salinity Laboratory, Riverside, California.
- Lesch, S.M., Strauss, D.J., Rhoades, J.D., 1995. Spatial Prediction of Soil Salinity Using Electromagnetic Induction Techniques: 2. An Efficient Spatial Sampling Algorithm Suitable for Multiple Linear Regression Model Identification and Estimation. *Water Resour. Res.* 31(2): 387-398.
- McArthur, E.D., 1981. Taxonomy, origin, and distribution of big sagebrush (*Artemisia tridentata*) and allies (subgenus *Tridentatae*). In: K.L. Johnson (Ed.), *Proceedings of the First Utah Shrub Ecology Workshop*, Ephraim, Utah.
- Minet, J., Laloy, E., Lambot, S., Vanclooster, M., 2011. Effect of high-resolution spatial soil moisture variability on simulated runoff response using a distributed hydrologic model. *Hydrol. Earth Syst. Sci.* 15(4): 1323-1338.
- Ochsner, T.E., Cosh, M.H., Cuenca, R.H., Dorigo, W.A., Draper, C.S., Hagimoto, Y., Kerr, Y.H., Njoku, E.G. Small, E.E., Zreda, M., 2013. State of the Art in Large-Scale Soil Moisture Monitoring. *Soil Sci. Soc. Am. J.* 77(6): 1888-1919.
- Olsen, H.R., Van Miegroet, H., 2010. Factors affecting carbon dioxide release from forest and rangeland soils in Northern Utah. *Soil Sci. Soc. Am. J.* 74(1): 282-291.
- Reynolds, S.G., 1970. The gravimetric method of soil moisture determination Part III An examination of factors influencing soil moisture variability. *J. Hydrol.* 11(3): 288-300.
- Robinson, D.A. Campbell, C.S., Hopmans, J.W., Hornbuckle, B.K., Jones, S.B., Knight, R., Ogden, F., Selker, J., Wendroth, O., 2008. Soil moisture measurement for ecological and hydrological watershed-scale observatories: a review. *Vadose Zone J.* 7(1): 358-389.
- Robinson, D.A., Jones, S.B., Wraith, J.M., Or, D., Friedman, S.P., 2003a. A review of advances in dielectric and electrical conductivity measurement in soils using time domain reflectometry. *Vadose Zone J.* 2(4): 444-475.
- Robinson, D.A., Schaap, M., Jones, S.B. Friedman, S.P., Gardner, C.M.K., 2003b. Considerations for improving the accuracy of permittivity measurement using TDR: Air/water calibration, effects of cable length. *Soil Sci. Soc. Am. J.* 76: 62-70.
- Rosenbaum, U., Huisman, J.A., Weuthen, A., Vereecken, H., Bogaen, H.R., 2010. Sensor-to-Sensor Variability of the ECH2O EC-5, TE, and 5TE Sensors in Dielectric Liquids. *Vadose Zone J.* 9(1): 181-186.

- Rosolem, R., Shuttleworth, W.J., Zreda, M., Franz, T.E., Zeng, X., Kurc, S.A., 2013. The Effect of Atmospheric Water Vapor on Neutron Count in the Cosmic-Ray Soil Moisture Observing System. *J. Hydrometeorol.* 14(5): 1659-1671.
- Scipal, K., Scheffler, C., Wagner, W., 2005. Soil moisture-runoff relation at the catchment scale as observed with coarse resolution microwave remote sensing. *Hydrol. Earth Syst. Sci. Discuss.* 2(2): 417-448.
- Seneviratne, S.I., Corti, T., Davin, E.L., Hirschi, M., Jaeger, E.B., Lehner, I., Orlowsky, B., Teuling, A.J., 2010. Investigating soil moisture–climate interactions in a changing climate: A review. *Earth-Sci. Rev.* 99(3–4): 125-161.
- Shuttleworth, W.J., M. Zreda, X. Zeng, C. Zweck, P.A. Ferre. 2010. The cosmic-ray Soil Moisture Observing System (COSMOS): A non-invasive, intermediate-scale soil moisture measurement network. In: C. Kirby, editor *Role of Hydrology in Managing Consequences of a Changing Global Environment*. Proceedings of the BHS Third International Symposium. British Hydrological Society, Newcastle University.
- Simunek, J., Sejna, M., Saito, H., Sakai, M., van Genuchten, M.T., 2008. The HYDRUS-1D software package for simulating the one-dimensional movement of water, heat, and multiple solutes in Variably-saturated Media. Department of environmental sciences university of California riverside, California.
- Topp, G.C., Davis, J.L., Annan, A.P., 1980. Electromagnetic determination of soil water content: Measurements in coaxial transmission lines. *Water Resour. Res.* 16(3): 574-582.
- Topp, G.C., Lapen, D.R., Young, G.D., Edwards, M., 2001. Evaluation of shaft-mounted TDT readings in disturbed and undisturbed media Second International Symposium and Workshop on Time Domain Reflectometry for Innovative Geotechnical Applications, Infrastructure Technology Institute-Northwestern University, Evanston, Illinois.
- Van Miegroet, H., Boettinger, J.L., Baker, M.A., Nielsen, J., Evans, D., Stum, A., 2005. Soil carbon distribution and quality in a montane rangeland-forest mosaic in northern Utah. *For. Ecol. Manage.* 220(1–3): 284-299.
- Vereecken, H., Huisman, J.A., Bogaen, H., Vanderborght, J., Vrugt, J.A., Hipmans, J.W., 2008. On the value of soil moisture measurements in vadose zone hydrology: A review. *Water Resour. Res.* 44(4), W00D06, doi: 10.1029/2008wr006829.
- Western, A.W., Grayson, R.B., 1998. The Tarrawarra data set: soil moisture patterns, soil characteristics, and hydrological flux measurements. *Water Resour. Res.* 34(10): 2765-2768.

- Woldeslassie, M., Van Miegroet, H., Gruselle, M.-C., Hambly, N., 2012. Storage and Stability of Soil Organic Carbon in Aspen and Conifer Forest Soils of Northern Utah. *Soil Sci. Soc. Am. J.* 76(6): 2230-2240.
- Zreda, M., Desilets, D., Ferré, T.P.A., Scott, R.L., 2008. Measuring soil moisture content non-invasively at intermediate spatial scale using cosmic-ray neutrons. *Geophys. Res. Lett.* 35(21): L21402.
- Zreda, M., Shuttleworth, W.J., Zeng, X., Zweck, C., Desilets, D., Franz, T., Rosolem, R., 2012. COSMOS: The COsmic-ray Soil Moisture Observing System. *Hydrol. Earth Syst. Sci. Discuss.* 9(4): 4505-4551.
- Zreda, M., Zeng, X., Shuttleworth, J., Zweck, C., Ferre, T., Franz, T. Rosolem, R., Desilets, D., Desilets, S., Womack, G., 2011. Cosmic-Ray Neutrons, An Innovative Method for Measuring Area-Average Soil Moisture. *GEWEX News* 21(3): 6-10.

Table 4-1. Tree size distribution and characteristics determined from seven-100 m² plots at the TWDEF research site, and the estimated aboveground and root biomass (Jenkins et al., 2003)

| Tree | Mean stem diameter (m) | Tree height (m) | Stem density (#/ha) | Root total (%) | ratio to biomass | Root distribution fraction above 0.3 m (%) | Dry AGB (kg/m ²) | Dry RB above 0.3 m (kg/m ²) |
|--------------|------------------------|-----------------|---------------------|----------------|------------------|--|------------------------------|---|
| aspen | 0.025 | 4.83 | 24 | 25.5 | | 40 | 0.002 | 0.0002 |
| | 0.075 | 7.16 | 33 | 20.5 | | 40 | 0.04 | 0.004 |
| | 0.125 | 9.48 | 33 | 19.6 | | 40 | 0.15 | 0.01 |
| | 0.175 | 11.81 | 61 | 19.3 | | 40 | 0.62 | 0.05 |
| | 0.225 | 14.13 | 66 | 19.1 | | 40 | 1.22 | 0.09 |
| | 0.275 | 16.46 | 24 | 18.9 | | 40 | 0.72 | 0.05 |
| | 0.325 | 18.78 | 24 | 18.9 | | 40 | 1.07 | 0.08 |
| | 0.375 | 21.11 | 9 | 18.8 | | 40 | 0.56 | 0.04 |
| | 0.425 | 23.43 | 14 | 18.8 | | 40 | 1.18 | 0.09 |
| conifer | 0.025 | 7.38 | 67 | 27.3 | | 40 | 0.01 | 0.0008 |
| | 0.075 | 9.11 | 34 | 22.9 | | 40 | 0.05 | 0.004 |
| | 0.125 | 10.84 | 74 | 22.1 | | 40 | 0.34 | 0.03 |
| | 0.175 | 12.57 | 60 | 21.7 | | 40 | 0.60 | 0.05 |
| | 0.225 | 14.30 | 54 | 21.5 | | 40 | 0.96 | 0.08 |
| | 0.275 | 16.04 | 27 | 21.4 | | 40 | 0.77 | 0.07 |
| | 0.325 | 17.77 | 13 | 21.4 | | 40 | 0.55 | 0.05 |
| | 0.375 | 19.50 | 13 | 21.3 | | 40 | 0.76 | 0.07 |
| | 0.425 | 21.23 | 7 | 21.3 | | 40 | 0.55 | 0.05 |
| | 0.475 | 22.96 | 13 | 21.2 | | 40 | 1.33 | 0.11 |
| Total | | | | | | | 11.48 | 0.93 |

Table 4-2. Summary of measured and derived parameters used in the universal calibration function (equation 4-4)

| No. | Parameters | Names | Units | Values |
|-----|---------------------|---|-------------------------|--------|
| 1 | ρ_b | soil bulk density | g/cm^3 | 0.93 |
| 2 | θ_v | Weighted soil moisture on the calibration day | m^3/m^3 | 0.134 |
| 3 | $z^*(\theta_v)$ | Effective depth on the calibration day | m | 0.23 |
| 4 | ρ_{SOC} | Soil organic carbon | g/g | 0.017 |
| 5 | ρ_τ | Lattice water content | g/g | 0.028 |
| 6 | ρ_v | Water vapor density on the calibration day | g/m^3 | 6 |
| 7 | N | Neutron count on the calibration day | cph | 1352 |
| 8 | N_0' | Site specific constant | cph | 2189 |

Table 4-3. Examples of numerically fitted (Hydrus-1D) soil hydraulic parameters for each vegetation type

| vegetation | Depth (m) | θ_r (m ³ /m ³) | θ_s (m ³ /m ³) | α (m ⁻¹) | n | Ks (m/day) |
|------------|-----------|--|--|-----------------------------|-------|------------|
| Aspen A1 | 0.10 | 0.059 | 0.794 | 0.444 | 2.106 | 2.159 |
| | 0.25 | 0.059 | 0.444 | 0.214 | 1.901 | 0.086 |
| | 0.5 | 0.04 | 0.490 | 0.228 | 1.632 | 0.046 |
| Conifer A1 | 0.10 | 0.045 | 0.442 | 0.338 | 1.333 | 0.121 |
| | 0.25 | 0.051 | 0.430 | 0.231 | 1.408 | 0.477 |
| | 0.5 | 0.044 | 0.428 | 0.099 | 1.642 | 0.014 |
| Grass A1 | 0.10 | 0.01 | 0.400 | 0.943 | 1.402 | 0.460 |
| | 0.25 | 0.053 | 0.600 | 0.441 | 1.761 | 0.012 |
| | 0.5 | 0.066 | 0.636 | 0.357 | 2.207 | 0.563 |
| Sage A1 | 0.10 | 0.015 | 0.513 | 0.966 | 1.665 | 1.113 |
| | 0.25 | 0.018 | 0.629 | 2.420 | 1.556 | 4.797 |
| | 0.5 | 0.045 | 0.68 | 0.4053 | 2.704 | 1.430 |

Table 4-4. Variogram nugget and sill from soil moisture measurements for each of four different sampling dates. The variogram was fitted using an exponential model. To the soil water moisture measurements obtained by a portable time domain reflectometry (TDR)

| Date | mean (m^3/m^3) | Nugget (m^6/m^6) | Sill (m^6/m^6) | Range (m) | R^2 | Nugget contribution |
|--------|-------------------------------------|---------------------------------------|----------------------------------|-----------|-------|------------------------|
| Jun 07 | 0.175 | 0.001023 | 0.01053 | 137 | 0.92 | 0.09 |
| Jul 06 | 0.088 | 0.000105 | 0.00243 | 90 | 0.91 | 0.04 |
| Aug 01 | 0.046 | 0.000171 | 0.00033 | -- | -- | 0.34 |
| Sep 02 | 0.094 | 0.00133 | 0.00068 | 195 | 0.93 | 0.66 |

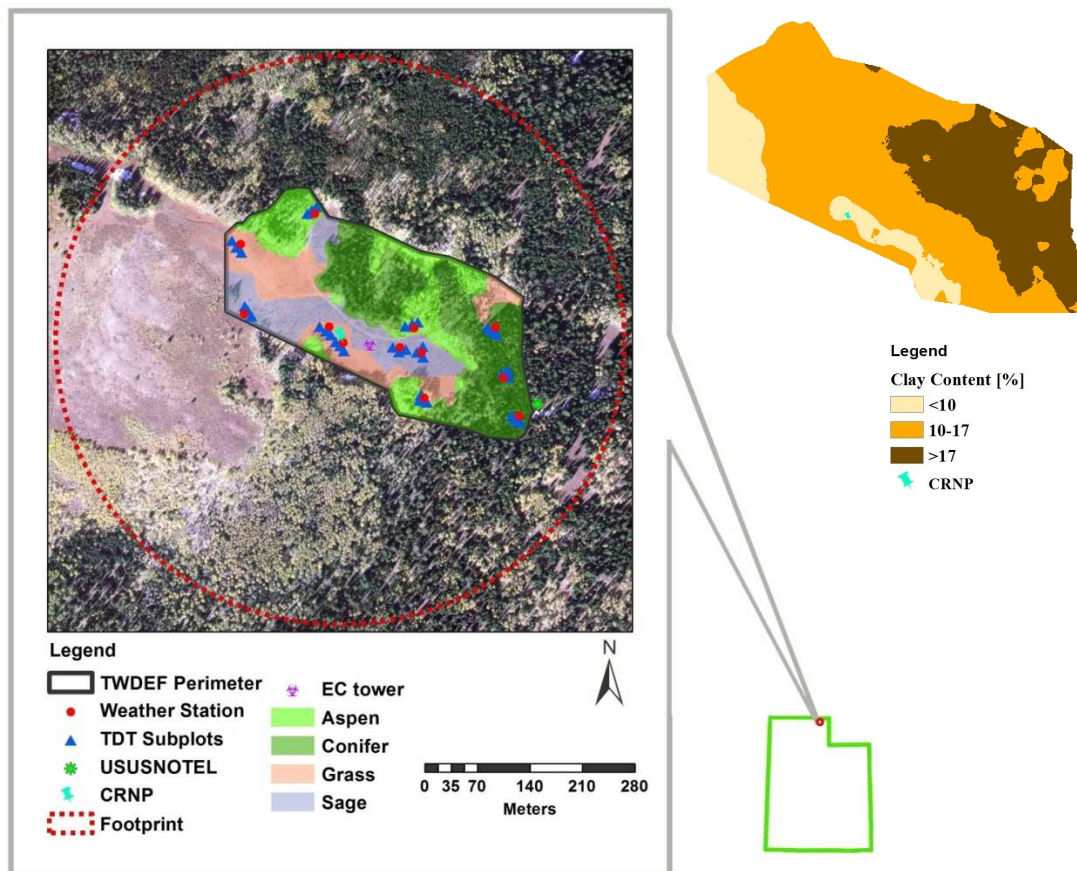


Figure 4-1. The overview of the TWDEF study site in the Northern Utah and the layout of the data collection network contained within the fenced perimeter. A Cosmic-ray Neutron Probe (CRNP) and its associated footprint are also shown. The time domain transmissometry (TDT) soil moisture sensors are shown as triangles around each plot weather station. The clay content (%) distribution inside the TWDEF site is displayed on the right upper corner.

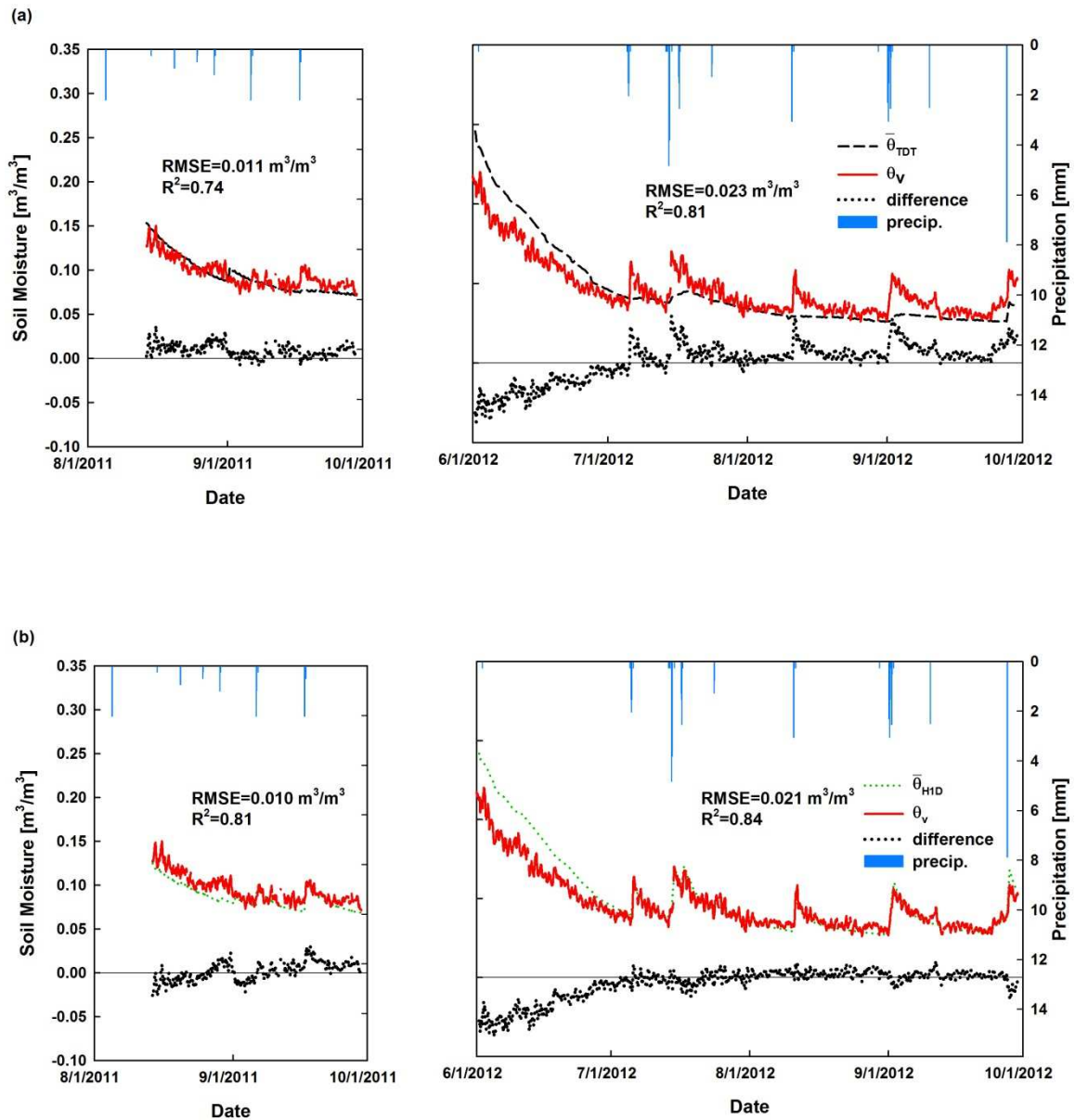


Figure 4-2. (a) Comparison between TDT weighted average soil moisture of 0.1 m, 0.25 m, and 0.5 m depth ($\bar{\theta}_{TDT}$) and the average areal soil moisture measured by CRNP (θ_v) during the growing seasons of 2011 and 2012. (b) Comparison between Hydrus-1D weighted soil moisture ($\bar{\theta}_{H1D}$) of 0.03 m, 0.05 m, 0.1 m, 0.25 m, and 0.5 m depth and the average areal soil moisture measured by CRNP (θ_v) during the growing seasons of 2011 and 2012. The soil moistures at 0.03 m and 0.05 m were extracted from the Hydrus-1D estimation. The soil moistures at 0.1 m, 0.25 m, and 0.5 m were measured by TDT sensors.

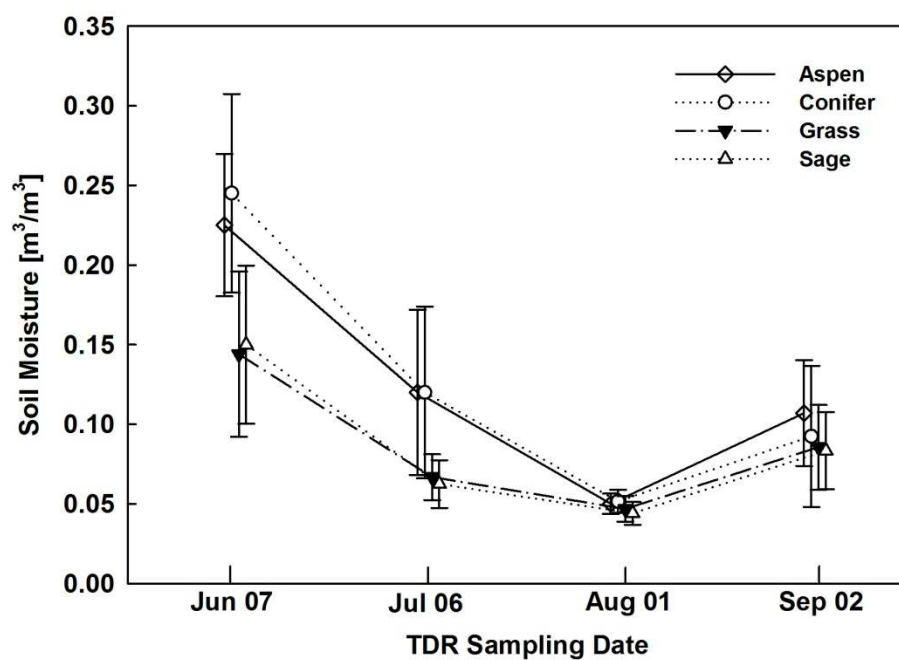


Figure 4-3. The seasonal evolution of soil moisture under the four vegetation types as measured by the portable time domain Reflectometry (TDR) probe on June 07, 2012, July 06, 2012, August 01, 2012, and September 02, 2012 at the TWDEF site.

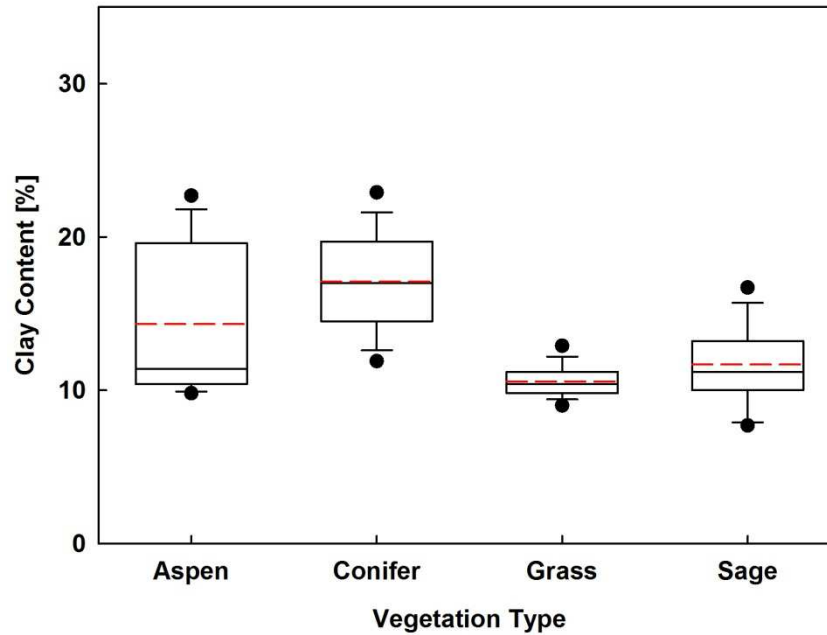


Figure 4-4. Clay content distribution within each vegetation type based on electromagnetic induction mapping and correlation between clay content and electrical conductivity (ECa). From top to bottom, the box chart shows the max value (top whisker), 75th percentile, mean (dash line), median (solid line), 25th percentile, and min value (bottom whisker) for each vegetation group, respectively. Dots indicate the 95th and 5th confidence interval.

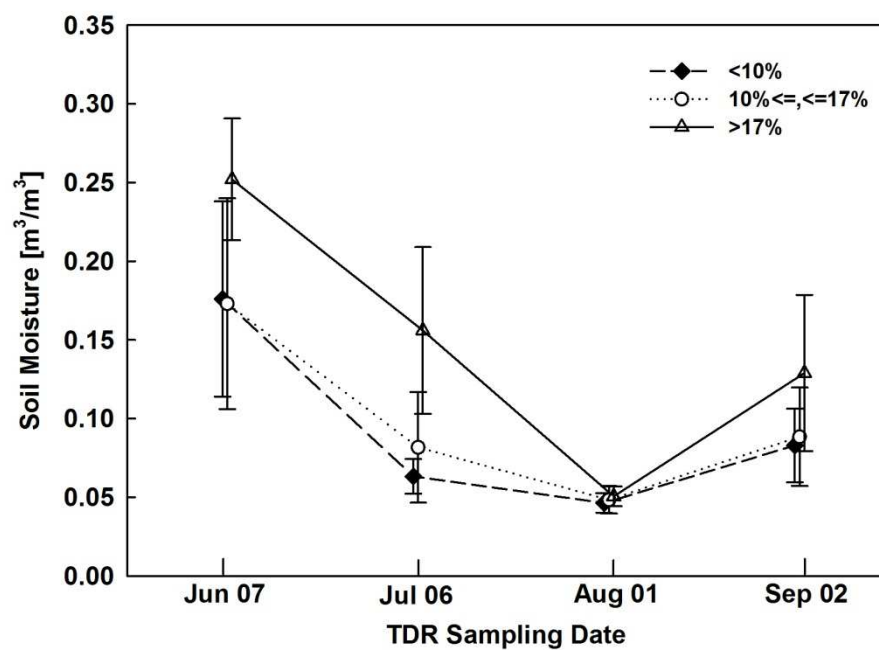


Figure 4-5. Temporal evolution of soil moisture during the summer of 2012 within each of 3 soil clay content regimes illustrated in Figure 1. The mean soil moisture flanked by one standard deviation for each soil clay fraction are plotted from portable TDR measurements made on June 07, 2012, July 06, 2012, August 01, 2012, and September 02, 2012 at the TWDEF.

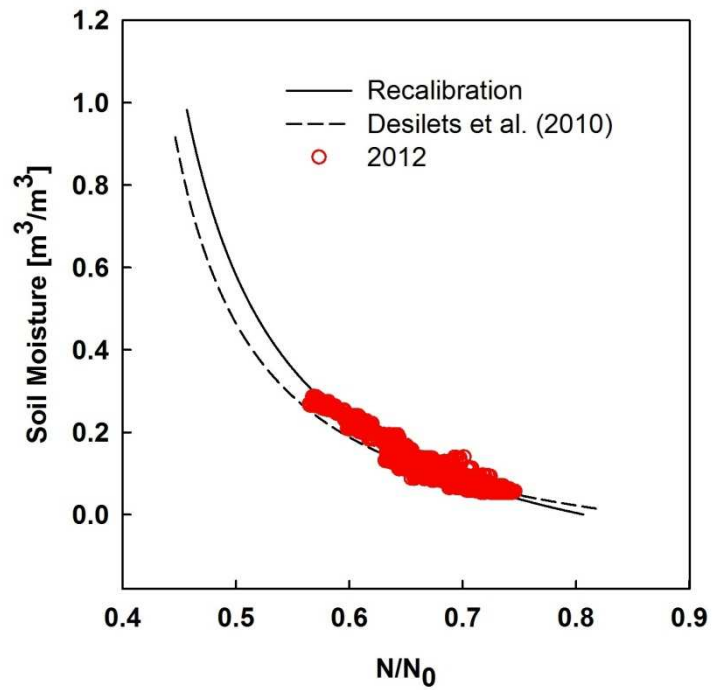


Figure 4-6. Comparison of CRNP-based soil moisture estimates as a function of fast neutron intensity using the parameters published by Desilets et al. (2010) against recalibrated parameters for the TWDEF. The discrete data points are derived from the Hydrus-1D weighted average areal soil moisture ($\bar{\theta}_{H1D}$) and the relative fast neutron intensity (N/N_0) obtained during the growing season of 2012.

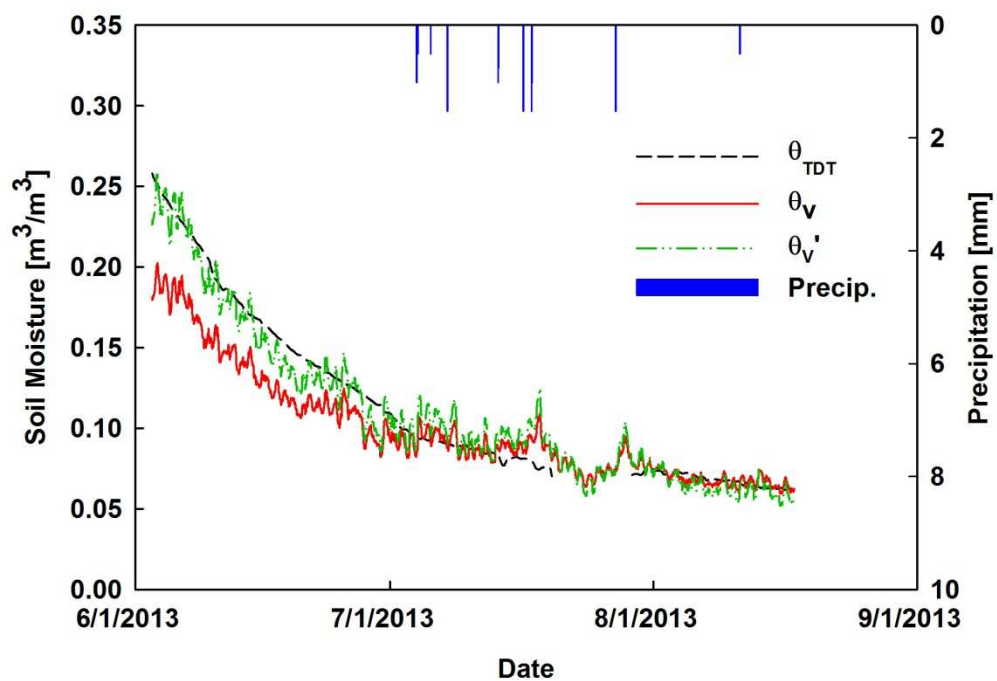


Figure 4-7. Comparison of soil moisture estimated from the weighted TDT sensors (θ_{TDT}), the universal calibration function (θ_v), and from the recalibrated parameters (θ_v') during the snow-free season of 2013.

CHAPTER 5

SUMMARY AND CONCLUSIONS

5.1 Summary of Findings

The results presented in the body of this dissertation included the descriptions of T.W. Daniel Experimental Forest (TWDEF) instruments and monitoring, and numerical ET simulations for four vegetation types (aspen, conifer, grass, and sage), and ET characteristics of each vegetation type. Furthermore, the estimation of areal-averaged soil moisture in the TWDEF using Cosmic-ray neutron probe (CRNP) was studied, improving the accuracy and capability of CRNP areal soil moisture estimation in a site as complex as the TWDEF.

In Chapter 2, I described a unique dataset obtained within the T.W. Daniel Experimental Forest (TWDEF), which is located in the Wasatch Mountains of Northern Utah. The TWDEF represents a high-elevation environmental research site collocated with the USU Doc Daniel SNOTEL site run by the USDA-NRCS. Environmental measurements were made within four common montane vegetation types of Northern Utah, namely: Aspen, conifer, grass, and sagebrush. The data set consisted of: (1) meteorological measurements from four primary automated micrometeorological towers (AMT) including air temperature and relative humidity, net radiation, precipitation, snow depth, and wind speed and direction as well as snow depth from the four primary AMT towers and eight secondary towers; (2) soil moisture and temperature from 36 plots at depths of 10 cm, 25 cm, and 50 cm; (3) precipitation, solar radiation, and water vapor and CO₂ flux from an eddy covariance tower; (4) areal-averaged soil moisture from a CRNP

sensor. This unique dataset is applicable to a variety of applications related to the description and modeling of the spatial and temporal snow accumulation, snow sublimation, snow melt infiltration, soil water storage, as well as enabling understanding of the ecological and hydrological responses to the climate change in Utah and the IMW region.

In Chapter 3, we used the meteorological data and soil moisture data measured in the TWDEF site to simulate the summer water use of the four vegetation types. The numerical model we chose in our study was Hydrus-1D, which is coupled with the Penman-Monteith equation and with the Feddes root-water uptake functions used to solve Richards equation through inverse fitting of the van-Genuchten hydraulic parameters. The Hydrus-1D numerical model was determined to be a valuable resource for simulating missing details of near-surface soil moisture after inverse fitting the model parameters to measured temporal records of soil moisture. Subsequent simulations of soil moisture proved invaluable for extending the information content of the soil profile and for simulating the soil evaporation and root water uptake to estimate ET. The simulated results showed that aspen had the highest water use during the growing seasons, followed by deep rooted conifer. The mean daily ET rates were 4.1-, 3.9-, 2.6-, 2.3- and 2.3-mm/day for aspen, deep rooted conifer, shallow rooted conifer, grass and sage, respectively. The typical hydrology of the TWDEF include a complete wetting of the soil profile by snowmelt followed by dry-down of the soil profile containing roots, with periodic rewetting of the surface by summer rains. Our study period included a record-breaking cool-wet year in 2011 and a recording-breaking dry-hot year in 2012. The

comparison of vegetation water use between these 2 years showed that the percentage of water use to total precipitation in the dry year was higher than in the wet year, likely a result of the shorter 'dry' season in the wet year. Considering the driest (2012) and wettest (2011) water years analyzed, the growing-season ET relative to the total annual precipitation ranged from 50.8% to 30.3% for aspen, 42.5% to 23.1% for conifer, 32.8% to 16.9% for grass/forbs and 33.3% to 17.7% for sage. This highlights the impact of vegetation water use on montane water availability where in dry years aspen consume half of the annual water. Although the conifer transpiration can potentially take place year-round, the summer-time ET is nearly 10% less than aspen. Aspen, grass and sage senesced or lost leaves, terminating water uptake from soil when soil moisture dropped below approximately $0.1 \text{ m}^3/\text{m}^3$ at the 10 cm depth each year. In contrast, the conifer appeared to transpire at low rates even under cold and dry conditions.

In Chapter 4, the comparison between the CRNP soil moisture measurements and in situ distributed TDT sensor soil moisture network measurements in this study showed that the near-surface soil moisture simulated by the Hydrus-1D could improve the correlation of these two soil moisture datasets, especially during rainfall events. The soil moisture distribution field and relative placement of the CRNP influence the readings of the CRNP. Soil moisture at the TWDEF site exhibits strong spatial structure (with a correlation length more than 100 m) during late spring/early summer following snowmelt, and tends to have a spatial Gaussian-like distribution when soil becomes dry. In addition, the CRNP was placed in a relatively dry spot in the TWDEF research site. As a result, the CRNP exhibited a dry bias at the beginning of the snow-free period. A site-specific

calibration function was employed for the CRNP at the TWDEF site, yielding a recalibrated function with coefficients of $a_0=0.120$, $a_1=0.367$, and $a_2=0.227$. The recalibration resulted in a RMSE (0.012) of less than half the original calibration RMSE (0.025).

5.2 Conclusions

From the ET simulations of the continuous four-year growing seasons, and their comparisons with observed soil moisture and eddy covariance measured ET, this research demonstrated that numerical simulation was a viable alternative method for the ET estimates for trees (e.g. aspen and conifer) and non-trees (e.g. grass and sage). From the statistical analysis of the four-year simulated ET, we found that when snowmelt fully recharges soil moisture, the total ET during the growing season for each vegetation type did not depend on the length of growing season or the depth of snowpack but primarily on the timing and amount of summer precipitation. Spring rainfall events had no significant effect on increasing total ET.

APPENDICES

(Coauthors' approval letters)

Ling Lv
Utah State University
Dept. Plants, Soils and Climate
4820 Old Main Hill
Logan, UT 84322-4820

07-09-2014

Jonathan Carlisle
Research Professional
Utah State University
Logan UT, 84322-4820
Email: jobie@usu.edu

Dear Carlisle,

I am in the process of preparing my dissertation in the Plants, Soils and Climate Department at Utah State University. I hope to complete in August 2014.

I am requesting your permission to include the attached paper, of which you are coauthor, as a chapter in my dissertation. I will include acknowledgments to your contributions as indicated. Please advise me of any changes you require.

Please indicate your approval of this request by signing in the space provided, attaching any other form or instruction necessary to confirm permission. If you have any questions, please contact me.

Thank you,

Yours Sincerely,

Ling Lv

I hereby give permission to Ling Lv to use and reprint all of the material that I have contributed to Chapter 2 of this dissertation.


Jonathan Carlisle

Ling Lv
Utah State University
Dept. Plants, Soils and Climate
4820 Old Main Hill
Logan, UT 84322-4820

07-09-2014

Trenton E. Franz
Assistant Professor
University of Nebraska-Lincoln,
School of Natural Resources,
607 Hardin Hall, Lincoln, NE, 68583
Email: Trenton.franz@unl.edu

Dear Dr. Franz,

I am in the process of preparing my dissertation in the Plants, Soils and Climate Department at Utah State University. I hope to complete in August 2014.

I am requesting your permission to include the attached paper, of which you are coauthor, as a chapter in my dissertation. I will include acknowledgments to your contributions as indicated. Please advise me of any changes you require.

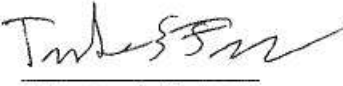
Please indicate your approval of this request by signing in the space provided, attaching any other form or instruction necessary to confirm permission. If you have any questions, please contact me.

Thank you,

Yours Sincerely,

Ling Lv

I hereby give permission to Ling Lv to use and reprint all of the material that I have contributed to Chapter 4 of this dissertation.


Trenton E. Franz

Ling Lv
Utah State University
Dept. Plants, Soils and Climate
4820 Old Main Hill
Logan, UT 84322-4820

07-09-2014

David A. Robinson
Research Scientist
NERC-Centre for Ecology & Hydrology
Environment Centre Wales,
Deiniol Rd., Bangor Gwynedd, LL57 2UW, UK
Email: davi2@ceh.ac.uk

Dear Dr. Robinson,

I am in the process of preparing my dissertation in the Plants, Soils and Climate Department at Utah State University. I hope to complete in August 2014.

I am requesting your permission to include the attached paper, of which you are coauthor, as a chapter in my dissertation. I will include acknowledgments to your contributions as indicated. Please advise me of any changes you require.

Please indicate your approval of this request by signing in the space provided, attaching any other form or instruction necessary to confirm permission. If you have any questions, please contact me.

Thank you,

Yours Sincerely,

Ling Lv

I hereby give permission to Ling Lv to use and reprint all of the material that I have contributed to Chapter 4 of this dissertation.



David A. Robinson

CURRICULUM VITAE

Ling Lv

CONTACT INFORMATION

| | |
|---|--|
| Department of Plants, Soils and Climate | Office: Agricultural Sciences 302A-C |
| Utah State University | E-mail: ling.lv@aggiemail.usu.edu |
| 4820 Old Main Hill | Phone (department): 435-797-2233 |
| Logan, UT, 84322-4820 | Fax (department): 435-7973376 |

RESEARCH INTERESTS

- Measuring and modeling land and atmosphere water exchange/interactions in the nature ecosystems
- Modeling of water infiltration/redistribution/loss in vadose zone
- Soil moisture measurement in intermediate- scale
- Geophysical methods to estimate areal soil moisture

EDUCATION

Ph.D.

Aug., 2009-Now

Utah State University, Logan, Utah, USA

Department of plants, Soils, and Climate

Ph.D. Student, Soil and Environmental Physics

- Dissertation Topic: “Linking Montane Soil Moisture Measurements to Evapotranspiration Using Inverse Numerical Modeling”
- Advisor: Scott B. Jones

Master of Agronomy

2006-2009

Northwest A&F University, Yangling, Shaanxi, China

Department of Environment and Resources

- Thesis Topic: “Urban Rainwater Utilization”
- Advisor: Pute Wu, Xining Zhao

Bachelor of Agronomy

2002-2006

Northwest A&F University, Yangling, Shaanxi, China

Department of Environment and Resources

- Project Topic: “the Wind Characteristics of the Mao Wu Su Sand Land”
- Advisor: Cha ying Liao

TRAINING EXPERIENCE

Geostatistical Analysis of Environmental Data Short Course. 2011. Utah State

University. Pierre Goovaerts, PGeostat, LLC.

NSF Workshop: “Science: Becoming the Messenger”

REFEREED PUBLICATIONS

Lv, L., Pute Wu, Xining Zhao. 2009. Research advance of urban rainwater utilization.

Science of Soil and Water Conservation. 7(1): 118-123.

Lv, L., Pute Wu, Xining Zhao. 2009. Calculating the available rainwater resources and

analyzing the benefits for Yangling urban area. Agricultural Research in the Arid

Areas. 27(5): 225-229.

MANUSCRIPTS IN PREPARATION

Lv, L., S.B. Jones, J. Carlisle: T.W. Daniel Experimental Forest, UT, United States. In preparation

Lv, L., S.B. Jones, L.E. Hips. Evapotranspiration in a Semi-arid Mountain Ecosystem from Integrating Numerical Modeling and Environmental Data. In preparation.

Lv, L., T.E. Franz, D.A. Robinson, S.B. Jones. Measured and Modeled Soil Moisture Compared with Cosmic-Ray Neutron Probe Estimates in a Mixed Forest. In preparation.

ABSTRACT OF PRESENTATIONS

Ling Lv, Scott B. Jones, Trenton Franz. 2013. A Cosmic-Ray Neutron Probe for Intermediate-Scale Estimates of Soil Moisture at the T.W. Daniel Experimental Forest. Annual Spring Runoff conference, Utah State University, Eccles Conference Center, Logan, UT, April 9-10.

Lv, Ling, Scott B. Jones, Lawrence E. Hips. 2012. Assessing Water Use in Semi-arid Montane Aspen, Conifer, Sage and Grass/Forbs Ecosystems using Measurements and Numerical Simulation. Soil Science Society of America International Annual Meeting, Cincinnati, Ohio, October 21-24.

Lv, Ling, Lawrence Hips, S.B. Jones. 2012. Water Use of Aspen, Conifer, Sage and Grass/Forbs Communities in a Semi-arid Montane Ecosystem. Annual Spring Runoff Conference, Utah State University, Eccles Conference Center, Logan, UT, April 3-4, 2012.

- Lv, Ling, Jobie Carlisle, Lawrence Hipps, Scott B. Jones. 2011. Modeling Evapotranspiration in a Semi-arid Mountain Ecosystem Integrating HYDRUS-1D and Weather Data. ASA, CSSA, and Soil Science Society of America International Annual Meetings, San Antonio, TX, October 16 – 19, 2011.
- Lv, Ling, Jobie Carlisle, S.B. Jones. 2011. Modeling Conifer Forest Evapotranspiration in a Semi-arid Mountain Ecosystem. Annual Spring Runoff Conference, Utah State University, Eccles Conference Center, Logan, UT, March 29-30.

HONORS & AWARDS

- Received Ph.D. Completion Fellowship. Provided by the office of Research and Graduate Studies, 2013.
- Received Outstanding Student Poster. Provided by the USU Water Initiative, 2013.
- Received RGS Graduate Student Travel Award. Provided by the office of Research and Graduate Studies, 2013.